7-31-2006

Chemosensory Responses in Azospirillum brasilense

Bonnie Baggett Stephens

CHEMOSENSORY RESPONSES IN *AZOSPRILLUM BRASILENSE*

by

BONNIE BAGGETT STEPHENS

Under the Direction of Gladys Alexandre

ABSTRACT

The ability to swim and navigate the surrounding environment confers an advantage to motile bacteria, allowing the occupation of niches that are optimum for survival and growth. Bacteria are too small to sense their environment spatially, so they must sense the environment temporally by comparing the past and present environments and altering their motility accordingly. Chemotaxis systems coordinate flagellar motility responses with temporal sensing of the environment.

Chemotaxis is proposed to be involved in plant root colonization by directing soil bacteria toward root exudates of various cereals, promoting growth. The nitrogen-fixing alpha-proteobacterium *Azospirillum brasilense* utilizes chemotaxis to navigate its environment by integrating various environmental signals into a chemotaxis signal transduction pathway.

In chemotaxis, transducers receive environmental sensory information and transmit the signal to the histidine kinase CheA, which relays the signal to the response regulator CheY. A novel chemotaxis transducer, Tlp1, has been identified and characterized as an energy sensor by constructing a *tlp1* mutant and performing behavioral and root colonization assays.

In order to adapt to changing environmental conditions, chemotactic microorganisms must employ a molecular "memory" comparing present environmental conditions to ones previously experienced and resetting the chemotaxis transducer to a prestimulatory status. A recently identified chemotaxis operon revealed a methyltransferase CheR and methylesterase CheB, comprising an adaptation system, suggesting that *A. brasilense* undergoes methylation-dependent taxis responses, contrary to previous reports. Chemotaxis and methanol release assays suggest that adaptation by methylation in locomotor behavior involves the presence of other unknown methylation systems, and the contribution of CheR and CheB to chemotactic and aerotactic responses is complex.

There is growing evidence that chemotaxis-like signal transduction pathways control a myriad of other cellular processes regulated in a temporal fashion. This would convey an advantage to cells by allowing modulation of cellular processes based on slight changes in environmental conditions and provide checkpoints for energetically consuming processes. Mutations in components of the chemotaxis-like signal transduction system revealed differences in cell size and exopolysaccharide production. This work shows that the signal transduction pathway of *A. brasilense* modulates cell length in response to changes in nutrient conditions, independently of growth rate.

INDEX WORDS: *Azospirillum brasilense*, signal transduction, chemotaxis, energy taxis, chemotaxis transducer, Tlp1, Tlp2, localization, CheA, CheB, CheR, CheBR, CheY methyltransferase, methylesterase, adaptation, methylation, cell size, flocculation, exopolysaccharide

CHEMOSENSORY RESPONSES IN *AZOSPRILLUM BRASILENSE*

by

BONNIE BAGGETT STEPHENS

A Dissertation Submitted in Partial Fulfillment of the Requirements for the Degree of

Doctor of Philosophy

in the College of Arts and Sciences

Georgia State University

2006

CHEMOSENSORY RESPONSES IN *AZOSPRILLUM BRASILENSE*

BY

BONNIE BAGGETT STEPHENS

Major Professor:	Gladys Alexandre
Committee:	John Hougthon
	Robert Simmons
	Phang C. Tai
	Igor Zhulin

Electronic Version Approved:

Office of Graduate Studies
College of Arts and Sciences
Georgia State University
August 2006

ACKNOWLEDGEMENTS

First, I'd like to thank the faculty and staff of the Georgia State University Biology department for this tremendous opportunity. I'd especially like to thank Dr. Gladys Alexandre, who has been an amazing mentor, teaching me to strive for excellence and thoroughness in all that I do and develop a curious scientific mind. I thank Dr. P.C. Tai and Dr. Igor Zhulin for their contributions and support, as well as Dr. Stephen Farrand for the opportunity to collaborate with his laboratory. I'd especially like to thank Dr. Robert Simmons who has shown tremendous patience teaching me about imaging, especially electron microscopy, and Dr. John Houghton who provided a "home away from home" with his mentorship and lab space.

I'd like to thank past and present members of the Alexandre lab for their support and assistance through the completion of this degree. Special mention is given to Lance Miller, Star Loar, and Annie Lin, who have all contributed ideas and provided helpful discussions. I would especially like to thank Mariam Wasim, a talented undergraduate student that I could always count on to lend a helping hand and Brook Danboise, whose friendship has been invaluable. I'd also like to thank the members of the Houghton lab, Anupama Shanmuganathan, Amrita Nargund, Suchita Sood, and Bishu Sapkota for taking me in as a member of their own laboratory; I will never forget your kindness.

I am grateful to my family for their love and support, and their teachings that everything should be done with excellence. I'd especially like to thank my husband, Josh, for is unfailing love, support, and patience though the completion of this degree.

TABLE OF CONTENTS

LIST OF TABLES

LIST OF FIGURES

LIST OF ABBREVIATIONS

HAMP	histidine kinase, adenylyl cyclase, methyl-accepting chemotaxis protein, and phosphatase
HCD	highly conserved domain
Htr	halobacterial transducers of rhodopsin
ETS	electron transport system
PMF	proton motive force
Tlp	transducer like protein
MCP	methyl-accepting chemotaxis protein
CPM	counts per minute
EPS	exopolysaccharide
TEM	transmission electron microscopy

CHAPTER ONE: GENERAL INTRODUCTION

CHEMOTAXIS

In 1676, using crude microscopes of his own construction, Antoni van Leeuwenhoek was the first to observe and document the existence of "wee animalcules" found swimming in a suspension of water (39). However, it was not until the late 19th century that Thomas Engelmann noticed that under a coverslip, bacteria accumulated and were actively swimming near sources of oxygen, but when an unfavorable chemical was added the cells slowed down and their motility changed (36). Since that time, the molecular mechanisms regulating such behavior have been extensively studied and bacterial chemotaxis is one of the best understood signal transduction systems.

The ability to swim and navigate the surrounding environment confers an advantage to motile bacteria, allowing the occupation of niches that are optimum for survival and growth. Bacteria are too small to sense their environment spatially, so they must sense the environment temporally by comparing the past environment to the present environment and altering their motility accordingly (26). Chemotaxis systems coordinate flagellar motility responses with temporal sensing of the environment. Chemotaxis is a generalized term describing the process by which cells respond to environmental conditions by moving towards favorable environmental conditions and away from unfavorable ones. In an isotropic environment, bacteria exhibit a "random walk" in which motile cells alternate between a series of runs (smooth swimming) and reorienting tumbles/reversals (changes in direction). When bacterial cells sense a favorable

environmental cue, the frequency of runs increases and tumbles/reversals decreases, resulting in the cell moving toward the favorable condition. On the other hand, when an unfavorable environmental cue is sensed, the walk is biased with a higher frequency of tumbles/reversals to move the cell away from this condition (15, 120). A variety of environmental cues can elicit a taxis response in bacterial cells including, but not limited to chemicals, pH, light, oxygen, reduction potential, magnetic field, temperature, osmolarity (1, 12, 19, 23, 24, 49, 79, 83, 92, 124, 164). These motility responses are regulated by a conserved two- component regulatory system in which a response regulator senses environmental stimuli via a sensory protein (chemotaxis transducer) and the response regulator (CheY), which binds to the flagellar motor resulting in a change in flagella rotation.

MOLECULAR MODELS FOR CHEMOTAXIS

Julius Adler was one of the pioneers in bacterial chemotaxis, choosing to study this phenomenon in the gamma-proteobacterium *Escherichia coli*. He determined that *E. coli* responds to chemicals independently of their metabolism (1). Since then, the *E. coli* chemotaxis signal transduction pathway has become one of the most well-studied two-component systems (127, 154). An environmental cue is sensed via chemotaxis transducers in a metabolism-independent ligand-binding mechanism. Each chemotaxis transducer has a chemical specificity. *E. coli* has five chemotaxis transducers. Four of these chemotaxis transducers Tsr (serine), Tar (aspartate and maltose), Trg (ribose and galactose), Tap (dipeptides) are prototypical chemotaxis transducers, which have a periplasmic sensing domain flanked by two helical membrane anchors and a cytoplasmic

signaling domain (77, 91, 133). The Aer (redox potential) chemotaxis transducer has a different topology consisting of cytoplasmic sensing and signaling domains.

E. coli has one set of chemotaxis genes encoding for the following signaling components: histidine kinase CheA, docking protein CheW, methyltransferase CheR, methylesterase CheB, response regulator CheY, and phosphatase CheZ. The signaling domain of chemotaxis transducers are linked to the histidine kinase CheA via a small docking protein, CheW (28). In response to the appropriate signal, CheA undergoes autophosphorylation and then phosphorylates CheY, which binds to the switch protein FliM on the flagellar motor, resulting in a change in rotation of the flagella (148, 160). The change in flagellar motor rotation is the basis by which cells can control their swimming direction (15, 81). *E. coli* cells swim by the counter clockwise (CCW) rotation of the flagellar motor bundling together five to eight flagella that push the cell forward. When the flagellar motor switches direction to clockwise (CW) rotation, the flagellar bundle is disrupted and the cell tumbles(150). In *E. coli*, the presence of attractants prevents the autophosphorylation of CheA, resulting in counterclockwise (CCW) rotation of the flagellar motor, biasing the cell toward smooth-swimming runs. In the absence of an attractant or in the presence of a repellent, CheA is activated, ultimately resulting in a change from CCW flagellar rotation to CW rotation, biasing the cells toward reorienting tumbles. The phosphatase CheZ is involved in terminating the excitory signal by increasing the rate of phosphate removal from phosphorylated CheY (95).

In order to effectively move along a gradient to the most favorable environmental conditions, the cell employs a molecular “memory”, comprised of a CheB methylesterase and a CheR methyltransferase, to temporally compare the previous environmental

condition experienced to the present environmental status. The CheR methyltransferase constitutively adds methyl groups from S-adenosylmethionine to the methylation domain of chemotaxis transducers (78, 132). The activated CheB methylesterase deamidates glutamine residues of the methylation domain of chemotaxis transducers and removes methyl groups as volatile methanol (69, 123). Activated CheA phosphorylates the methylesterase CheB at a much slower rate than it phosphorylates CheY, creating a feedback loop that "resets" the chemotaxis transducers to prestimulatory bias, allowing the cell to compare the current environmental condition to the one previously sensed.

A second well understood two-component chemotaxis system is found in the gram-positive bacterium *Bacillus subtilis*. *B. subtilis* has ten chemotaxis transducers, most of which have a prototypical topology similar to those of *E. col*i (45, 46, 51, 52, 62, 75). However, they differ from *E. coli* chemotaxis transducers due to the presence of two pairs of C-terminal insertion/deletions of 14 amino acids as well as different sites for methylation (82, 173). Similar to *E. coli*, *B. subtilis* has one set of chemotaxis genes, homologous to all of the chemotaxis proteins found in *E. coli* with the exception of the CheZ phosphatase. Just as observed in *E. coli*, a chemotaxis transducer detects an environmental signal, and the histidine kinase CheA is autophosphorylated. However, in *B. subtilis*, CheA is activated in the presence of an attractant and binding of the phosphorylates CheY to the flagellar motor results in smooth swimming (21).

One of the primary differences between the chemotaxis signal transduction pathways of *E. coli* and *B. subtilis* is with the adaptation mechanism. For example, the *B. subtilis* chemotaxis transducer McpB has different methylation sites on its C-terminal region, each with a different role. Methylation of Glu637 brings about adaptation to

attractants, while Glu630 and Glu637 bring about adaptation to the removal of an attractant (173), which results in methanol evolution by CheB from both the addition and removal of an attractant (73, 147). *B. subtilis* has additional adaptational proteins not present in *E. coli.* CheV is an adaptational protein that couples to and is phosphorylated by CheA, which brings about adaptation, possibly in a methylation-independent manner (68). CheC is another adaptational protein that can hydrolyze phosphorylated CheY, thereby affecting adaptation (139). CheD plays a role fulfilled by CheB in *E. coli;* CheD deamidates glutamine residues of chemotaxis transducers that is necessary to achieve full methylation and activation of chemotaxis transducers (80).

CHEMOTAXIS TRANSDUCERS

Chemotaxis transducers receive sensory information in chemotaxis and transmit the environmental signal to the histidine kinase CheA. These transducers are comprised of two elements: a sensing domain and a signaling module (169). Sensing domains can be located either in the periplasm or the cytoplasm and are generally not conserved. This region of the chemotaxis transducer specifies the environmental cues sensed and thus will show little conservation except amongst transducers that sense similar environmental cues.

Domains

The sensing domain is often (but not always) connected to the signaling region via a linker or HAMP domain (histidine kinase, adenylyl cyclase, methyl-accepting chemotaxis protein, and phosphatase), which has been shown to be an integral part of

transducing the environmental signal from the sensing domain to the signaling domain of the transducer by sensing conformational changes of the transducer.

In *E. coli*, the C-terminal region is comprised of two methylation domains flanking a highly conserved domain, HCD (34, 138). The methylation domains contain glutamate residues that are methylated and demethylated by the CheB/CheR adaptation system allowing the transducer to be reset into a prestimulus sensing mode (27, 134). The HCD is the site of interaction between the chemotaxis transducer and the CheW docking protein. The sequence of the HCD is highly conserved and found in transducer sequences of both Bacteria and Archaea (169). Chemotaxis transducers can be divided into three classes based on the presence or absence of two pairs of insertion/deletions (indels) consisting of fourteen amino acids (82). Class I transducers do not have any indels, and chemotaxis transducers from enteric bacteria such as *E. coli* fall into this class. Class II transducers have two indel regions flanking the HCD domain; the FrzCD transducer from *M. xanthus* falls into this category. *B. subtilis* transducers, such as McpB, fall into class III transducers by possessing two indel regions at the beginning and end of the methylation region in addition to the same indel regions as Class II transducers (82).

The different classes of chemotaxis transducers contain different sites of methylation within the methylation region of the C-terminal region of the transducer. These sites are responsible for the formation of volatile methanol in response to different stimuli. The sites of methylation of the class I *E. coli* chemotaxis transducer Tar include the glutamate residues 295, 302, 309, and 491 (144, 145). Methylation of any of the sites result in methanol evolution in response to negative stimuli (70, 122, 146). However, the methylation sites of the class III chemotaxis transducer McpB of *B. subtilis* include three

glutamate residues 630, 637, and 371. However, unlike the methylation sites of *E. coli*, each methylation site has a different function. Methanol is evolved from either Glu 371 or Glu630 upon positive stimulation and from Glu 630 and 637 upon negative stimulation (173). However, the patterns of methanol evolution in response to both positive and negative stimuli cannot be generalized based on the categorization of the chemotaxis transducer. For example, the class I chemotaxis transducers of *Rhodobacter sphaeroides* possess conserved glutamate residues possibly involved in adaptation (94). However, these transducers evolve methanol in response to positive stimuli, unlike the *E. coli* or *B. subtilis* models (94). This is not surprising since *R. sphaeroides* has multiple chemotaxis-like systems that regulate functions other than motility (see below). As more information is gained regarding the functions and interactions of the various components of chemotaxis-like signal transduction systems of other species, such systems will begin to emerge as models in place of *E. coli* and *B. subtilis*.

The C-terminal regions of the *E. coli* chemotaxis transducers (Tsr and Tar) contain an NWETF pentapeptide motif at the C-terminal end of the chemotaxis transducer, which serves as a CheR methyltransferase binding site (38, 163). This NWETF motif has not been identified in chemotaxis transducers of *R. sphaeroides*, although two chemotaxis transducers McpA and TlpT contain similar motifs, GWEDF and GFEDF (respectively). This is interesting since $CheR_2$ can complement an *E. coli* strain lacking CheR, which suggests that $CheR_2$ interacts with both motifs or a different conserved region of chemotaxis transducers (94). *B. subtilis* chemotaxis transducers such as McpB also lack a NWETF pentapeptide motif. Instead, it possesses an FKIE motif that

is required for expression of the transducer, and may serve a function similar to the NWETF motif in *E. coli* (172).

Localization

In order to integrate various environmental signals, motile bacteria possess a signal amplification system that allows for detection of differences of only a few molecules occupying ligand-binding transducers. It has been recently proposed that clustering of chemotaxis transducers might be involved in signal amplification as well as in signal transduction during chemotaxis (71, 125, 127, 128). In the membrane, chemotaxis transducers exist as homodimers and are further grouped together as trimers (9). Chemotaxis transducers are typically clustered at the cell poles, which was first observed in *E. coli* and *Caulobacter crescentus* and then in several other bacterial and archeal species, suggesting that it is a conserved feature of chemotaxis transducers (7, 47, 53, 74, 89, 90). This type of arrangement allows for interactions between transducers. Chemotaxis transducers exist in specific stoichiometric ratios within the cell. For example, in *E. coli* Tsr and Tar are highly abundant with thousands of copies per cell, while Tap, Trg, and Aer are of low abundance with only a few hundred copies per cell (84). Additionally, the components of the chemotaxis signal transduction pathway in *E. coli* have been shown to localize to the pole of the cells (89, 129), which is thought to be important for the formation of tight clusters of the chemotaxis proteins resulting in signal amplification and adaptation (29, 35).

DIVERSITY IN CHEMOTAXIS: A PARADIGM SHIFT?

While *E. coli* is the best understood model for chemotaxis, there is evidence that the signal transduction system is also one of the most simple. Experimental evidence in addition to genomic research indicates that there are major departures from the generalized chemotaxis scheme of *E. coli* including differences such as multiple copies of various chemotaxis homologs, additional chemotaxis proteins, fusion proteins, variations of sensory input proteins, as well as multiple signal transduction pathways. The type and range of environmental cues varies with each microorganism, and each system has evolved for the optimum survivability in the particular niche occupied. No other chemotaxis system has been studied as intensively as that of *E. coli*, but as more experimental and genomic research becomes available, it is clear that the model established in *E. coli* is quite simple and does not represent the majority of chemotaxis systems.

Variations on a theme: multiple chemotaxis systems

Sinorhizobium meliloti

Departures from the *E. coli* paradigm of chemotaxis are observed in several well-studied species of proteobacteria. One example is the soil bacterium *Sinorhizobium meliloti*. *S. melilioti* is a free-living alpha-proteobacterium often found living in the rhizosphere or root nodules of various plants such as alfalfa and converts atmospheric nitrogen into ammonia, which is taken up by the plant. *S. meliloti* has two sets of chemotaxis genes (42, 48). *CheOp*$_1$ is the major chemotaxis operon and contains *cheY*$_1$, *cheA*, *cheW*, *cheR*, *cheB*, *cheY*$_2$, and *cheD* (131). Unlike *E. coli*, *S. meliloti* has two

response regulators, CheY1 and CheY2 and lacks a CheZ phosphatase (48). Each of these response regulators has a different function and work together to modulate motility responses. CheY2 is the master control for flagellar rotation while CheY1 modulates the speed (130). Upon activation, CheA phosphorylates CheY2. Since *S. meliloti* lacks a CheZ phosphatase to extinguish the signal, excess phosphorylated CheY2 transfers a phosphate group back to CheA. The phosphate group is subsequently transferred to CheY1, which acts as a phosphate sink, accelerating the deactivation of phosphorylated CheY2 (130). Hence, it was proposed that multiple CheY homolog may compensate for the lack of CheZ phosphatase in some bacterial species.

Rhodobacter sphaeroides

Another example of such a departure from the *E. coli* model is with the metabolically diverse *Rhodobacter sphaeroides*. *R. sphaeroides* is a free-living alpha-proteobacterium that moves by the rotation of a single subpolar flagellum. Unlike *E. coli*, the flagella rotates CCW in response to a positive stimulus (an attractant) and stops in response to a negative stimulus (repellent) by changing its structure from helical to coiled(10). Motile cells of *R. sphaeroides* possess three sets of chemotaxis genes, two of which are essential for chemotaxis and one that is of unknown function. The three sets of chemotaxis genes are comprised of the following chemotaxis homologs: *che*Op$_1$ contains *cheY*$_1$, *cheA*$_1$, *cheW*$_1$, *cheR*$_1$, and *cheY*$_2$; *che*Op$_2$ contains *cheY*$_3$, *cheA*$_2$, *cheW*$_2$, *cheW*$_3$, *cheR*$_2$, *cheB*$_1$, and *tlpC*; *che*Op$_3$ contains *cheA*$_4$, *cheR*$_3$, *cheB*$_2$, *cheW*$_4$, *slp*, *tlpT*, *cheY*$_6$, and *cheA*$_3$ (50, 114, 157). Additionally, *R. sphaeroides* has a CheBRA fusion protein and an addition *cheY*$_4$ (88, 121). Deletion of any of the *che*Op$_1$ components results only in a

minor behavioral change, while deletion of any of the *che*Op_2 or *che*Op_3 components abolishes normal chemosensory and photosensory responses (50, 93, 94, 114). $CheY_4$ was also shown to be essential for chemotaxis (121).

The different components of the two the chemotaxis signal transduction pathways controlling chemotaxis in *R. sphaeroides* are localized to different regions within the bacterial cell. The components of *che*Op_2 ($CheA_2$, $CheW_2$, and $CheW_3$) are localized to the poles of the cell along with transmembrane chemotaxis transducers, while the components of *che*Op_3 ($CheA_3$, $CheA_4$, $CheW_4$, and TlpT) are localized in the cytoplasm in a cluster along with cytoplasmic chemotaxis transducers; no proteins were localized to both locations (155). The localization of these sets of proteins to different locations within the cell may prevent cross-talk between the components of these two systems. It has been shown that the Such physical separation would be required to prevent related systems from interacting with each other, especially given the number of two-component signal transduction pathways present in any one given bacterial cell may be as high as 130 (11).

Rhodospirillum centenum

Rhodospirillum centenum is a photosynthetic alpha-proteobacterium that has the ability to differentiate into different cell types. *R. centenum* swims using a single polar flagellum and is capable of swarming on a surface using 2-4 lateral flagella that are different from the polar flagellum and produced only when cells are grown on surfaces (16). *R. centenum* has three chemotaxis operons, one which controls chemotaxis, phototaxis, and motility. The *che*$_1$ operon encodes for chemotaxis homologs to most of

the proteins found in the *E. coli* chemotaxis operon such as CheW, CheY, CheB, and CheR; additionally, the operon contains a CheA-CheY hybrid protein (63). The motility phenotypes of mutant cells of the *R. sphaeroides* chemotaxis genes is similar to that observed in E. coli, suggesting that the signal transduction pathway ultimately acts on the flagellar motor in a manner similar to that observed in *E. coli* (65, 109, 110). However, a mutation in the *cheY* gene resulted in a rapid reversal phenotype unlike a mutation in its *E. coli* counterpart that is locked into a smooth-swimming phenotype. Also, a mutation in CheY does not abolish chemotaxis and prevents swarming on surfaces, indicating that this response regulator does not control rotation of the polar flagella but most likely controls rotation of lateral flagella (65). This operon controls chemotaxis and phototactic behavior similar to the chemotaxis operon in *E. coli* (54, 65).

Halobacterium salinarum

The differences observed from the chemotaxis signaling pathway of *E. coli* is not limited to Bacteria, but also extends to Archaea. The archaeon *Halobacterium salinarum* is a halophilic microorganism that has adapted to growth under conditions of high salinity (4.3 M) (33). It is polarly flagellated and swims by the bundling of 5-10 flagellar filaments and reorients itself by a switch in the rotation of the flagella, resulting in a reversal (3). Genome sequence analysis reveals that *H. salinarum* has at least 17 che-like transducers and a set of *B. subtilis che*-homologs including *cheA*, *cheB*, *cheC* (two, $cheC_1$ and $cheC_2$), *cheD*, *cheR*, *cheY*, and *cheW* (two, $cheW_1$, $cheW_2$) (100).

H. salinarum senses light stimuli by transmembrane photoreceptors known as sensory rhodopsins (SR) that are homologous to chemotaxis transducers. These sensory

rhodopsins are coupled to halobacterial transducers of rhodopsin (Htr) that sense the conformational state of the receptor-transducer complex and relay the environmental cue to the histidine kinase CheA, which is autophosphorylated and subsequently phosphorylated CheY, which binds to the flagellar motor, resulting in a change in swimming direction (116-118). *H. salinarum* senses orange light as an attractant by the SRI-HtrI photoreceptive protein complex, which results in decreased switching of flagellar rotation yielding longer runs (59, 166). UV and blue light is sensed as a repellent by the SRII-HtrII photoreceptive protein complex (59, 168), which yields a higher number of reorienting reversals.

Helicobacter pylori

Regulation of chemotaxis and motility is also important for pathogenic microorganisms. *Helicobacter pylori* is an epsilon-proteobacteria that is responsible for type B gastritis and ulcers (25, 112). *H. pylori* cells are sense urea and amino acids as attractants and bile salts as repellents (32, 162, 167). Chemotaxis has been shown to play an important role in host colonization and infection by *H. pylori* because non-chemotactic mutants are attenuated in their ability to cause disease in animal infection models (96, 108, 143). The chemotaxis system of *H. pylori* is comprised of 3 prototypical chemotaxis transducers, 1 cytoplasmic chemotaxis transducer, CheW, CheA-$CheY_2$ fusion protein, $CheY_1$, and three CheV protein homologs (8, 149). By constructing mutant strains separating the CheA-ChY_2 fusion protein and purifying the components of the chemotaxis signal transduction pathway, it has been demonstrated *in vitro* that $CheY_1$, $CheY_2$, and all three CheV proteins have the ability to dephosphorylate CheA (66).

Phosphorylated CheY can also phosphorylate CheA-$CheY_2$, suggesting that the CheY receiver domain of the fusion protein can act as a phosphate sink similar to $CheY_1$ in *S. meliloti*, playing a role in terminating the excitation signal (43, 130).

H. pylori has approximately five polar flagella that it uses to swim in patterns of short straight runs interrupted by frequent direction changes (40). A CheY1 mutant results in a tumbling motility phenotype, and a CheA-Y_2 mutant results in a smooth-running motility phenotype, suggesting that $CheY_2$, phosphorylated by CheA interacts with the flagellar motor switch, similar to the observed in *E. coli* (40).

Diversity in chemotaxis: answers yet to be uncovered

There is growing evidence that one set of chemotaxis genes with one copy of each gene is not typical of most chemotactic microorganisms. Many chemotaxis operons contain multiple copies of genes including those encoding for fusion proteins. For example, many organisms have a CheA-Y fusion protein that is shown to functionally act as a histidine kinase as well as a response regulator, interacting with the flagellar motor. However, the mechanism of such interactions remains unclear, since CheA is typically coupled to chemotaxis transducers via the CheW docking protein, and phosphorylated CheY binds to the flagellar motor, how are such interactions accomplished? Also, genes present in an operon typically suggest interactions between the resulting proteins. However, when some mutations in a chemotaxis operon affect motility and others do not, what is the function of these additional proteins?

Adaptation: many ways to a common end

Rhodobacter sphaeroides

The adaptational mechanism of *R. sphaeroides* also appears to be different than that observed for either the *E. coli* or *B. subtilis* models. The CheB1 and CheR2 proteins from the second operon are believed to be the principal methylesterase and methyltransferase (94). In *E. coli* methyl groups are removed as methanol from chemotaxis transducers by an activated CheB methylesterase in response to a negative stimulus, such as the removal of an attractant (70). However, in *R. sphaeroides*, methanol release is observed in the presence of a positive stimulus (94). Additionally, disruption of the cheR1 gene found in the first operon, the function of which is unknown, does not result in any chemotaxis defects, but results in methanol release upon both the addition and removal of an attractant, similar to the pattern observed in *B. subtilis* (94). These observations suggest that *R. sphaeroides* has a novel system of adaptation unlike either *E. coli* or *B. subtilis*.

Halobacterium salinarum

Just as in *E. coli* and *B. subtilis*, *H. salinarum* has the ability to adapt to its surrounding environmental conditions. As described above, *H. salinarum* has homologs of the adaptation system of *B. subtilis,* and adaptation is mediated by methylation and demethylation of transducers (2, 100, 103, 135). Therefore, it is not surprising that *H. salinarum* evolves methanol in response to both attractant and repellent chemical and light stimuli just as observed in *B. subtilis* (2, 135). The general model proposed for adaptation is the methylation and demethylation of certain glutamate residues on the C-

terminal region of chemotaxis transducers (37). However, mutation of these methylation sites on the photoreceptive protein complexes results in cells that retain the ability to adapt to the light stimulus. This led the authors to suggest that methylation of the transducer sensing the light stimulus may not be required and probably occurs by an adaptational mechanism faster that the CheB/CheR adaptation system that functions in *E. coli* and *B. subtilis* (111).

H. salinarum also senses oxygen gradients (20, 86, 136). Motile cells of *H. salinarum* respond to an increase in oxygen concentration as an attractant response with smooth swimming and to a decrease in oxygen as a repellent response by tumbling (86). In *E. coli*, it has been established that adaptation in response to oxygen occurs via a methylation-independent mechanism, unlike response to most chemicals, which occurs via a methylation-dependent mechanism (102, 161). However, it has been demonstrated *in H. salinarum* that unlike *E. coli*, adaptation to oxygen is methylation-dependent. Both oxygen addition and removal resulted in methanol release in *H. salinarum*, similar to the pattern observed in response to chemicals and light and similar to the pattern observed in *B. subtilis* (86, 147).

Helicobacter pylori

H. pylori cells do not possess homologs to the adaptation proteins CheB and CheR. Instead, it has been proposed that the three CheV proteins facilitate adaptation during chemotaxis similar to the role of the CheV homolog from *B. subtilis* that has been shown to participate in adaptation in this species. Mutations in each of the *H. pylori* CheV proteins showed that only $CheV_1$ has a reduced swarming phenotype on soft-agar

plates, but its role in the signal transduction pathway of *H. pylori* remains to be uncovered (113).

Adaptation: answers yet to be uncovered

The CheB and CheR adaptation system in *E. coli* is relatively simple to understand. There is only one set of chemotaxis genes, and these adaptation proteins affect the sensitivity of chemotaxis transducers to environmental stimuli. However, as more genomic and experimental data becomes available, and it becomes apparent that the *E. coli* represents a minority of systems more questions arise. For example, how do multiple CheB and CheR proteins interact with different signal transduction pathways? Also, in addition to chemotaxis transducers, what other proteins are dependent on the chemotaxis CheB and CheR proteins for methylation and demethylation? It has been shown that several adaptation systems are methylation-independent, relying on adaptational proteins other than CheB and CheR, but the interactions and mechanisms of most of these systems remains to be elucidated.

Chemotaxis-like pathways regulate functions other than chemotaxis

Chemotaxis signal transduction pathways typically control motility responses to environmental cues. However, unlike the relatively simple chemotaxis models of *E. coli* and *B. subtilis*, which each contain one set of chemotaxis genes, there are many bacterial species that contain multiple che-like signal transduction pathways. There is growing evidence that other che-like signal transduction pathways control a myriad of other cellular processes that can be regulated in a temporal fashion. This would convey an

advantage to cells by allowing modulation of cellular processes based on slight changes in environmental conditions and provide checkpoints for energy consuming processes.

Escherichia coli

Although only one set of chemotaxis genes are present in *E. coli*, this signal transduction pathway also functions to control a process other than chemotaxis. When grown on various solid surfaces, *E. coli* cells are capable of producing hyper-flagellated swarm cells that can quickly colonize a surface (54). This behavioral response is mediated by the chemotaxis signal transduction pathway of *E. coli* (54, 126). Mutations in the components of the operon result in strains that have altered abilities to differentiate into swarm cells (30). Chemotaxis mutants on swarm agar are drier than the wild type cells, and it has been suggested that the flagellar filament itself senses the environment to modulate a feedback loop, preventing flagellin export (156).

Rhodospirillum centenum

Unlike *E. coli* that uses one chemotaxis system to regulate two different functions, *R. centenum* has two additional che-like operons, each with a unique output. The che_1 operon of *R. centenum* controls chemotaxis and phototaxis (as described above). Just like *E. coli*, *R. centenum* has the ability to differentiate from swim cells to swarm cells. In *R. centenum* this differentiation is temperature dependent (16). However, *R. centenum* possesses an entire set of che-like proteins involved in this differentiation. The che_2 operon encodes for CheW, CheB, CheR, CheY, and CheA homologs to the *E. coli* chemotaxis signal transduction pathway and has been shown to control flagella

biosynthesis (16). Mutations in these components of the signal transduction system result in cells that have altered flagella phenotypes, some mutants producing hyper-flagellated cells and other cells lacking flagella (16). Under appropriate conditions, all mutants, with the exception of an operon knock-out mutant and a CheY mutant, which do not produce flagella, are capable of displaying normal chemotaxis, indicating that this operon only indirectly affects chemotaxis, but its main function is regulation of flagella biosynthesis.

R. centenum possesses a third chemotaxis operon that encodes for CheY1, two CheW proteins (CheW3a and CheW3b), CheR3, CheA3, CheB3, a CheA-CheY hybrid protein (CheA3), and response-regulator sensor kinase hybrid (CheS) (17). Just as observed with the other two operons, mutations in this operon cause either induction or a delay in cyst development (17). One of the first steps in cyst-cell development is the ejection of flagella (18). Some mutants of both the che2 and che3 operons lack flagella, which suggests that these two pathways may share the same signaling output, most likely through cross-talk with one another (17). The chemotaxis mutants in the Che3 system that lack flagella include only the proteins involved in adaptation: CheB3, CheR3, and CheA3. This suggests that the Che3 pathway may be involved with adaptation that ultimately affects the signaling of the Che2 pathway, resulting in defects in flagella biosynthesis. Therefore, the Che3 system could have two possible outputs: (i) timing of cyst cell development and (ii) adaptation affecting the Che2 pathway, controlling flagella biosyntehesis (17).

Myxococcus xanthus

Myxococcus xanthus is a non-flagellated delta-proteobacterium that feeds on nutrients or other microorganisms in the environment. Under nutrient-limiting conditions, *M. xanthus* can differentiate into fruiting bodies that form spores. The multi-cellular lifestyle of *M. xanthus* is regulated by cell-to-cell signaling and coordination of motility with environmental conditions to form fruiting bodies (72). *M. xanthus* moves on surfaces by gliding motility and possesses both social and adventurous motility systems. Adventurous (A) motility refers to individual cell movement, and social (S) motility is the movement of cells in groups(60, 61). S motility occurs by the extension and retrataction of type IV pili (67, 137).

In order to coordinate this behavior, *M. xanthus* uses che-like signal transduction systems. *M. xanthus* has eight chemotaxis-like operons, of which the function of only four have been described. Both the Frz signal transduction pathway and(158) the Che4 signal transduction pathway are involved in S-motility (153, 159). The *frz* (che1) operon is comprised of FrzCD (chemotaxis transducer homolog), FrzA (CheW homolog), FrzG (CheB homolog), FrzF (CheR homolog), FrzE (CheA-CheY fusion), FrzZ (CheY-CheY fusion), and FrzB. The Frz system coordinates both A and S motility. Mutations in the components of the Frz system result in cells that rarely reverse direction or reverse direction frequently, which do not swarm well (22). This is reminiscent of the *E. coli* chemotaxis pathway in which mutations in the chemotaxis genes results in cells that are locked into an either smooth swimming or tumbly phenotype. Additionally, a Che4 signal transduction pathway also controls cell reversal in *M. xanthus*. The *che4* operon is comprised of a chemotaxis transducer homolog, two CheW proteins, a hybrid CheA-

CheY protein, and a CheR protein (153). In a strain displaying only S motility, it was shown that deletion of *cheY*$_4$ or the entire operon resulted in cells that displayed enhanced swarming and development. It was also shown that cells lacking *cheY*$_4$ or the chemotaxis transducer no longer coordinated a higher velocity with a reduced reversal frequency, which suggests that multiple pathways coordinate this behavior (153).

A third chemotaxis operon in *M. xanthus* encodes for two chemotaxis transducers (Mcp3A, McpB), CheW, a hybrid CheA, CheB, and CheR. Interestingly, this operon lacks a CheY response regulator. Mutations in each of the components of this operon did not result in any motility defects, suggesting that this operon does not control motility. However, it was observed that mutations in the genes of this chemotaxis-like operon resulted in cells that prematurely entered myxospore development, but did not produce viable spores. Therefore, the authors hypothesized that the Che3 system of controlled the expression of developmental genes, and expression studies of developmentally controlled genes confirmed this hypothesis. Analysis of the gene context of the operon revealed the presence of a response regulator, CrdA, an NtrC-like transcriptional regulator, immediately upstream of this operon. To determine if CheA3 was the associated kinase for CrdA, a yeast-two hybrid analysis was performed and indicated that there was a strong interaction between these two proteins(76). A mutation in *crdA* resulted in a strain that was developmentally delayed, in contrast to the phenotype observed with the Che3 mutatants. The CrdA response regulator was linked to the chemotaxis-like signal transduction pathway by the construction of a CrdA/Mcp3 double mutant, which yielded a CrdA mutant phenotype, opposite of an Mcp3 mutant phenotype. This supports the idea that the Che3 signal transduction pathway regulates CrdA, which regulates

developmental gene expression (76). This finding linked this chemotaxis system to the regulation of gene expression, which is like most two-component systems that regulate gene expression except for the presence of CheB and CheR; most two-component systems regulate gene expression based on environmental conditions. However, this finding is vastly different from other chemotaxis systems where the activity of CheY homologs is modulated, which typically regulates motility (76).

The *dif* (che2) operon contains homologs to a chemotaxis transducer, CheW, CheY, CheA, and CheC proteins. Mutations in this operon resulted in S-motility defects such as the lack of extracellular matrix production required for pilus retraction (85, 165). Under conditions of starvation, mutations in the *dif* operon result in cells that are defective in S-motility, demonstrated by their inability to aggregate and form spores (14, 165). Since, the *dif* operon is required for S-motility, and the che4 operon displays enhanced S-motility, a *che4* operon mutation in various *dif* operon mutant strain backgrounds produced phenotypes indistinguishable from the *dif* operon mutant strain alone, suggesting that the Che4 signal transduction system requires a functional Dif signal transduction system for proper signal transduction (153).

Chemotaxis-like pathways regulate functions other than chemotaxis: answers yet to be uncovered

There are many microorganisms that have chemotaxis-like systems controlling functions other than chemotaxis, and genomic data is quickly unveiling the presence of multiple systems of unknown function. An advantage to using a chemotaxis-like system to regulate other functions is the ability to temporally modulate cellular processes that are

energetically expensive and provide a checkpoint before committing the cell's resources to such courses. However, there are many unanswered questions regarding such systems. First, how are such processes regulated? Many systems have CheB and CheR homologs, suggesting that there may be methylation-dependent regulation. What is the target of their activity? In motility, the response regulator CheY binds to the flagellar motor resulting in a change of flagella rotation. In systems controlling functions other than motility, what is the target of CheY, and how does it regulate other cellular processes? The presence of multiple chemotaxis-like systems also means the presence of multiple chemotaxis homologs. How is cross-talk between these systems prevented or is this a common phenomenon? If cross-talk does occur, how is it regulated?

ENERGY TAXIS

Microorganisms have evolved to monitor their intracellular energy levels. This motile behavior is known as energy taxis (for reviews see references (5, 142)). Energy taxis couples the locomotor behavior of the cell to its metabolism (141). During normal metabolism and energy generation, the electrons are donated to the electron transport system (ETS) by an oxidizable substrate, and are passed through the respiratory chain, terminating at an electron acceptor, such as oxygen. The electrons are transferred by a series of oxidation-reduction reactions resulting in an accumulation of protons on the outside of the membrane and the generation of a proton motive force . Energy taxis transducers sense an increase or decrease in energy levels (PMF or redox) originating in the electron transport system. The chemotaxis signal transduction pathway similar to that used for sensing extracellular cues is used for energy taxis. Energy taxis has been

described in various microorganisms, and phylogenetic analysis of sequenced genomes suggests that there are many transducers that are potential energy sensors (5). There are two energy taxis transducers in *E. coli*, Aer and Tsr . The serine transducer, Tsr, is a ligand-binding chemotaxis transducer that also senses energy. The N-terminal sensing domain of Tsr does not contain any known motifs for co-factor binding, and the mechanism of energy sensing by Tsr is unknown. Other energy taxis transducers have been identified in other organisms such as *Pseudomonas putida* (101), *Campylobacter jejuni* (57, 58), *Desulfovibrio vulgaris* (41), and *Rhodosprillum centenum* (64). It is apparent that energy taxis is not an isolated phenomenon, and that energy taxis transducers are widespread throughout nature. However, the mechanisms regarding energy taxis are only beginning to be understood in the well-studied model, *E. coli*. Given the relative simplicity of the signal transduction pathway of *E. coli*, it is easy to imagine much more intricate and complex methods of energy sensing in other organisms.

AZOSPIRILLUM BRASILENSE

Azospirilla are free-living, nitrogen-fixing alpha-proteobacteria that live in association with the rhizosphere of various crops of agronomic importance, such as wheat, maize, and rice, promoting plant growth (105, 106). Azospirilla are small, curved rods approximately 2.0 to 3.0 μm in length and 1.0 μm in width and are motile in both liquid and semisolid surface by the use of a single polar flagellum or several lateral flagella (97-99).

Azospirillum spp. colonize the surface of root hairs in a mutually beneficial association (105). In addition to fixing atmospheric nitrogen, colonization of the

rhizosphere by Azospirilla results in morphological and physiological changes to the roots, resulting in increased water and mineral uptake from the environment (104). It is hypothesized that motility and chemotaxis are important for the colonization of plant roots, since chemotactic strains of *Azospirillum* have an advantage in root colonization over non-chemotactic strains (151, 152, 171). Azospirilla are chemotactic toward organic acids, sugars, amino acids, aromatic compounds, and root exudates (13, 56, 87, 115, 170).

Azospirillum have the ability to aggregate, which is a survival mechanism under stressful environmental conditions that can affect dispersal and survival in the soil (119). *A. brasilense* is currently used as a biofertilizer worldwide (105). The ability of cells to flocculate leads to potential biofertilizer applications such as increased survivability and adhesiveness (119).

Unlike *E. coli* where chemotaxis is predominantly metabolism-independent, metabolism-dependent chemotaxis, known as energy taxis, has been described as the dominant behavior in *A. brasilense* (1, 4). *A. brasilense* displays energy related responses such as aerotaxis, redox taxis, and taxis to alternative terminal electron acceptors. *A. brasilense* requires a functional electron transport system and the ability to metabolize a chemoeffector for normal chemotaxis (4). This is unlike *E. coli*, in which structural analogs of chemoeffectors trigger chemotaxis (1).

Recently, a chemotaxis operon was identified in *A. brasilense* by complementation of generally non-chemotactic mutants. This operon contains homologs to the central excitation and adaptation pathways in *E. coli* (55). Interestingly the CheA homolog has seven transmembrane regions, which have not been observed in any other bacterial species (G. Alexandre, I.B. Zhulin unpublished data). This chemotaxis operon

also contains CheB and CheR homologs, suggesting methylation-dependent behavior, contrary to previous reports (170). While the chemotaxis operons of *E. coli* and *A. brasilense* share many components, the mechanisms of excitation and signal termination may differ between these distantly-related species. Complementation of *E. coli* strains deficient for CheW or CheY with the corresponding *A. brasilense* homologs, in addition to the sequence analysis of the proteins, indicate that the input components of chemotaxis signal transduction systems are more conserved than the output components. The ability of CheW but not CheY to restore function in *E. coli* strains lacking these proteins suggests differences in signal termination and bacterial flagellar motors between *E. coli* and *A. brasilense* (6).

Several alpha-proteobacterial species contain multiple chemotaxis-like genes organized into multiple operons. In comparing gene order and composition of the operons, the operons can be organized into three groups (55). The chemotaxis operon of *A. brasilense* is most related to similar operons in *Caulobacter crescentus*, *Rhodospeudomonas palustris*, *Magnetospirillum magnetotacticum*, and *Rhodospirillum centenum*. However, there is not a correlation between the function of the operon and its grouping. For example, this gene cluster is the major chemotaxis operon in *R. centenum*, but is not the major operon for *C. crescentus* (55).

A better understanding of the mechanisms underlying chemosensory responses in beneficial soil bacteria such as *A. brasilense* will provide a foundation for the development of strains that can better colonize the rhizosphere of agronomically important crops. Since the dominant behavior of *A. brasilense* is energy taxis, an understanding of how this phenomenon contributes to rhizosphere colonization is

important. While energy taxis is the prevailing behavior in *A. brasilense*, there is evidence that this is not its only behavior. This dissertation describes an energy taxis transducer (Tlp1) that promotes plant root colonization as well as the presence of another chemotaxis transducer that does not appear to be an energy sensor (Chapter 2).

Previously, chemotaxis responses in *A. brasilense* were reported to be methylation-independent. However, the discovery of a methylesterase CheB and methyltransferase CheR homolog in a recently identified chemotaxis operon suggested otherwise. A study of the chemotaxis signal transduction pathway of *A. brasilense* revealed that some responses are methylation-dependent and others are methylation independent, and that the contributions of CheB and CheR to the chemotactic and aerotactic behavior of *A. brasilense* are complex. Interestingly, it was determined that while this chemotaxis operon contributes to motility, this is not its primary function (Chapter 3).

Therefore, the function of this operon was characterized. It is known that bacteria can regulate their cell size in response to environmental conditions, but the mechanisms of regulation have remained unknown. It was determined that this chemotaxis-like operon of *A. brasilense* regulates cell size in response to nutrient conditions independent of growth rate. Additionally, this operon has an impact on other cellular processes related to cell size such as EPS production. This is the first known mechanism of cell size regulation in a bacterium in response to environmental cues (Chapter 4).

Taken together, the chemosensory responses in *A. brasilense* are complex and an in-depth study of such the signal transduction pathways of this organism will lead to a

better understanding of the overall ecology of this microorganism as well as provide information for the generation of strains optimized for use as a biofertilizer.

REFERENCES

1. Adler, J. 1969. Chemoreceptors in bacteria. Science 166:1588-97.

2. Alam, M., M. Lebert, D. Oesterhelt, and G. L. Hazelbauer. 1989. Methyl-accepting taxis proteins in Halobacterium halobium. Embo J 8:631-9.

3. Alam, M., and D. Oesterhelt. 1984. Morphology, function and isolation of halobacterial flagella. J Mol Biol 176:459-75.

4. Alexandre, G., S. E. Greer, and I. B. Zhulin. 2000. Energy taxis is the dominant behavior in Azospirillum brasilense. J Bacteriol 182:6042-8.

5. Alexandre, G., S. E. Greer-Phillips, and I. B. Zhulin. 2004. Ecological role of energy taxis in microorganisms. FEMS Microbiol. Rev. 28:113-126.

6. Alexandre, G., and I. B. Zhulin. 2003. Different evolutionary constraints on chemotaxis proteins CheW and CheY revealed by heterologous expression studies and protein sequence analysis. J Bacteriol 185:544-52.

7. Alley, M. R., J. R. Maddock, and L. Shapiro. 1992. Polar localization of a bacterial chemoreceptor. Genes Dev 6:825-36.

8. Alm, R. A., L. S. Ling, D. T. Moir, B. L. King, E. D. Brown, P. C. Doig, D. R. Smith, B. Noonan, B. C. Guild, B. L. deJonge, G. Carmel, P. J. Tummino, A. Caruso, M. Uria-Nickelsen, D. M. Mills, C. Ives, R. Gibson, D. Merberg, S. D. Mills, Q. Jiang, D. E. Taylor, G. F. Vovis, and T. J. Trust. 1999. Genomic-sequence comparison of two unrelated isolates of the human gastric pathogen Helicobacter pylori. Nature 397:176-80.

9. Ames, P., C. A. Studdert, R. H. Reiser, and J. S. Parkinson. 2002. Collaborative signaling by mixed chemoreceptor teams in Escherichia coli. Proc Natl Acad Sci U S A 99:7060-5.

10. Armitage, J. P., and R. M. Macnab. 1987. Unidirectional, intermittent rotation of the flagellum of Rhodobacter sphaeroides. J Bacteriol 169:514-8.

11. Ashby, M. K. 2004. Survey of the number of two-component response regulator genes in the complete and annotated genome sequences of prokaryotes. FEMS Microbiol Lett 231:277-81.

12. Baracchini, O., and J. C. Sherris. 1959. The chemotactic effect of oxygen on bacteria. J Pathol Bacteriol 77:565-74.

13. Barak, R., I. Nur, and Y. Okon. 1983. Detection of chemotaxis in Azospirillum brasilense. Journal of Applied Bacteriology 162:399-403.

14. Bellenger, K., X. Ma, W. Shi, and Z. Yang. 2002. A CheW homologue is required for Myxococcus xanthus fruiting body development, social gliding motility, and fibril biogenesis. J Bacteriol 184:5654-60.

15. Berg, H. C., and D. A. Brown. 1972. Chemotaxis in Escherichia coli analysed by three-dimensional tracking. Nature 239:500-4.

16. Berleman, J. E., and C. E. Bauer. 2005. A che-like signal transduction cascade involved in controlling flagella biosynthesis in Rhodospirillum centenum. Mol Microbiol 55:1390-402.

17. Berleman, J. E., and C. E. Bauer. 2005. Involvement of a Che-like signal transduction cascade in regulating cyst cell development in Rhodospirillum centenum. Mol Microbiol 56:1457-66.

18. Berleman, J. E., B. M. Hasselbring, and C. E. Bauer. 2004. Hypercyst mutants in Rhodospirillum centenum identify regulatory loci involved in cyst cell differentiation. J Bacteriol 186:5834-41.

19. Bespalov, V. A., I. B. Zhulin, and B. L. Taylor. 1996. Behavioral responses of Escherichia coli to changes in redox potential. Proc Natl Acad Sci U S A 93:10084-9.

20. Bibikov, S. I., and V. P. Skulachev. 1989. Mechanisms of phototaxis and aerotaxis in Halobacterium halobium. FEBS Lett 243:303-306.

21. Bischoff, D. S., R. B. Bourret, M. L. Kirsch, and G. W. Ordal. 1993. Purification and characterization of Bacillus subtilis CheY. Biochemistry 32:9256-61.

22. Blackhart, B. D., and D. R. Zusman. 1985. "Frizzy" genes of Myxococcus xanthus are involved in control of frequency of reversal of gliding motility. Proc Natl Acad Sci U S A 82:8767-70.

23. Blakemore, R. 1975. Magnetotactic bacteria. Science 190:377-9.

24. Blakemore, R. P. 1982. Magnetotactic bacteria. Annu Rev Microbiol 36:217-38.

25. Blaser, M. J. 1992. Helicobacter pylori: its role in disease. Clin Infect Dis 15:386-91.

26. Block, S. M., J. E. Segall, and H. C. Berg. 1982. Impulse responses in bacterial chemotaxis. Cell 31:215-26.

27. Borkovich, K. A., L. A. Alex, and M. I. Simon. 1992. Attenuation of sensory receptor signaling by covalent modification. Proc Natl Acad Sci U S A 89:6756-60.

28. Borkovich, K. A., N. Kaplan, J. F. Hess, and M. I. Simon. 1989. Transmembrane signal transduction in bacterial chemotaxis involves ligand-dependent activation of phosphate group transfer. Proc Natl Acad Sci U S A 86:1208-12.

29. Bray, D., M. D. Levin, and C. J. Morton-Firth. 1998. Receptor clustering as a cellular mechanism to control sensitivity. Nature 393:85-8.

30. Burkart, M., A. Toguchi, and R. M. Harshey. 1998. The chemotaxis system, but not chemotaxis, is essential for swarming motility in Escherichia coli. Proc Natl Acad Sci U S A 95:2568-73.

31. Butler, S. L., and J. J. Falke. 1998. Cysteine and disulfide scanning reveals two amphiphilic helices in the linker region of the aspartate chemoreceptor. Biochemistry 37:10746-56.

32. Cerda, O., A. Rivas, and H. Toledo. 2003. Helicobacter pylori strain ATCC700392 encodes a methyl-accepting chemotaxis receptor protein (MCP) for arginine and sodium bicarbonate. FEMS Microbiol Lett 224:175-81.

33. Christian, J. H., and J. A. Waltho. 1962. Solute concentrations within cells of halophilic and non-halophilic bacteria. Biochim Biophys Acta 65:506-8.

34. Danielson, M. A., R. B. Bass, and J. J. Falke. 1997. Cysteine and disulfide scanning reveals a regulatory alpha-helix in the cytoplasmic domain of the aspartate receptor. J Biol Chem 272:32878-88.

35. Duke, T. A., and D. Bray. 1999. Heightened sensitivity of a lattice of membrane receptors. Proc Natl Acad Sci U S A 96:10104-8.

36. Engelmann, T. W. 1881. Bacterium photometricum: an article on the comparative physiology o fthe sense for light and colour. Arch. Ges. Physiol. Bonn. 30:95-124.

37. Falke, J. J., R. B. Bass, S. L. Butler, S. A. Chervitz, and M. A. Danielson. 1997. The two-component signaling pathway of bacterial chemotaxis: a molecular view of signal transduction by receptors, kinases, and adaptation enzymes. Annu Rev Cell Dev Biol 13:457-512.

38. Feng, X., A. A. Lilly, and G. L. Hazelbauer. 1999. Enhanced function conferred on low-abundance chemoreceptor Trg by a methyltransferase-docking site. J Bacteriol 181:3164-71.

39. Ford, B. J. 1991. The Leeuwenhoek Legacy. Biopress, Bristol/Farrand Press, London.

40. Foynes, S., N. Dorrell, S. J. Ward, R. A. Stabler, A. A. McColm, A. N. Rycroft, and B. W. Wren. 2000. Helicobacter pylori possesses two CheY response regulators and a histidine kinase sensor, CheA, which are essential for chemotaxis and colonization of the gastric mucosa. Infect Immun 68:2016-23.

41. Fu, R., J. D. Wall, and G. Voordouw. 1994. DcrA, a c-type heme-containing methyl-accepting protein from Desulfovibrio vulgaris Hildenborough, senses the oxygen concentration or redox potential of the environment. J Bacteriol 176:344-50.

42. Galibert, F., T. M. Finan, S. R. Long, A. Puhler, P. Abola, F. Ampe, F. Barloy-Hubler, M. J. Barnett, A. Becker, P. Boistard, G. Bothe, M. Boutry, L. Bowser, J. Buhrmester, E. Cadieu, D. Capela, P. Chain, A. Cowie, R. W. Davis, S. Dreano, N. A. Federspiel, R. F. Fisher, S. Gloux, T. Godrie, A. Goffeau, B. Golding, J. Gouzy, M. Gurjal, I. Hernandez-Lucas, A. Hong, L. Huizar, R. W. Hyman, T. Jones, D. Kahn, M. L. Kahn, S. Kalman, D. H. Keating, E. Kiss, C. Komp, V. Lelaure, D. Masuy, C. Palm, M. C. Peck, T. M. Pohl, D. Portetelle, B. Purnelle, U. Ramsperger, R. Surzycki, P. Thebault, M. Vandenbol, F. J. Vorholter, S. Weidner, D. H. Wells, K. Wong, K. C. Yeh, and J. Batut. 2001. The composite genome of the legume symbiont Sinorhizobium meliloti. Science 293:668-72.

43. Garcia, J. R., F. Jaumann, S. Schulz, A. Krause, J. Rodriguez-Jimenez, U. Forssmann, K. Adermann, E. Kluver, C. Vogelmeier, D. Becker, R. Hedrich, W. G. Forssmann, and R. Bals. 2001. Identification of a novel, multifunctional beta-defensin (human beta-defensin 3) with specific antimicrobial activity. Its interaction with plasma membranes of Xenopus oocytes and the induction of macrophage chemoattraction. Cell Tissue Res 306:257-64.

44. Gardina, P. J., and M. D. Manson. 1996. Attractant signaling by an aspartate chemoreceptor dimer with a single cytoplasmic domain. Science 274:425-6.

45. Garrity, L. F., and G. W. Ordal. 1997. Activation of the CheA kinase by asparagine in Bacillus subtilis chemotaxis. Microbiology 143:2945-51.

46. Garrity, L. F., S. L. Schiel, R. Merrill, J. Reizer, M. H. Saier, Jr., and G. W. Ordal. 1998. Unique regulation of carbohydrate chemotaxis in Bacillus subtilis by the phosphoenolpyruvate-dependent phosphotransferase system and the methyl-accepting chemotaxis protein McpC. J Bacteriol 180:4475-80.

47. Gestwicki, J. E., A. C. Lamanna, R. M. Harshey, L. L. McCarter, L. L. Kiessling, and J. Adler. 2000. Evolutionary conservation of methyl-accepting chemotaxis protein location in Bacteria and Archaea. J Bacteriol 182:6499-502.

48. Greck, M., J. Platzer, V. Sourjik, and R. Schmitt. 1995. Analysis of a chemotaxis operon in Rhizobium meliloti. Mol Microbiol 15:989-1000.

49. Grishanin, R. N., I. I. Chalmina, and I. B. Zhulin. 1991. Behavior of Azospirillum brasilense in a spatial gradient of oxygen and in a 'redox' gradient of an artificial electron acceptor. Journal of General Microbiology 137:2781-2785.

50. Hamblin, P. A., B. A. Maguire, R. N. Grishanin, and J. P. Armitage. 1997. Evidence for two chemosensory pathways in Rhodobacter sphaeroides. Mol Microbiol 26:1083-96.

51. Hanlon, D. W., and G. W. Ordal. 1994. Cloning and characterization of genes encoding methyl-accepting chemotaxis proteins in Bacillus subtilis. J Biol Chem 269:14038-46.

52. Hanlon, D. W., M. M. Rosario, G. W. Ordal, G. Venema, and D. Van Sinderen. 1994. Identification of TlpC, a novel 62 kDa MCP-like protein from Bacillus subtilis. Microbiology 140 (Pt 8):1847-54.

53. Harrison, D. M., J. Skidmore, J. P. Armitage, and J. R. Maddock. 1999. Localization and environmental regulation of MCP-like proteins in Rhodobacter sphaeroides. Mol Microbiol 31:885-92.

54. Harshey, R. M., and T. Matsuyama. 1994. Dimorphic transition in Escherichia coli and Salmonella typhimurium: surface-induced differentiation into hyperflagellate swarmer cells. Proc Natl Acad Sci U S A 91:8631-5.

55. Hauwaerts, D., G. Alexandre, S. K. Das, J. Vanderleyden, and I. B. Zhulin. 2002. A major chemotaxis gene cluster in Azospirillum brasilense and relationships between chemotaxis operons in alpha-proteobacteria. FEMS Microbiol Lett 208:61-7.

56. Heinrich, D., and D. Hess. 1985. Chemotactic attraction of Azospirillum lipoferum by wheat roots and characterization of some attractants. Canadian Journal of Microbiology 31:26-31.

57. Hendrixson, D. R., B. J. Akerley, and V. J. DiRita. 2001. Transposon mutagenesis of Campylobacter jejuni identifies a bipartite energy taxis system required for motility. Mol Microbiol 40:214-24.

58. Hendrixson, D. R., and V. J. DiRita. 2004. Identification of Campylobacter jejuni genes involved in commensal colonization of the chick gastrointestinal tract. Mol Microbiol 52:471-84.

59. Hildebrand, E., and A. Schimz. 1986. Integration of photosensory signals in Halobacterium halobium. J Bacteriol 167:305-11.

60. Hodgkin, J., and D. Kaiser. 1979. Genetics of gliding motility in Myxococcus xanthus (Myxobacterales): genes controlling movement of single cells. molecular and general genetics 171:167-176.

61. Hodgkin, J., and D. Kaiser. 1979. Genetics of gliding motility in Myxococcus xanthus (Myxobacterales): two gene systems control movement. molecular and general genetics 171:177-191.

62. Hou, S., R. W. Larsen, D. Boudko, C. W. Riley, E. Karatan, M. Zimmer, G. W. Ordal, and M. Alam. 2000. Myoglobin-like aerotaxis transducers in Archaea and Bacteria. Nature 403:540-4.

63. Jiang, Z. Y., and C. E. Bauer. 1997. Analysis of a chemotaxis operon from Rhodospirillum centenum. J Bacteriol 179:5712-9.

64. Jiang, Z. Y., and C. E. Bauer. 2001. Component of the Rhodospirillum centenum photosensory apparatus with structural and functional similarity to methyl-accepting chemotaxis protein chemoreceptors. J Bacteriol 183:171-7.

65. Jiang, Z. Y., H. Gest, and C. E. Bauer. 1997. Chemosensory and photosensory perception in purple photosynthetic bacteria utilize common signal transduction components. J Bacteriol 179:5720-7.

66. Jimenez-Pearson, M. A., I. Delany, V. Scarlato, and D. Beier. 2005. Phosphate flow in the chemotactic response system of Helicobacter pylori. Microbiology 151:3299-311.

67. Kaiser, D., and C. Crosby. 1983. Cell movement and its coordination in swarms of Myxococcus xanthus. Cell Motility Cytoskeleton 3:227-245.

68. Karatan, E., M. M. Saulmon, M. W. Bunn, and G. W. Ordal. 2001. Phosphorylation of the response regulator CheV is required for adaptation to attractants during Bacillus subtilis chemotaxis. J Biol Chem 276:43618-26.

69. Kehry, M. R., M. W. Bond, M. W. Hunkapiller, and F. W. Dahlquist. 1983. Enzymatic deamidation of methyl-accepting chemotaxis proteins in Escherichia coli catalyzed by the cheB gene product. Proc Natl Acad Sci U S A 80:3599-603.

70. Kehry, M. R., T. G. Doak, and F. W. Dahlquist. 1984. Stimulus-induced changes in methylesterase activity during chemotaxis in Escherichia coli. J Biol Chem 259:11828-35.

71. Keymer, J. E., R. G. Endres, M. Skoge, Y. Meir, and N. S. Wingreen. 2006. Chemosensing in Escherichia coli: two regimes of two-state receptors. Proc Natl Acad Sci U S A 103:1786-91.

72. Kim, S. K., D. Kaiser, and A. Kuspa. 1992. Control of cell density and pattern by intercellular signaling in Myxococcus development. Annu Rev Microbiol 46:117-39.

73. Kirby, J. R., C. J. Kristich, S. L. Feinberg, and G. W. Ordal. 1997. Methanol production during chemotaxis to amino acids in Bacillus subtilis. Mol Microbiol 24:869-78.

74. Kirby, J. R., T. B. Niewold, S. Maloy, and G. W. Ordal. 2000. CheB is required for behavioural responses to negative stimuli during chemotaxis in Bacillus subtilis. Mol Microbiol 35:44-57.

75. Kirby, J. R., M. M. Saulmon, C. J. Kristich, and G. W. Ordal. 1999. CheY-dependent methylation of the asparagine receptor, McpB, during chemotaxis in Bacillus subtilis. J Biol Chem 274:11092-100.

76. Kirby, J. R., and D. R. Zusman. 2003. Chemosensory regulation of developmental gene expression in Myxococcus xanthus. Proc Natl Acad Sci U S A 100:2008-13.

77. Kondoh, H., C. B. Ball, and J. Adler. 1979. Identification of a methyl-accepting chemotaxis protein for the ribose and galactose chemoreceptors of Escherichia coli. Proc Natl Acad Sci U S A 76:260-4.

78. Kort, E. N., M. F. Goy, S. H. Larsen, and J. Adler. 1975. Methylation of a membrane protein involved in bacterial chemotaxis. Proc Natl Acad Sci U S A 72:3939-43.

79. Krikos, A., M. P. Conley, A. Boyd, H. C. Berg, and M. I. Simon. 1985. Chimeric chemosensory transducers of Escherichia coli. Proc Natl Acad Sci U S A 82:1326-30.

80. Kristich, C. J., and G. W. Ordal. 2002. Bacillus subtilis CheD is a chemoreceptor modification enzyme required for chemotaxis. J Biol Chem 277:25356-62.

81. Larsen, S. H., R. W. Reader, E. N. Kort, W. W. Tso, and J. Adler. 1974. Change in direction of flagellar rotation is the basis of the chemotactic response in Escherichia coli. Nature 249:74-7.

82. Le Moual, H., and D. E. Koshland, Jr. 1996. Molecular evolution of the C-terminal cytoplasmic domain of a superfamily of bacterial receptors involved in taxis. J Mol Biol 261:568-85.

83. Li, C., A. J. Boileau, C. Kung, and J. Adler. 1988. Osmotaxis in Escherichia coli. Proc Natl Acad Sci U S A 85:9451-5.

84. Li, M., and G. L. Hazelbauer. 2004. Cellular stoichiometry of the components of the chemotaxis signaling complex. J Bacteriol 186:3687-94.

85. Li, Y., H. Sun, X. Ma, A. Lu, R. Lux, D. Zusman, and W. Shi. 2003. Extracellular polysaccharides mediate pilus retraction during social motility of Myxococcus xanthus. Proc Natl Acad Sci U S A 100:5443-8.

86. Lindbeck, J. C., E. A. Goulbourne, Jr., M. S. Johnson, and B. L. Taylor. 1995. Aerotaxis in Halobacterium salinarium is methylation-dependent. Microbiology 141 (Pt 11):2945-53.

87. Lopez-de-Victoria, G., and C. R. Lovell. 1993. Chemotaxis of Azospirillum Species to Aromatic Compounds. Appl Environ Microbiol 59:2951-2955.

88. Mackenzie, C., M. Choudhary, F. W. Larimer, P. F. Predki, S. Stilwagen, J. P. Armitage, R. D. Barber, T. J. Donohue, J. P. Hosler, J. E. Newman, J. P. Shapleigh, R. E. Sockett, J. Zeilstra-Ryalls, and S. Kaplan. 2001. The home stretch, a first analysis of the nearly completed genome of Rhodobacter sphaeroides 2.4.1. Photosynth Res 70:19-41.

89. Maddock, J. R., and L. Shapiro. 1993. Polar location of the chemoreceptor complex in the Escherichia coli cell. Science 259:1717-23.

90. Maki, N., J. E. Gestwicki, E. M. Lake, L. L. Kiessling, and J. Adler. 2000. Motility and chemotaxis of filamentous cells of Escherichia coli. J Bacteriol 182:4337-42.

91. Manson, M. D., V. Blank, G. Brade, and C. F. Higgins. 1986. Peptide chemotaxis in E. coli involves the Tap signal transducer and the dipeptide permease. Nature 321:253-6.

92. Manten, A. 1948. Phototaxis in the purple bacterium Rhodospirillum rubrum and the relationship between phototaxis and photosynthesis. Antonie van Leeuwenhoek 14:65-86.

93. Martin, A. C., G. H. Wadhams, and J. P. Armitage. 2001. The roles of the multiple CheW and CheA homologues in chemotaxis and in chemoreceptor localization in Rhodobacter sphaeroides. Mol Microbiol 40:1261-72.

94. Martin, A. C., G. H. Wadhams, D. S. Shah, S. L. Porter, J. C. Mantotta, T. J. Craig, P. H. Verdult, H. Jones, and J. P. Armitage. 2001. CheR- and CheB-dependent chemosensory adaptation system of Rhodobacter sphaeroides. J Bacteriol 183:7135-44.

95. McEvoy, M. M., A. Bren, M. Eisenbach, and F. W. Dahlquist. 1999. Identification of the binding interfaces on CheY for two of its targets, the phosphatase CheZ and the flagellar switch protein fliM. J Mol Biol 289:1423-33.

96. McGee, D. J., M. L. Langford, E. L. Watson, J. E. Carter, Y. T. Chen, and K. M. Ottemann. 2005. Colonization and inflammation deficiencies in Mongolian gerbils infected by Helicobacter pylori chemotaxis mutants. Infect Immun 73:1820-7.

97. Moens, S., K. Michiels, V. Keijers, F. Van Leuven, and J. Vanderleyden. 1995. Cloning, sequencing, and phenotypic analysis of laf1, encoding the flagellin of the lateral flagella of Azospirillum brasilense Sp7. J Bacteriol 177:5419-26.

98. Moens, S., K. Michiels, and J. Vanderleyden. 1995. Glycosylation of the flagellin of the polar flagellum of Azospirillum brasilense, a Gram-negative nitrogen-fixing bacterium. Microbiology 141:2651-2657.

99. Moens, S., M. Schloter, and J. Vanderleyden. 1996. Expression of the structural gene, laf1, encoding the flagellin of the lateral flagella in Azospirillum brasilense Sp7. J Bacteriol 178:5017-9.

100. Ng, W. V., S. P. Kennedy, G. G. Mahairas, B. Berquist, M. Pan, H. D. Shukla, S. R. Lasky, N. S. Baliga, V. Thorsson, J. Sbrogna, S. Swartzell, D. Weir, J. Hall, T. A. Dahl, R. Welti, Y. A. Goo, B. Leithauser, K. Keller, R. Cruz, M. J. Danson, D. W. Hough, D. G. Maddocks, P. E. Jablonski, M. P. Krebs, C. M. Angevine, H. Dale, T. A. Isenbarger, R. F. Peck, M. Pohlschroder, J. L. Spudich, K. W. Jung, M. Alam, T. Freitas, S. Hou, C. J. Daniels, P. P. Dennis, A. D. Omer, H. Ebhardt, T. M. Lowe, P. Liang, M. Riley, L. Hood, and S. DasSarma. 2000. Genome sequence of Halobacterium species NRC-1. Proc Natl Acad Sci U S A 97:12176-81.

101. Nichols, N. N., and C. S. Harwood. 2000. An aerotaxis transducer gene from Pseudomonas putida. FEMS Microbiol Lett 182:177-83.

102. Niwano, M., and B. L. Taylor. 1982. Novel sensory adaptation mechanism in bacterial chemotaxis to oxygen and phosphotransferase substrates. Proc Natl Acad Sci U S A 79:11-5.

103. Nordmann, B., M. R. Lebert, M. Alam, S. Nitz, H. Kollmannsberger, D. Oesterhelt, and G. L. Hazelbauer. 1994. Identification of volatile forms of methyl groups released by Halobacterium salinarium. J Biol Chem 269:16449-54.

104. Okon, Y., and Y. Kapulnik. 1986. Development and function of Azospirillum-inoculated roots. Plant Soil 90:3-16.

105. Okon, Y., and C. A. Labandera-Gonzalez. 1994. Agronomic applications of Azospirillum: an evaluation of 20 years worldwide field inoculation. Soil Biol. Biochem. 26:1591-1601.

106. Okon, Y., and J. Vanderleyden. 1997. Root-associated Azosprillum species can stimulate plants. ASM News 63:366-370.

107. Oosawa, K., and M. Simon. 1986. Analysis of mutations in the transmembrane region of the aspartate chemoreceptor in Escherichia coli. Proc Natl Acad Sci U S A 83:6930-4.

108. Ottemann, K. M., and A. C. Lowenthal. 2002. Helicobacter pylori uses motility for initial colonization and to attain robust infection. Infect Immun 70:1984-90.

109. Parkinson, J. S. 1976. cheA, cheB, and cheC genes of Escherichia coli and their role in chemotaxis. J Bacteriol 126:758-70.

110. Parkinson, J. S. 1978. Complementation analysis and deletion mapping of Escherichia coli mutants defective in chemotaxis. J Bacteriol 135:45-53.

111. Perazzona, B., and J. L. Spudich. 1999. Identification of methylation sites and effects of phototaxis stimuli on transducer methylation in Halobacterium salinarum. J Bacteriol 181:5676-83.

112. Peterson, W. L. 1991. Helicobacter pylori and peptic ulcer disease. N Engl J Med 324:1043-8.

113. Pittman, M. S., M. Goodwin, and D. J. Kelly. 2001. Chemotaxis in the human gastric pathogen Helicobacter pylori: different roles for CheW and the three CheV paralogues, and evidence for CheV2 phosphorylation. Microbiology 147:2493-504.

114. Porter, S. L., A. V. Warren, A. C. Martin, and J. P. Armitage. 2002. The third chemotaxis locus of Rhodobacter sphaeroides is essential for chemotaxis. Mol Microbiol 46:1081-94.

115. Reinhold, B., T. Hurek, and I. Fendrik. 1985. Strain-specific chemotaxis of Azospirillum spp. J Bacteriol 162:190-5.

116. Rudolph, J., and D. Oesterhelt. 1995. Chemotaxis and phototaxis require a CheA histidine kinase in the archaeon Halobacterium salinarium. Embo J 14:667-73.

117. Rudolph, J., and D. Oesterhelt. 1996. Deletion analysis of the che operon in the archaeon Halobacterium salinarium. J Mol Biol 258:548-54.

118. Rudolph, J., N. Tolliday, C. Schmitt, S. C. Schuster, and D. Oesterhelt. 1995. Phosphorylation in halobacterial signal transduction. Embo J 14:4249-57.

119. Sadasivan, L., and C. A. Neyra. 1985. Flocculation in Azospirillum brasilense and Azospirillum lipoferum: exopolysaccharides and cyst formation. J Bacteriol 163:716-23.

120. Segall, J. E., S. M. Block, and H. C. Berg. 1986. Temporal comparisons in bacterial chemotaxis. Proc Natl Acad Sci U S A 83:8987-91.

121. Shah, D. S., S. L. Porter, D. C. Harris, G. H. Wadhams, P. A. Hamblin, and J. P. Armitage. 2000. Identification of a fourth cheY gene in Rhodobacter sphaeroides and interspecies interaction within the bacterial chemotaxis signal transduction pathway. Mol Microbiol 35:101-12.

122. Shapiro, M. J., I. Chakrabarti, and D. E. Koshland, Jr. 1995. Contributions made by individual methylation sites of the Escherichia coli aspartate receptor to chemotactic behavior. Proc Natl Acad Sci U S A 92:1053-6.

123. Sherris, D., and J. S. Parkinson. 1981. Posttranslational processing of methyl-accepting chemotaxis proteins in Escherichia coli. Proc Natl Acad Sci U S A 78:6051-5.

124. Shi, W., M. J. Lentz, and J. Adler. 1993. Behavioral responses of Escherichia coli to changes in temperature caused by electric shock. J Bacteriol 175:5785-90.

125. Shimizu, T. S., N. Le Novere, M. D. Levin, A. J. Beavil, B. J. Sutton, and D. Bray. 2000. Molecular model of a lattice of signalling proteins involved in bacterial chemotaxis. Nat Cell Biol 2:792-6.

126. Silverman, M., and M. Simon. 1976. Operon controlling motility and chemotoxis in E. coli. Nature 264:577-80.

127. Sourjik, V. 2004. Receptor clustering and signal processing in E. coli chemotaxis. Trends Microbiol 12:569-76.

128. Sourjik, V., and H. C. Berg. 2004. Functional interactions between receptors in bacterial chemotaxis. Nature 428:437-41.

129. Sourjik, V., and H. C. Berg. 2000. Localization of components of the chemotaxis machinery of Escherichia coli using fluorescent protein fusions. Mol Microbiol 37:740-51.

130. Sourjik, V., and R. Schmitt. 1998. Phosphotransfer between CheA, CheY1, and CheY2 in the chemotaxis signal transduction chain of Rhizobium meliloti. Biochemistry 37:2327-35.

131. Sourjik, V., W. Sterr, J. Platzer, I. Bos, M. Haslbeck, and R. Schmitt. 1998. Mapping of 41 chemotaxis, flagellar and motility genes to a single region of the Sinorhizobium meliloti chromosome. Gene 223:283-90.

132. Springer, M. S., M. F. Goy, and J. Adler. 1979. Protein methylation in behavioural control mechanisms and in signal transduction. Nature 280:279-84.

133. Springer, M. S., M. F. Goy, and J. Adler. 1977. Sensory transduction in Escherichia coli: two complementary pathways of information processing that involve methylated proteins. Proc Natl Acad Sci U S A 74:3312-6.

134. Springer, W. R., and D. E. Koshland, Jr. 1977. Identification of a protein methyltransferase as the cheR gene product in the bacterial sensing system. Proc Natl Acad Sci U S A 74:533-7.

135. Spudich, E. N., T. Takahashi, and J. L. Spudich. 1989. Sensory rhodopsins I and II modulate a methylation/demethylation system in Halobacterium halobium phototaxis. Proc Natl Acad Sci U S A 86:7746-50.

136. Stoeckenius, W., E. K. Wolff, and B. Hess. 1988. A rapid population method for action spectra applied to Halobacterium halobium. J Bacteriol 170:2790-5.

137. Sun, H., D. R. Zusman, and W. Shi. 2000. Type IV pilus of Myxococcus xanthus is a motility apparatus controlled by the frz chemosensory system. Curr Biol 10:1143-6.

138. Surette, M. G., and J. B. Stock. 1996. Role of alpha-helical coiled-coil interactions in receptor dimerization, signaling, and adaptation during bacterial chemotaxis. J Biol Chem 271:17966-73.

139. Szurmant, H., T. J. Muff, and G. W. Ordal. 2004. Bacillus subtilis CheC and FliY are members of a novel class of CheY-P-hydrolyzing proteins in the chemotactic signal transduction cascade. J Biol Chem 279:21787-92.

140. Tatsuno, I., M. Homma, K. Oosawa, and I. Kawagishi. 1996. Signaling by the Escherichia coli aspartate chemoreceptor Tar with a single cytoplasmic domain per dimer. Science 274:423-5.

141. Taylor, B. L., and I. B. Zhulin. 1998. In search of higher energy: metabolism-dependent behaviour in bacteria. Mol Microbiol 28:683-90.

142. Taylor, B. L., I. B. Zhulin, and M. S. Johnson. 1999. Aerotaxis and other energy-sensing behavior in bacteria. Annu Rev Microbiol 53:103-28.

143. Terry, K., S. M. Williams, L. Connolly, and K. M. Ottemann. 2005. Chemotaxis plays multiple roles during Helicobacter pylori animal infection. Infect Immun 73:803-11.

144. Terwilliger, T. C., E. Bogonez, E. A. Wang, and D. E. Koshland, Jr. 1983. Sites of methyl esterification on the aspartate receptor involved in bacterial chemotaxis. J Biol Chem 258:9608-11.

145. Terwilliger, T. C., and D. E. Koshland, Jr. 1984. Sites of methyl esterification and deamination on the aspartate receptor involved in chemotaxis. J Biol Chem 259:7719-25.

146. Terwilliger, T. C., J. Y. Wang, and D. E. Koshland, Jr. 1986. Kinetics of receptor modification. The multiply methylated aspartate receptors involved in bacterial chemotaxis. J Biol Chem 261:10814-20.

147. Thoelke, M. S., J. R. Kirby, and G. W. Ordal. 1989. Novel methyl transfer during chemotaxis in Bacillus subtilis. Biochemistry 28:5585-9.

148. Toker, A. S., and R. M. Macnab. 1997. Distinct regions of bacterial flagellar switch protein FliM interact with FliG, FliN and CheY. J Mol Biol 273:623-34.

149. Tomb, J. F., O. White, A. R. Kerlavage, R. A. Clayton, G. G. Sutton, R. D. Fleischmann, K. A. Ketchum, H. P. Klenk, S. Gill, B. A. Dougherty, K. Nelson, J. Quackenbush, L. Zhou, E. F. Kirkness, S. Peterson, B. Loftus, D. Richardson, R. Dodson, H. G. Khalak, A. Glodek, K. McKenney, L. M. Fitzegerald, N. Lee, M. D. Adams, E. K. Hickey, D. E. Berg, J. D. Gocayne, T. R. Utterback, J. D. Peterson, J. M. Kelley, M. D. Cotton, J. M. Weidman, C. Fujii, C. Bowman, L. Watthey, E. Wallin, W. S. Hayes, M. Borodovsky, P. D. Karp, H. O. Smith, C. M. Fraser, and J. C. Venter. 1997. The complete genome sequence of the gastric pathogen Helicobacter pylori. Nature 388:539-47.

150. Turner, L., W. S. Ryu, and H. C. Berg. 2000. Real-time imaging of fluorescent flagellar filaments. J Bacteriol 182:2793-801.

151. Vande Broek, A., M. Lambrecht, and J. Vanderleyden. 1998. Bacterial chemotactic motility is important for the initiation of wheat root colonization by Azospirillum brasilense. Microbiology 144 (Pt 9):2599-606.

152. Vande Broek, A., M. Lambrecht, and J. Vanderleyden. 1995. The role of bacterial motility, chemotaxis, and attachment in bacteria-plant interactions. Mol. Plant-Microbe Interactions 8:800-810.

153. Vlamakis, H. C., J. R. Kirby, and D. R. Zusman. 2004. The Che4 pathway of Myxococcus xanthus regulates type IV pilus-mediated motility. Mol Microbiol 52:1799-811.

154. Wadhams, G. H., and J. P. Armitage. 2004. Making sense of it all: bacterial chemotaxis. Nat Rev Mol Cell Biol 5:1024-37.

155. Wadhams, G. H., A. V. Warren, A. C. Martin, and J. P. Armitage. 2003. Targeting of two signal transduction pathways to different regions of the bacterial cell. Mol Microbiol 50:763-70.

156. Wang, Q., A. Suzuki, S. Mariconda, S. Porwollik, and R. M. Harshey. 2005. Sensing wetness: a new role for the bacterial flagellum. Embo J 24:2034-42.

157. Ward, M. J., D. M. Harrison, M. J. Ebner, and J. P. Armitage. 1995. Identification of a methyl-accepting chemotaxis protein in Rhodobacter sphaeroides. Mol Microbiol 18:115-21.

158. Ward, M. J., and D. R. Zusman. 1999. Motility in Myxococcus xanthus and its role in developmental aggregation. Curr Opin Microbiol 2:624-9.

159. Ward, M. J., and D. R. Zusman. 1997. Regulation of directed motility in Myxococcus xanthus. Mol Microbiol 24:885-93.

160. Welch, M., K. Oosawa, S. Aizawa, and M. Eisenbach. 1993. Phosphorylation-dependent binding of a signal molecule to the flagellar switch of bacteria. Proc Natl Acad Sci U S A 90:8787-91.

161. Wong, L. S., M. S. Johnson, I. B. Zhulin, and B. L. Taylor. 1995. Role of methylation in aerotaxis in Bacillus subtilis. J Bacteriol 177:3985-91.

162. Worku, M. L., Q. N. Karim, J. Spencer, and R. L. Sidebotham. 2004. Chemotactic response of Helicobacter pylori to human plasma and bile. J Med Microbiol 53:807-11.

163. Wu, J., J. Li, G. Li, D. G. Long, and R. M. Weis. 1996. The receptor binding site for the methyltransferase of bacterial chemotaxis is distinct from the sites of methylation. Biochemistry 35:4984-93.

164. Yamamoto, K., R. M. Macnab, and Y. Imae. 1990. Repellent response functions of the Trg and Tap chemoreceptors of Escherichia coli. J Bacteriol 172:383-8.

165. Yang, Z., Y. Geng, D. Xu, H. B. Kaplan, and W. Shi. 1998. A new set of chemotaxis homologues is essential for Myxococcus xanthus social motility. Mol Microbiol 30:1123-30.

166. Yao, B., Y. Wang, K. Hu, D. Chen, Y. Zheng, and M. Lei. 2002. Mechanisms of pulse response and differential response of bacteriorhodopsin and their relations. Photochem Photobiol 76:545-8.

167. Yoshiyama, H., H. Nakamura, M. Kimoto, K. Okita, and T. Nakazawa. 1999. Chemotaxis and motility of Helicobacter pylori in a viscous environment. J Gastroenterol 34 Suppl 11:18-23.

168. Zhang, W., A. Brooun, M. M. Mueller, and M. Alam. 1996. The primary structures of the Archaeon Halobacterium salinarium blue light receptor sensory rhodopsin II and its transducer, a methyl-accepting protein. Proc Natl Acad Sci U S A 93:8230-5.

169. Zhulin, I. B. 2001. The superfamily of chemotaxis transducers: from physiology to genomics and back. Adv Microb Physiol 45:157-98.

170. Zhulin, I. B., and J. P. Armitage. 1993. Motility, chemokinesis, and methylation-independent chemotaxis in Azospirillum brasilense. J Bacteriol 175:952-8.

171. Zhulin, I. B., V. A. Bespalov, M. S. Johnson, and B. L. Taylor. 1996. Oxygen taxis and proton motive force in Azospirillum brasilense. J Bacteriol 178:5199-204.

172. Zimmer, M. A., H. Szurmant, M. M. Saulmon, M. A. Collins, J. S. Bant, and G. W. Ordal. 2002. The role of heterologous receptors in McpB-mediated signalling in Bacillus subtilis chemotaxis. Mol Microbiol 45:555-68.

173. Zimmer, M. A., J. Tiu, M. A. Collins, and G. W. Ordal. 2000. Selective methylation changes on the Bacillus subtilis chemotaxis receptor McpB promote adaptation. J Biol Chem 275:24264-72.

CHAPTER TWO: CHEMOTAXIS TRANSDUCERS IN *AZOSPIRILLUM BRASILENSE*

PART A: A published manuscript

An Energy Taxis Transducer Promotes Root Colonization by *Azospirillum brasilense*

Suzanne E. Greer-Phillips,[1] Bonnie B. Stephens,[2] and Gladys Alexandre[3]

Greer-Phillips, S.E., B.B. Stephens, and G. Alexandre. 2004. An Energy Taxis Transducer Promotes Root Colonization by *Azospirillum brasilense.* J. Bacteriol. 186: 6595-6604.

1. Graduate student who identified Tlp1, performed respiration assays, bioinformatics analysis, and contributed to the writing of the manuscript

2. Graduate student who performed behavioral assays (swarm plates, anaerobic swarm plates, aerotaxis, and miniplug), and contributed to the writing of the manuscript

3. Professor and mentor who provided laboratory space and equipment and supervised the project, and performed plant-root colonization assays, and contributed to the writing of the manuscript

An Energy Taxis Transducer Promotes Root Colonization by *Azospirillum brasilense*

RUNNING TITLE: Energy taxis transducer in *A. brasilense*

Suzanne E. Greer-Phillips,[1,†] Bonnie B. Stephens,[2] and Gladys Alexandre[1,2*]

Department of Microbiology and Molecular Genetics, School of Medicine, Loma Linda University, Loma Linda, California,[1] Department of Biology, Georgia State University, Atlanta, Georgia[2]

*Corresponding author

Phone: 404-651-2786

Fax: 404-651-2509

E-mail: biogaa@langate.gsu.edu

[†]Present address: Department of Plant Pathology, University of California at Riverside, Riverside, CA 92521

ABSTRACT

Motility responses triggered by changes in the electron transport system are collectively known as energy taxis. In *Azospirillum brasilense*, energy taxis was shown to be the principal form of locomotor control. In the present study, we have identified a novel chemoreceptor-like protein, named Tlp1, which serves as an energy taxis transducer. The Tlp1 protein is predicted to have an N-terminal periplasmic region and a cytoplasmic C-terminal signaling module homologous to those of other chemoreceptors. The predicted periplasmic region of Tlp1 comprises a conserved domain that is found in two types of microbial sensory receptors: chemotaxis transducers and histidine kinases. However, the function of this domain is currently unknown. We characterized the behavior of a *tlp1* mutant by a series of spatial and temporal gradient assays. The *tlp1* mutant is deficient in (i) chemotaxis to several rapidly oxidizable substrates, (ii) taxis to terminal electron acceptors (oxygen and nitrate), and (iii) redox taxis. Taken together, the data strongly suggest that Tlp1 mediates energy taxis in *A. brasilense*. Using qualitative and quantitative assays, we have also demonstrated that the *tlp1* mutant is impaired in colonization of plant roots. This finding supports the hypothesis that energy taxis and therefore bacterial metabolism might be key factors in determining host specificity in *Azospirillum*-grass associations.

INTRODUCTION

Azospirillum brasilense, a free-living diazotroph that belongs to the alpha-subdivision of proteobacteria, associates with the roots of many agriculturally important crops, including wheat, corn, and rice. Azospirilla colonize the root surface and may

significantly promote plant growth and crop yield, properties that make them attractive candidates for the development of biological fertilizers for these crops (26-28). The ability of *Azospirillum* to attain significant populations on the root surfaces of the host is essential for its beneficial effect on plant growth and requires that the bacteria come in close contact with the roots (9, 27, 28, 35). The abilities of sensing chemicals released by the host plant and navigating toward the root system are likely to be important for the establishment of bacteria, including *Azospirillum* (9, 10, 42), in the rhizosphere. Experimental evidence supporting this hypothesis was obtained by demonstrating that nonchemotactic and nonmotile mutants of *A. brasilense* are severely impaired in surface colonization of wheat roots (41). Although there is no strict host specificity in *Azospirillum*-plant associations, a strain-specific chemotaxis was reported: strains isolated from the rhizosphere of a particular grass demonstrated preferential chemotaxis toward chemicals found in root exudates of that grass (31). These results suggested that chemotaxis may contribute to host-plant specificity and could largely be determined by metabolism (31).

Most motility responses in *A. brasilense* are a particular form of metabolism-dependent taxis called energy taxis (1). In energy taxis, a flow of reducing equivalents through an electron transport system is required for a behavioral response. Thus, energy taxis typically encompasses various (but not all) types of aerotaxis, taxis to alternative electron acceptors, phototaxis, redox taxis, and chemotaxis to oxidizable substrates (donors of reducing equivalents) (4, 38, 39).

Aerotaxis is the strongest behavioral response in *A. brasilense*. It guides the bacteria to an oxygen concentration optimal for energy generation and nitrogen fixation

(8, 52). It has also recently been shown that a functional electron transport system is required not only for aerotaxis and taxis to alternative electron acceptors, as expected, but also for chemotaxis, suggesting that *A. brasilense* is attracted to most chemicals via energy taxis (1). In addition, redox molecules that interact directly with the electron transport system and inhibit the flow of reducing equivalents through the respiratory chain are repellents for *A. brasilense*. Therefore, the signal for major behavioral responses in *A. brasilense* originates within the electron transport system (1). In energy taxis, any changes in electron transport trigger a behavioral response: changes leading to a step-up in intracellular energy level produce an attractant signal, whereas a step-down in energy level causes a repellent signal (4, 38, 39). Because energy taxis couples energy metabolism and motility, this behavior may be significant in the ecology of *Azospirillum* spp. and other species that are not dependent on specific plant signals to form associations with host plants (2).

Motility responses in bacteria depend on the cellular signal transduction machinery that transmits information from the environment to the motility apparatus. The molecular mechanism governing bacterial chemotaxis is best understood in *Escherichia coli* (15, 36). Changes in concentration of various effectors are detected by specialized transmembrane chemoreceptors, also termed methyl-accepting chemotaxis proteins (MCPs) or transducers. Upon binding of a chemoeffector, chemotaxis transducers undergo conformational changes that are transmitted to the flagellar motors by a phosphoryl transfer cascade between cytoplasmic signal transduction proteins. The CheA histidine kinase, which is docked to chemoreceptors via CheW, serves as a phosphodonor for CheY. In its phosphorylated form, CheY is able to bind to the switch of the flagellar

motor, an event that changes the direction of rotation of the flagellum and causes the cell to tumble (36). Two additional proteins, CheB methylesterase and CheR methyltransferase, comprise the adaptation pathway (15, 36). *E. coli* has five chemotaxis transducers: four transmembrane MCPs (Tsr, Tar, Trg, and Tap) (15) and one membrane-associated cytoplasmic receptor (Aer) (13, 30).

The chemotaxis operon in *A. brasilense* has recently been identified, and it has been shown that the operon comprises genes coding for the central excitation and adaptation chemotaxis pathway, which is homologous to that of *E. coli*. Mutations in the *A. brasilense* chemotaxis operon abolish taxis to all known stimuli and affect the pattern of motility (20), suggesting that this operon is the major regulator of motile behavior. It has also been shown that, despite their divergence in sequence, the chemotaxis proteins of *A. brasilense* are functional homologs of their *E. coli* counterparts (5).

In this study, we describe the first chemoreceptor identified in *A. brasilense*, Tlp1 (for transducer-like protein 1), and demonstrate that it serves as an energy taxis transducer. We also show that Tlp1 promotes colonization of plant roots by *A. brasilense*. This finding is significant because it provides experimental support for the hypothesis that energy taxis, and therefore bacterial metabolism, might be a key factor in determining the host specificity in *Azospirillum*-grass associations. To our knowledge, Tlp1 is the only chemotaxis transducer with a known function that is directly implicated in host-microbe interactions.

MATERIALS AND METHODS

Media, bacterial strains, and growth conditions. *A. brasilense* Sp7 (ATCC 29145), a wild type for chemotaxis, was used throughout this study. Bacterial strains and plasmids are listed in Table 2.1. The *A. brasilense* cells were grown at 28°C in a minimal medium (MMAB) (43) supplemented with the carbon source of choice at a final concentration of 10 mM. For aerobic growth, the cells were incubated at 200 rpm on a rotary shaker. For anaerobic growth, cells were incubated in a GasPak anaerobic system (Becton Dickinson Microbiology Systems, Cockeysville, Md.). The growth medium was supplemented with the antibiotics kanamycin (30 µg/ml) and tetracycline (10 µg/ml) for *A. brasilense*. Ampicillin (100 µg/ml) was used with *E. coli*.

Growth of the wild-type strain Sp7 and the *tlp1* mutant (see below) was compared by following the optical density at 600 nm (OD_{600}) over time of cultures in MMAB minimal medium containing either malate, fumarate, succinate, or fructose as the sole carbon source at two different concentrations, 5 and 10 mM (final concentration).

Identification of a new chemotaxis transducer. Twenty-four sequences of transducer-like proteins and MCPs from the α-proteobacteria *Caulobacter crescentus*, *Rhodobacter capsulatus*, *Rhodobacter sphaeroides*, *Rhizobium leguminosarum*, *Rhizobium meliloti*, *Agrobacterium tumefaciens*, and the γ-proteobacterium *E. coli* were aligned with CLUSTAL_X (40). A 16-residue highly conserved domain (HCD) sequence (NLLALNAGVEAARAG) was identified in the C-terminal region, and a degenerate oligonucleotide (HCD probe) (5'-

Table 2.1 Strains and plasmids used in this study

Strain or plasmid	Properties	Reference or source
Strains		
E. coli		
DH5α	General cloning strain	Gibco-BRL
S17-1	*thi endA recA hsdR* with RP4-2Tc::Mu- Km::Tn*7* Integrated in chromosome	(34)
A. brasilense		
Sp7	Wild-type strain; ATCC 29145	(37)
SG323	*tlp1* mutant; Km^r	This work
Plasmids		
pSG312	pUC18 with a 1.6-kb EcoRI/SalI fragment from pHCD12	This work
pSG316	pUC18 with a 2.9-kb EcoRI/BstBI fragment from pHCD12	This work
pSG318	pSG312 with the Km^r cassette from pHP45Ω-Km blunt inserted in the StuI site (plus direction); Km^r Ap^r	This work
pSG319	pSUP202 with EcoRI linearized pSG318 inserted at the EcoRI site; Tc^r Km^r Ap^r	This work
pHCD12	pLAFR1 clone from genome bank of *A. brasilense* Sp7, containing *tlp1*, Tc^r	This work
pHP45Ω-Km	Ap^r Km^r	(16)
pRK2013	Helper plasmid, carries *tra* genes; Km^r	(17)
pSUP202	Mobilizable plasmid, suicide vector for *A. brasilense*; Cm^r Tc^r Ap^r	(34)
pUC18	Cloning vector; Ap^r	(48)

AACCTGCTGGCCCTGAACGCCGGCGTCGAGGCCGCCCGCGCCGGC) was synthesized (Sigma Genosys, The Woodlands, Tex.) and labeled with digoxigenin-11-ddUTP with the DIG Oligonucleotide 3'End labeling kit (Roche Applied Science, Indianapolis, Ind.). The *A. brasilense* Sp7 genomic library in the pLAFR1 cosmid (44) was screened with the HCD probe by colony hybridization according to the manufacturer's protocols (Roche Applied Science). One of the cosmids yielding a positive hybridization with the probe was named pHCD12 (Table 2.1). The pHCD12 cosmid was digested with several enzymes and rehybridized with the probe to identify smaller restriction fragments suitable for sequencing. A 1.6-kb EcoRI/SalI fragment and a 2.9-kb BstBI/EcoRI fragment that still hybridized with the HCD probe were subcloned into pUC18 digested with the same enzymes, resulting in plasmids pSG312 and pSG316, respectively (Table 2.1). Direct sequencing and primer walking from pHCD12, pSG312, and pSG316 were used in automated DNA sequencing (ABI Prism) to obtain the DNA sequence of the region encompassing the *tlp1* gene and flanking regions.

Recombinant DNA techniques. Preparation of cosmid, plasmid, and genomic DNA, transformations, restriction endonuclease digestions, DNA extraction from agarose gels, ligation reactions; PCR and Southern hybridization, and DNA transformation into *E. coli* were carried out by standard protocols (33) and the manufacturers' instructions. The enzymes for DNA manipulation and PCR amplification were purchased from Roche Applied Science, New England Biolabs (Beverly, Mass.) and Epicentre (Madison, Wis.). To construct a *tlp1* insertion mutant, an *aphII* cassette (encoding Km^r and two transcription stop signals) was obtained from pHP45Ω-Km digested with BamHI (16) and

polished with the Klenow fragment of DNA polymerase I (New England Biolabs). The cassette was blunt-end ligated at an StuI site within the *tlp1* gene cloned into pSG312, resulting in plasmid pSG318. The pSG318 construct contains the kanamycin cassette in the same orientation of transcription as the *tlp1* gene (Table 2.1). pSG318 was linearized by digestion with EcoRI and ligated into the pSUP202 suicide vector, also digested with EcoRI, yielding pSG319 (Table 2.1). The pSG319 plasmid was introduced into *A. brasilense* by triparental mating with the pRK2013 vector as a helper, as described previously (20). Recombinants were screened for the loss of the recombinant plasmid and for double homologous recombination by replica plating on the appropriate antibiotics (Km^r and Tet^s). The correct allelic replacement in putative mutants was verified by PCR and Southern hybridization, with DNA fragments from the *tlp1* gene, the suicide vector, and the Km^r cassette as probes. One of the *tlp1* mutants (SG323) was chosen for further characterization.

Computational DNA and protein sequence analysis. Computational gene finding was carried out using the FramePlot program, which is designed to predict protein-coding regions in bacterial DNA with a high G+C content (21). The start codon of the *tlp1* gene was verified with the GeneMarkS program (11). Similarity searches against the nonredundant database at the National Center for Biotechnology Information (Bethesda, Md.) were carried out with the BLASTP and PSI-BLAST programs (6). Domain architecture of the predicted Tlp1 protein was obtained by searching against the SMART domain database (24). Multiple-sequence alignment of the conserved N-terminal periplasmic region of Tlp1 (residues 78 to 176) was constructed with CLUSTAL_X (40).

A bootstrapped neighbor-joining tree was generated from the multiple alignment with the MEGA phylogenetic package (22).

Behavioral assays. The swarm plate and temporal gradient assays for chemotaxis and the miniplug assay for redox taxis and chemotaxis in *A. brasilense* were performed essentially as previously described (1). For swarm plate assays, the same number of cells of the wild type and the mutant were inoculated by using a 5-μl aliquot of cells in exponential phase adjusted to the same OD_{600} value. The final concentration of the chemical to be tested as a chemoeffector was 10 mM. Taxis on swarm plates under anaerobic conditions was assessed with nitrate as a terminal electron acceptor, succinate or fructose as an electron donor, and the sole carbon source in the MMAB medium (43) lacking ammonium ions. The plates were incubated under anaerobic conditions in a GasPak anaerobic system (Becton Dickinson) and were inoculated with cells previously grown anaerobically with nitrate as a terminal electron acceptor in minimal liquid medium. The final concentration of nitrate was 10 mM. The optimum concentrations of the carbon sources added as electron donors to observe a sharp chemotaxis ring in this assay were determined in preliminary experiments and corresponded to 5 mM for succinate and 10 mM for fructose.

The spatial gradient assay for aerotaxis was used as previously described, with modifications (1). Cells were washed three times and resuspended in chemotaxis buffer (10 mM phosphate buffer [pH 7.0], 1 mM EDTA). Nine microliters of cells was mixed with 1 μl of the appropriate carbon source to give a final concentration of 2.5 mM and introduced into an optically flat capillary tube. The positions of the aerotactic bands

formed by the wild type and the *tlp1* mutant in the capillary tube were compared by measuring the relative distance of each aerotactic band from the meniscus. The temporal gradient assay for aerotaxis was used to measure the time until adaptation to oxygen removal and was performed as described by Zhulin et al. (52). Response times were measured in triplicate in three independent experiments.

Measurement of respiration. Respiration (oxygen consumption) in bacterial suspensions of the wild type (Sp7) and the *tlp1* mutant was measured as previously described (1).

Preparation of wheat seeds and plant root colonization assays. Seeds of wheat (*Triticum aestivum* cv. Jagger) were provided by R. L. Bowden (U.S. Department of Agriculture-Agricultural Research Service, Manhattan, Kans.). Seeds were surface-sterilized as described by Ramos et al. (29) and germinated by incubation in the dark for 3 days on nutrient agar plates (8 g of Bacto nutrient broth/liter and 15 g of agar/liter) at 23°C. *A. brasilense* cells (Sp7 and the *tlp1* mutant) were harvested at mid-logarithmic-growth phase (OD_{600}, 0.4), washed three times in sterile chemotaxis buffer, and concentrated to 10^8 cells/ml. The density of the cell suspensions was verified by serial dilution and plating onto MMAB plates. For each strain, 10^7 cells were added to 26- by 150-mm glass tubes containing 15 ml of molten Farhaeus semisoft agar (4% [wt/vol] agar) (50). After the agar had solidified, one sterile germinated seedling was aseptically transferred into each tube. The seedlings were grown at 23°C, with a photoperiod of 16 h of light and 8 h of dark. Ten days after inoculation, the seedlings were washed briefly in

sterile chemotaxis buffer to remove excess agar still adhering to the roots, blotted briefly on sterile Whatman 3MM filter paper, and weighed. Equal-sized roots from five plants were individually crushed in 50 ml of sterile chemotaxis buffer with a Waring blender. Serial dilutions were plated on MMAB medium supplemented with kanamycin (25 µg/ml) and incubated for 4 days at 28°C to count colonies of the *tlp1* mutant.

In situ detection of bacteria on the root surface. To monitor the pattern of colonization of the surface of sterile wheat roots, we introduced a stable plasmid, pJBA21TC, that constitutively expresses *gusA* from the P*aph* promoter (45) from *E. coli* into the wild-type strain Sp7 and the *tlp1* mutant of *A. brasilense* by triparental matings, as described previously (44). There was no difference in the growth of *A. brasilense* Sp7 and *tlp1* cells carrying the pJBA21TC plasmid. This plasmid contains the *parDE* genes and was reported to be very stable under nonselective conditions (45). Similarly, we found that this plasmid was stable in *A. brasilense* for at least 100 generations under nonselective conditions. Sterile wheat seedlings were prepared and inoculated as described above. The ß-glucuronidase activity was measured 10 days after inoculation on seedlings with equal-sized roots by the procedure described by Ramos et al. (29), except that the final concentration of 5-bromo-4-chloro-3-indoxyl-ß-D-glucuronide used was 100 µg/ml. The root systems of at least five plants were visually inspected and photographed.

Statistical analysis of data. A two-tailed *t* test, assuming unequal variances and with a 0.01 confidence level, was used to determine if the differences between the mutant and the wild type in the spatial gradient assay for aerotaxis and in the spatial gradient assay

for chemotaxis and anaerobic nitrate taxis were statistically significant. A *t* test, with similar parameters, was also performed to compare the respiration rates of the wild type and the *tlp1* mutant. Data obtained for these two strains in the quantitative colonization of wheat were compared by analysis of variance.

Nucleotide sequence accession number. The nucleotide sequences determined in this study have been deposited in the GenBank database under the accession number AY584240.

RESULTS

Identification of the *tlp1* gene, sequence analysis, and mutant construction. The genome of *A. brasilense* has not yet been sequenced. Therefore, the genomic library of *A. brasilense* Sp7 (20) was screened by colony hybridization with a degenerate probe to the HCD of the chemoreceptors (23, 51). This screen resulted in the identification of several candidate cosmids, including pHCD12. Sequencing and analysis of the pHCD12 insert revealed a 1,995-bp open reading frame encoding a putative chemoreceptor-like protein that we named Tlp1. Eleven base pairs upstream of the predicted start codon of the *tlp1* gene was a predicted ribosomal binding site, as identified by the GeneMark program (11). A gene coding for a cytochrome *c* was identified immediately downstream and in the opposite orientation of *tlp1*. An open reading frame coding for a hypothetical protein was detected upstream and in the opposite orientation of the *tlp1* gene (Fig. 2.1A).

The inferred Tlp1 protein has a predicted molecular mass of 70 kDa. It has a membrane topology typical of classical transmembrane chemoreceptors (Fig. 2.1B). Two

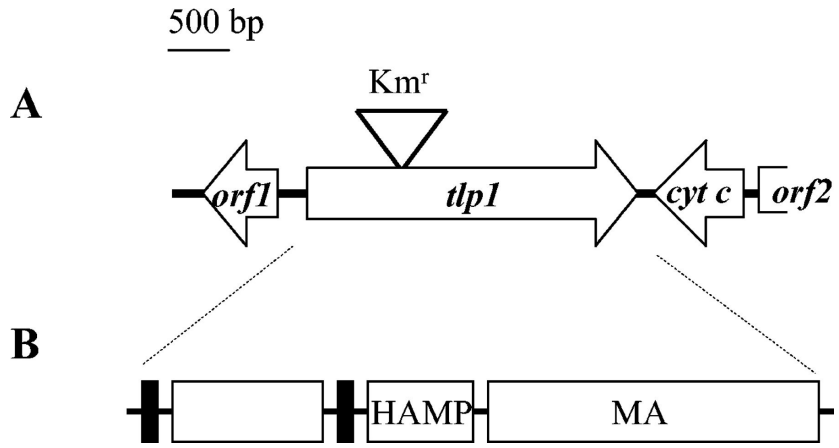

Fig. 2.1. Physical map of the 4,113-bp DNA region encompassing the *tlp1* gene (A) and predicted domain architecture of Tlp1 (B). (A) The arrows indicate the direction of transcription. The triangle above the *tlp1* gene indicates the insertion of the Km^r cassette. (B) Domains in the predicted Tlp1 protein, as defined by the SMART database (24): HAMP domain (7) ; MA, methyl-accepting chemotaxis-like domain (23). Black rectangles depict transmembrane regions.

transmembrane regions demarcate the N-terminal periplasmic domain of Tlp1, and the C-terminal region consists of a HAMP (histidine kinases, adenylyl cyclases, methyl binding proteins, and phosphatases) domain (7) and a signaling module containing the HCD and two methylation regions typical of chemoreceptors (23). Similarity searches using the BLASTP program (6) revealed that the Tlp1 C-terminal signaling module is homologous to those of chemoreceptors from closely related α-proteobacteria, namely *Magnetospirillum magnetotacticum*, *Rhodospirillum rubrum*, *Rhodopseudomonas palustris*, and *Bradyrhizobium japonicum* (data not shown). PSI-BLAST searches with the N-terminal periplasmic region of Tlp1 followed by multiple alignment of related sequences showed that it comprises a novel domain of unknown function (Fig. 2.2). This domain was found exclusively in the extracellular regions of two classes of receptor proteins from various distantly related bacterial species: chemotaxis transducers and sensor histidine kinases (Fig. 2.3).

Computational analysis did not suggest any specific sensory function for Tlp1. There are no known conserved motifs for binding prosthetic groups. Interestingly, there is a conserved set of aromatic amino acids (Phe102, Tyr152, and Tyr156) (Fig. 2.2) that is usually present in the contact sites where two proteins interact (25).

We constructed a mutant defective in the *tlp1* gene (SG323) and characterized its motile behavior by a variety of qualitative and quantitative assays. The average swimming speed and reversal frequency of the mutant were essentially the same as that of the wild type. Growth of the mutant in rich and minimal media containing various chemicals as a sole carbon source (see Material and Methods) was indistinguishable from that of the wild type.

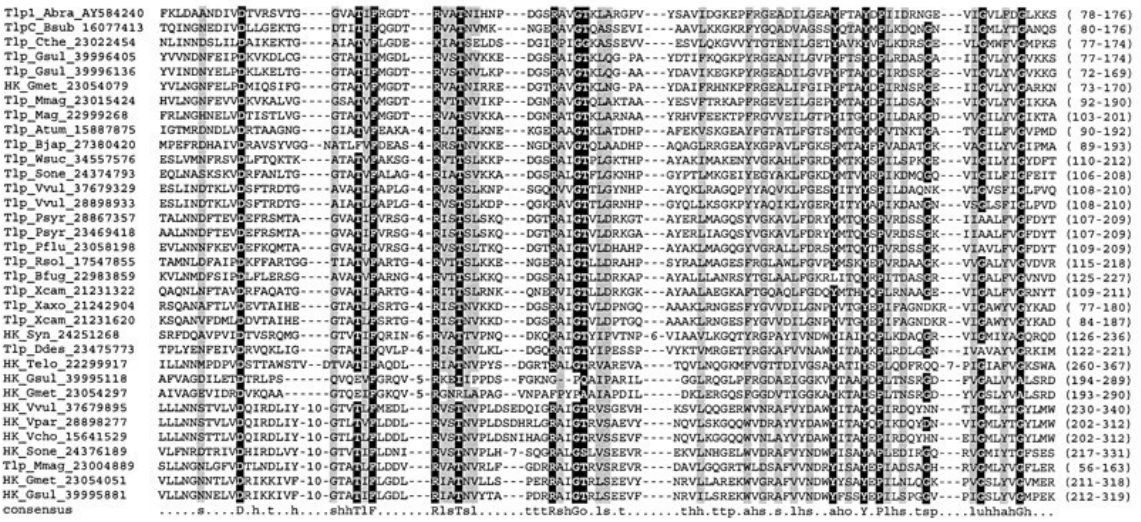

Fig. 2.2. A protein domain family exemplified by the N-terminal periplasmic region of Tlp1 from *A. brasilense*. Multiple alignment of homologous amino acid sequences was constructed with the CLUSTAL_X program (40). The start and end positions (domain boundaries) are shown to the right of each sequence. A consensus for multiple alignment (85% threshold) determined by using the CONSENSUS script (www.bork.embl-heidelberg.de/Alignment/consensus.html) is shown at the bottom. Identical residues are highlighted in black, and chemically similar residues are highlighted in gray. Each sequence in the alignment is identified by its GenBank protein identification number (except for the Tlp1 protein, for which the GenBank accession number of the corresponding DNA region is given) and by the abbreviated name of the organism. Abbreviations: HK, histidine kinase; Abra, *A. brasilense*; Atum, *A. tumefaciens*; Bjap, *B. japonicum*; Bsub, *B. subtilis*; Cthe, *Clostridium thermocellum*; Ddes, *Desulfovibrio desulfuricans*; Gmet, *G. metallireducens*; Gsul, *Geobacter sulfurreducens;* Mmag, *M. magnetotacticum*, Mag, *Magnetococcus* sp.; Pflu, *P. fluorescens*; Psyr, *Pseudomonas syringae*; Rsol, *Ralstonia solanacearum;* Bfug, *Burkholderia fungorum*; Sone, *Shewanella oneidensis;* Syn, *Synechococcus*; Telo, *Thermosynechococcus elongatus*; Vcho, *Vibrio cholerae*; Vpar, *Vibrio parahaemolyticus*; Vvul, *Vibrio vulnificus;* Wsuc, *Wolinella succinogenes;* Xaxo, *Xanthomonas axonopodis*; Xcam, *Xanthomonas campestris*.

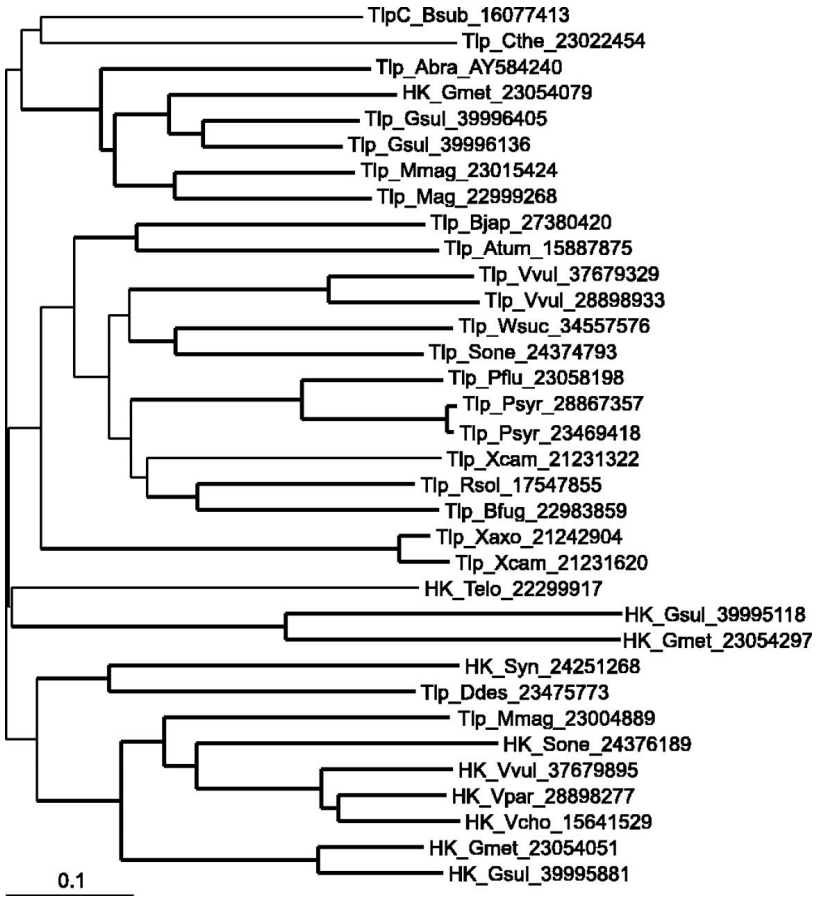

Fig. 2.3. Neighbor-joining tree showing the phylogenetic relationships within the protein domain family exemplified by the N-terminal periplasmic region of Tlp1 from *A. brasilense*. The tree was constructed from the multiple alignment shown in Fig. 2.2 with the MEGA phylogenetic package (22). Thick lines mark branches with significant (≥ 60%) bootstrap support (1,000 replicates). GenBank accession numbers and species abbreviations are the same as defined in the legend to Fig. 2.2.

The *tlp1* mutant is impaired in chemotaxis to rapidly oxidizable substrates.

Chemotaxis to various carbon sources known to be attractants for *A. brasilense* was tested on swarm plates (1). Selected results are shown in Fig. 2.4. We found that chemotaxis to amino acids and certain sugars (galactose and ribose) was indistinguishable in the mutant and the wild type. However, the mutant was significantly impaired in chemotaxis to organic acids, glycerol, and maltose. The results of the swarm plate assay also indicated that the *tlp1* mutant might be impaired in chemotaxis to fructose, but the difference was not statistically significant.

In swarm plates, bacteria metabolize the carbon source and move along its gradient. Therefore, in this assay, the size of the chemotactic ring is affected by both chemotaxis and metabolism. We have shown that there was no difference in growth between the mutant and wild-type cells on organic acids, sugars, and glycerol. Therefore, we infer that the diminished diameters of the chemotactic rings in these experiments are due to a defect in chemotaxis.

It is important to stress that chemotaxis was not abolished in the *tlp1* mutant and that the mutant only displayed a reduced ability to move along gradients of oxidizable substrates (Fig. 2.4). The difference in the behavior of the wild type and the *tlp1* mutant was most significant in the presence of substrates that were previously identified as the strongest chemoattractants for *A. brasilense*, such as sugars and organic acids (1). We have confirmed the chemotaxis phenotype by two additional behavioral assays: a miniplug method and a quantitative temporal gradient assay (Table 2.2). Cell metabolism is not required for the formation of the gradient of the chemoeffector tested in either assay. We found that the *tlp1* mutant was significantly impaired in taxis to chemicals that

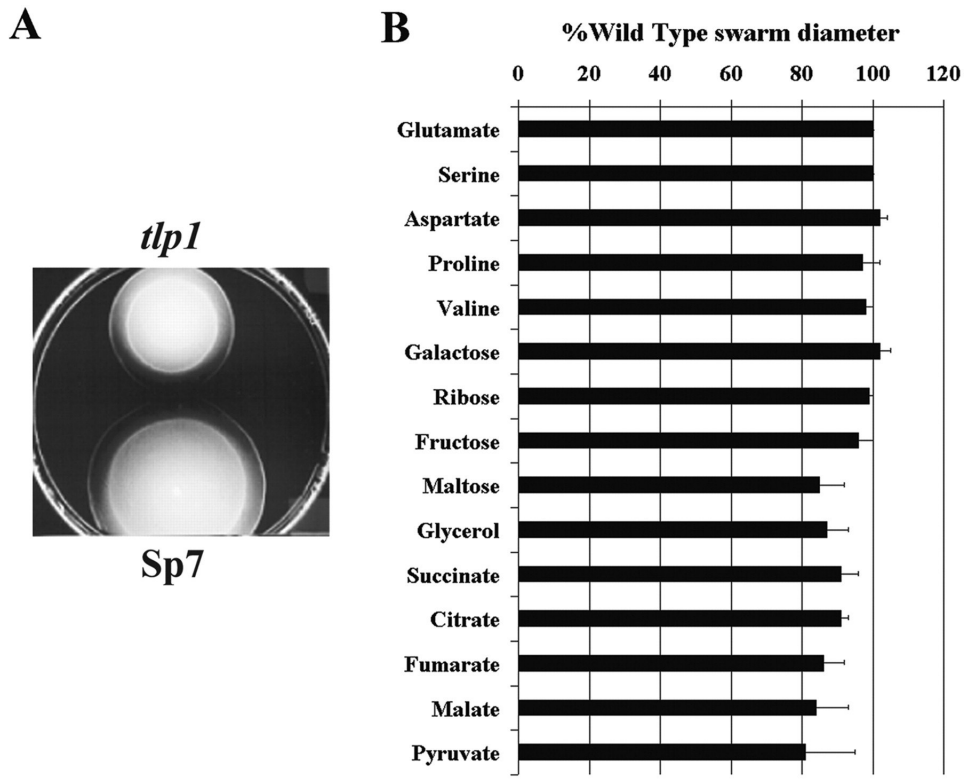

Fig. 2.4. The *tlp1* mutant is deficient in chemotaxis. Chemotaxis of the *A. brasilense* wild-type strain (Sp7) and the *tlp1* mutant was compared by the swarm plate assay. Swarm diameters were measured after incubation at 28°C for 48 h. (A) Representative swarm plate with fumarate as the sole carbon source. (B) The average swarm diameters are expressed as the percentage relative to that of wild-type strain (defined as 100%). Error bars represent standard deviations from the mean calculated from at least six repetitions. Differences in the swarming diameters of the wild type and the *tlp1* mutant were found to be statistically significant with the following chemoeffectors: maltose, glycerol, succinate, citrate, fumarate, malate, and pyruvate.

Table 2.2. Chemotaxis of *A. brasilense* wild type and *tlp1* mutant in spatial (miniplug) and temporal gradient assays

Attractant[a]	Threshold in miniplug Assay (μM)		Mean response time ± SD temporal assay[b]	
	Sp7	*tlp1*	Sp7	*tlp1*
Fructose	0.1	1	72±5	66±5
Fumarate	1	10	78±4	43±3
Malate	1	100	71±10	46±7
Succinate	1	100	67±8	47±5
Glycerol	10	100	37±7	32±5
Aspartate	100	100	28±7	21±6

[a] Cells were grown with the chemical to be tested as an attractant and prepared as described in Materials and Methods.

[b] The chemicals were tested at a final concentration of 10 mM. Values are in seconds

are strong attractants for *A. brasilense*, whereas no significant difference could be detected in the response of the wild type and the *tlp1* mutant to weaker chemoeffectors, such as amino acids. Data from both the temporal gradient assay and the miniplug method also suggested that the *tlp1* mutant was deficient in chemotaxis to fructose, a strong attractant for *A. brasilense*. Altogether, these results suggest that the *tlp1* mutant is deficient in chemotaxis to rapidly oxidizable substrates that have been previously shown to elicit energy taxis in *A. brasilense* (1).

The *tlp1* mutant is impaired in taxis to electron acceptors. Aerotaxis is the strongest motility response in *A. brasilense* (8, 52) and is part of the overall energy taxis in this organism (1). We measured aerotaxis in the *tlp1* mutant and the wild type by the capillary assay described previously (1, 52). Cells in a minimal medium placed in an optically flat capillary tube form an aerotactic band at a preferred oxygen concentration within 0.5 to 5 min. In aerotaxis, cells respond to changes in the rate of electron transport between the electron donor (substrate) and electron acceptor (oxygen) (1, 39, 52). Because the substrate in the capillary is distributed uniformly in the cell suspension, the behavior observed in this assay is in response to the oxygen gradient formed by oxygen diffusion into the capillary tube and oxygen consumption by respiring cells. The *tlp1* mutant cells were capable of aerotaxis, i.e., they formed a sharp aerotactic band similar to that of the wild type; however, the band formed by the mutant was always located closer to the meniscus relative to the wild type, i.e., it formed at a higher oxygen concentration (Fig. 2.5A). This behavior was consistent regardless of the electron donor used (Fig. 2.5B).

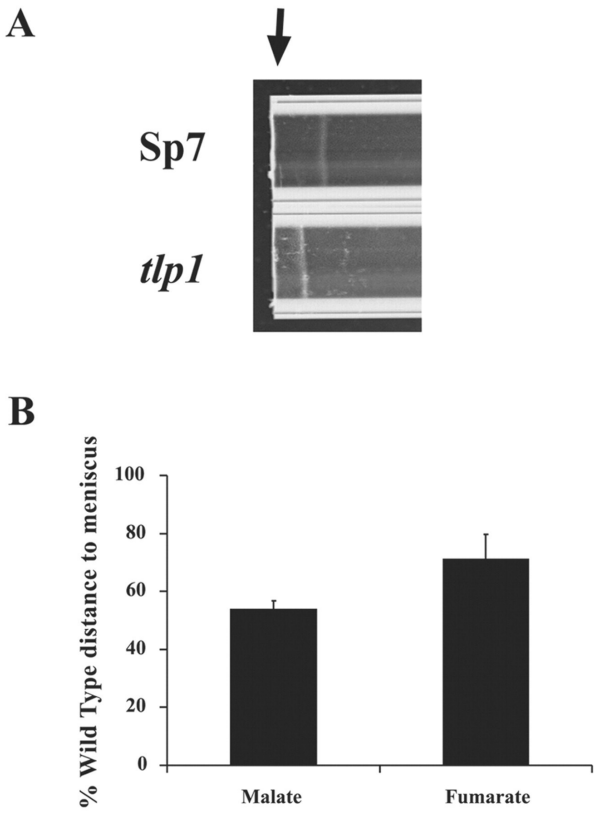

Fig. 2.5. The *tlp1* mutant is altered for aerotaxis. The ability of the *A. brasilense* wild-type strain (Sp7) and the *tlp1* mutant to form a sharp aerotactic band in a gradient of oxygen formed in a capillary tube was compared. (A) Representative capillary assay for aerotaxis showing the position of the aerotactic band in the gradient for the wild-type strain (Sp7) and the *tlp1* mutant. The arrow indicates the position of the meniscus at the air-liquid interface. Fumarate (2.5 mM) was added as the sole carbon and energy source to the suspension of motile cells. Magnification, x35. (B) The average distances of the aerotactic band to the meniscus expressed as a percentage of the distance for the wild-type strain (defined as 100%). Malate or fumarate was added at 2.5 mM as the sole substrate to the suspension of motile cells, and the distance of the aerotactic band to the meniscus was measured. Error bars represent standard deviations from the mean calculated from three independent experiments. Similar results were obtained with succinate as the sole carbon source.

Furthermore, we measured oxygen consumption (respiration) by the mutant and wild type. We found no difference in the respiration rates of the wild type and the *tlp1* mutant with malate, fumarate, or fructose as a substrate (data not shown), whereas the differences in the position of the aerotactic band were statistically significant.

We confirmed that the *tlp1* mutant was impaired in aerotaxis by measuring the response time of cells to the removal of oxygen in a temporal gradient assay. The wild-type cells adapted to the repellent effect of oxygen removal in 35 ± 2 s, whereas cells of the *tlp1* mutant responded in 24 ± 2 s (five independent experiments).

To determine whether the difference in the behavior of the wild type and the *tlp1* mutant is limited to oxygen sensing or is representative of overall energy taxis, we compared tactic responses under anaerobic conditions in the presence of NO_3^- as an alternative electron acceptor. We found that the *tlp1* mutant cells had a reduced response in a spatial gradient assay, regardless of the electron donor used in this experiment (Fig. 2.6).

The *tlp1* mutant is less sensitive to the repellent effect of a substituted quinone.

Substituted quinones, such as 1,4-benzoquinone, are redox-active chemicals that trigger a repellent response for *A. brasilense* by interfering with electron transport through the respiratory chain (1, 19). We compared the wild type (Sp7) and *tlp1* mutant responses to 10 µM 1,4-benzoquinone by two methods: a miniplug assay and a temporal gradient assay. In both assays, the *tlp1* mutant showed a significantly reduced response to the redox repellent. The threshold in the miniplug assay was 100 µM for Sp7 and 1,000 µM for the *tlp1* mutant. The response time in the temporal gradient assay was 93 ± 15 s for Sp7 and 55 ± 6 s for the *tlp1* mutant (means ± standard deviations). A higher

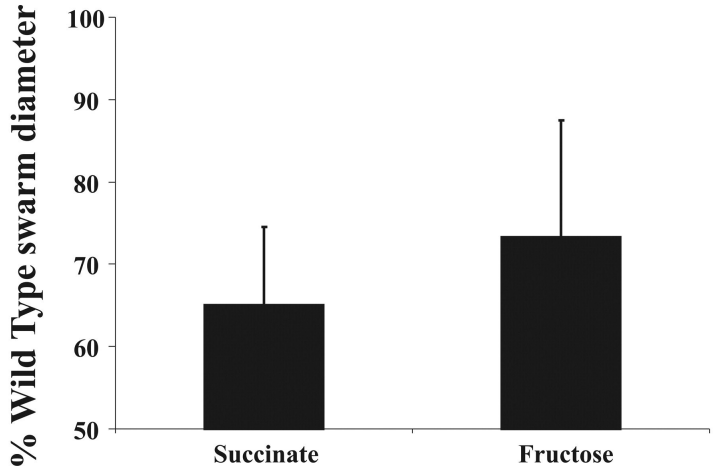

Fig. 2.6. The *tlp1* mutant shows altered energy taxis under anaerobic conditions. Tactic responses of the *A. brasilense* wild-type strain (Sp7) and the *tlp1* mutant were measured in the presence of nitrate as electron acceptor and succinate or fructose as electron donor. Plates were incubated anaerobically. Control plates containing no electron acceptor or no electron donor did not support growth. The average swarm diameters are expressed as a percentage of the wild-type swarm diameter (defined as 100%). Error bars represent standard deviation from the mean calculated from three independent experiments. The differences in the swarm diameters of the wild type and the *tlp1* mutant were statistically significant.

concentration of repellent was required to elicit the response from the mutant in a spatial gradient assay, and the mutant was also less sensitive (i.e., had a shorter response time) than the wild type in a temporal gradient assay. Because the *tlp1* mutant was impaired in all behavioral responses that are known to constitute energy taxis in *A. brasilense*, we conclude that Tlp1 is an energy taxis transducer.

The *tlp1* mutant is impaired in colonization of plant roots. The construction and characterization of a mutant of *A. brasilense* lacking an energy taxis transducer and significantly impaired in energy taxis provided us with the unique opportunity to investigate the role of this behavior in colonization of plant roots. We employed a qualitative (46) and a quantitative (3) assay to compare the ability of the *tlp1* mutant and the wild type to colonize the surface of sterile wheat roots. In the first approach, the spatial pattern of root colonization was visualized by detecting ß-glucuronidase activity constitutively expressed from a stable plasmid, pJBA21TC (45), introduced in both strains. The wild type and the mutant cells were inoculated individually under sterile conditions at a final concentration of approximately 10^7 cells/ml to 10 different sterile wheat plants, and the plants were incubated for 10 days. Figure 2.7A shows the dramatic difference in the efficiency of root surface colonization between the mutant and the wild type.

We confirmed this difference in a quantitative assay by determining the number of wild-type and *tlp1* cells colonizing the root surface of wheat plants 10 days after inoculation under conditions similar to those used for the qualitative assay (Fig. 2.7B). In agreement with the results from the qualitative assay, we found that the number of *tlp1*

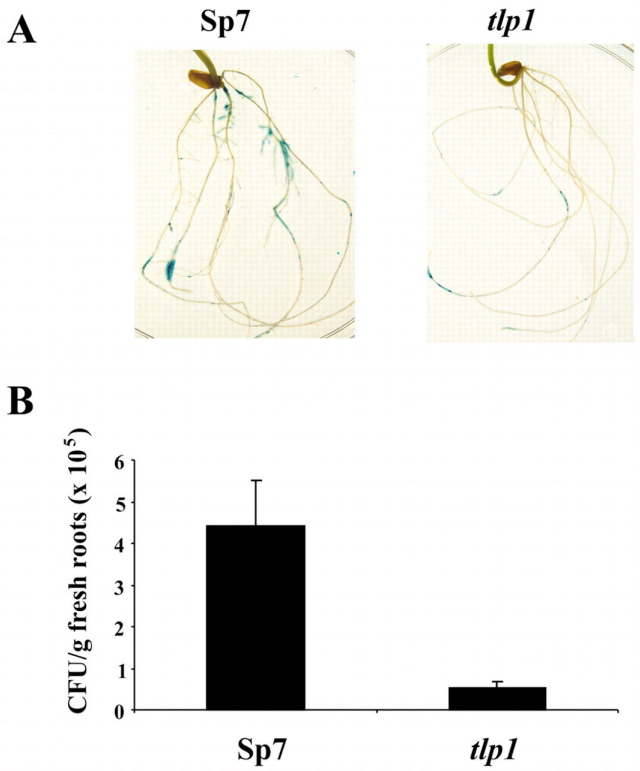

Fig. 2.7. The *tlp1* mutant is impaired in colonization of wheat root surfaces. (A) The pattern of root surface colonization was visualized on wheat roots 10 days after inoculation with similar levels of the *A. brasilense* Sp 7 wild type and the *tlp1* mutant. Each strain harbored plasmid pJBA21TC, which constitutively expresses ß-glucuronidase, with activity indicated by the blue color. (B) Colonization levels of wheat roots by *A. brasilense* wild-type strain Sp7 and the *tlp1* mutant 10 days after inoculation with similar numbers of cells. The error bars represent the standard deviations about the mean calculated for five plants. Similar results were obtained in three independent experiments.

mutant cells recovered from the wheat root surface was significantly lower than the number of wild-type cells. In summary, the data indicate that the *tlp1* mutant is impaired in colonization of wheat root surfaces and suggest that energy taxis contributes to root colonization in *A. brasilense*.

DISCUSSION

During energy taxis, cells seek a position in gradients of metabolized compounds at which the intracellular energy level is optimum. This behavior in *E. coli* has been studied extensively (12, 13, 18, 30, 32) and has been described for other bacterial species, including *A. brasilense* (1). However, the Aer and Tsr chemotaxis transducers of *E. coli* are the only two proteins that have been conclusively shown to transduce signals from energy taxis (13, 30).

We have identified and characterized a novel energy taxis transducer in *A. brasilense*. The Tlp1 protein has a predicted membrane topology typical of classical transmembrane receptors in *E. coli* (15); however, its extracellular domain has no sequence similarity to the N-terminal domains of *E. coli* chemoreceptors and a rather limited similarity in the C-terminal domain. Tlp1 contains the cytoplasmic C-terminal signaling module, which consists of an HCD (23) flanked by methylation helices. The C-terminal domain of Tlp1 is highly similar to those of most closely related α-proteobacterial species.

The predicted periplasmic N-terminal domain is the first member of a newly identified domain family, which is found in two types of microbial sensor molecules: chemotaxis transducers and sensor histidine kinases. Such domain sharing between

different classes of microbial sensors has recently been described for several unrelated extracellular sensory domains in prokaryotes (53). The presence of a conserved sensory domain in different classes of signal transduction proteins clearly indicates its importance to the biology of the organisms.

The N-terminal domain of Tlp1 is more closely related to a homologous domain of a histidine kinase from a distantly related delta-proteobacterial species, *Geobacter metallireducens*, than to homologous domains of chemotaxis transducers from closely related α-proteobacterial species. This relationship is indicative of an independent evolutionary history of the extracellular and intracellular domains of Tlp1, which is consistent with the recently reported independent domain evolution of cyanobacterial chemotaxis transducers (47). The biological function of the newly identified domain remains unknown.

The following experimental results strongly indicate that Tlp1 mediates energy taxis in *A. brasilense*, likely by monitoring a parameter linked to the electron transport system. In the absence of a functional Tlp1 transducer, mutant cells did not respond as effectively as cells of the wild type to gradients of electron donors (rapidly oxidizable substrates) or to terminal electron acceptors (oxygen or nitrate under anaerobic conditions) and were less sensitive to the repellent effect of a competitive electron transport inhibitor (a substituted quinone). All our results were consistent with the hypothesis that Tlp1 is an energy taxis transducer.

Although Tlp1 is an energy taxis transducer, the *tlp1* mutant does not have a null phenotype. Therefore, we conclude that there are other energy taxis transducers in *A. brasilense*. Similarly, mutation of either Aer or Tsr, the two energy taxis transducers in *E.*

coli, does not result in a null phenotype for energy taxis because the intact transducer can compensate for the mutated one (30). In addition, the *aer* and *tsr* mutants form an aerotactic band in a capillary at a lower or higher oxygen concentration, respectively, than wild-type cells (30), which is similar to the behavior of the *tlp1* mutant.

The molecular mechanism of energy sensing is understood only for the Aer transducer of *E. coli* (12, 32). The Aer transducer has a PAS domain and a flavin-adenine dinucleotide cofactor that is proposed to sense redox potential via interaction with a component of the electron transport system (12, 32). The molecular mechanism by which Tlp1 senses energy remains unknown, as it is for Tsr, and Tlp1 has a membrane topology similar to that of Tsr. The N-terminal periplasmic domain of the Tsr chemoreceptor lacks any oxygen- or redox-responsive prosthetic group. Similarly, sequence analysis of Tlp1 did not reveal any conserved motifs for putative binding sites for oxygen-and redox-responsive cofactors. It is important to mention that, although Tsr and Tlp1 are both energy taxis transducers, there is no sequence similarity between their N-terminal periplasmic domains. Whether Tsr and Tlp1 sense energy via similar mechanisms remains to be determined.

The involvement of microbial chemotaxis in colonization of plant roots has been previously addressed (for a review, see reference 42). However, most of these studies used genetically uncharacterized mutants with chemotactic behavior that was not analyzed. Only recently, the role of chemotaxis in root colonization by *Pseudomonas fluorescens* has been demonstrated directly by using a *cheA* mutant (14). Similarly, a *R. leguminosarum* mutant deficient in a chemotaxis transducer was shown to be less

competitive in nodulation of the host plant (49). However, the function of this transducer in *R. leguminosarum* and the behavior of the corresponding mutant were not established. Root exudates serve as growth substrates for soil microorganisms. This factor ultimately contributes to the selection of the soil bacteria that colonize the rhizosphere by affecting the growth of bacteria in the vicinity of the roots. It was previously suggested that root colonization by azospirilla is dependent on the bacterial metabolism, and metabolism-dependent chemotaxis was proposed to contribute to host selection by the bacteria (31). It has been demonstrated that metabolism-dependent chemotaxis in *A. brasilense* is largely energy taxis (1). The findings of the present study suggested that energy taxis might be involved in root colonization and the establishment of *Azospirillum*-grass associations. The identification of Tlp1 as an energy taxis transducer in *A. brasilense* allowed us to test this hypothesis. We have determined that a *tlp1* mutant is significantly less efficient than the wild-type strain in root colonization when sterile wheat seedlings were inoculated to in vitro. Since the *tlp1* mutant had a reduced ability to navigate in gradients of chemoeffectors that affect intracellular energy levels, it is likely that the smaller populations of the *tlp1* mutant resulted from reduced sensitivity of the mutant to root-generated gradients of chemoeffectors that affect energy levels.

It was previously proposed that active motility and chemotaxis to chemicals present in cereal root exudates are responsible for the first steps of root colonization in various host microbe associations, including in *Azospirillum* spp. (41, 42). Our results suggest that energy taxis is important for the establishment of *A. brasilense* in the rhizosphere of wheat. We hypothesize that previously observed strain-specific chemotaxis of *Azospirillum* to chemicals typical of plant root exudates (31) can be

attributed to energy taxis. Through energy taxis, azospirilla are attracted to a broad range of chemicals that support metabolism. Such metabolites are found in the root exudates of various host plants. This broad response is in contrast to the strict host specificity in which specific chemical signals establish the association. It is therefore tempting to speculate that energy taxis might be a significant factor that contributes to the broad host specificity seen in *Azospirillum*-plant associations.

A recent analysis of the number of chemotaxis transducers in different microbial genomes indicates that many soil bacteria possess significantly more chemoreceptors than the model organisms studied for chemotaxis (*E. coli* and *Bacillus subtilis*). The sensory specificity for the large majority of these transducers is unknown (2). However, given that chemotaxis is probably a major factor in bacterial adaptation to changing conditions, future studies focusing on characterizing the sensory specificity of chemotaxis transducers should unravel the diversity of environmental cues that trigger adaptive responses in microorganisms. They will also aid in defining how chemotaxis contributes to the biology of these organisms.

This work was supported in part by a National Science Foundation CAREER award (MCB-0347218), the Georgia Research Foundation, and the Office of Institutional Research, Georgia State University (to G.A.).

ACKNOWLEDGMENTS

We thank Jos Vanderleyden (Katholieke Universiteit Leuven, Leuven, Belgium) for providing the *A. brasilense* Sp7 genomic library, Robert L Bowden (USDA-ARS,

Manhattan, Kans.) for providing the wheat seeds, and Anna Skorupska (M. Curie-Sklodowska University, Lublin, Poland) for the pJBA21TC plasmid. We are grateful to Barry Taylor and Igor Zhulin for access to their laboratories' facilities at the early stage of this project. We thank Mark Johnson, Barry Taylor, Igor Zhulin, and Sandy Parkinson for expert advice, stimulating discussions, and critical reading of the manuscript.

REFERENCES

1. **Alexandre, G., S. E. Greer, and I. B. Zhulin.** 2000. Energy taxis is the dominant behavior in *Azospirillum brasilense*. J. Bacteriol. **182:**6042-6048.

2. **Alexandre, G., S. E. Greer-Phillips, and I. B. Zhulin.** 2004. Ecological role of energy taxis in microorganisms. FEMS Microbiol. Rev. **28:**113-126.

3. **Alexandre, G., C. Jacoud, D. Faure, and R. Bally.** 1996. Population dynamics of a motile and non-motile *Azospirillum lipoferum* strain during rice colonization and motility variation in the rhizosphere. FEMS Microbiol. Ecol. **19:**271-278.

4. **Alexandre, G., and I. B. Zhulin.** 2001. More than one way to sense chemicals. J. Bacteriol. **183:**4681-4686.

5. **Alexandre, G., and I. B. Zhulin.** 2003. Different evolutionary constraints on chemotaxis proteins CheW and CheY revealed by heterologous expression studies and protein sequence analysis. J. Bacteriol. **185:**544-552.

6. **Altschul, S. F., T. L. Madden, A. A. Schaffer, J. Zhang, Z. Zhang, W. Miller, and D. J. Lipman.** 1997. Gapped BLAST and PSI-BLAST: a new generation of protein database search programs. Nucleic Acids Res. **25:**3389-3402.

7. **Aravind, L., and C. P. Ponting.** 1999. The cytoplasmic helical linker domain of receptor histidine kinase and methyl-accepting proteins is common to many prokaryotic signalling proteins. FEMS Microbiol. Lett. **176:**111-116.

8. **Barak, R., I. Nur, Y. Okon, and Y. Henis.** 1982. Aerotactic response of *Azospirillum brasilense*. J. Bacteriol. **152:**643-649.

9. **Bashan, Y.** 1986. Migration of the rhizosphere bacteria *Azospirillum brasilense* and *Pseudomonas fluorescens* towards wheat roots in the soil. J. Gen. Microbiol. **132:**3407-3414.

10. **Bashan, Y., and G. Holguin.** 1994. Root-to-root travel of the beneficial soil bacterium *Azospirillum brasilense*. Appl. Environ. Microbiol. **60:**2120-2131.

11. **Besemer, J., A. Lomsadze, and M. Borodovsky.** 2001. GeneMarkS: a self-training method for prediction of gene starts in microbial genomes. Implications for finding sequence motifs in regulatory regions. Nucleic Acids Res. **29:**2607-2618.

12. **Bibikov S. I., L. A. Barnes, Y. Gitin, and J. S. Parkinson.** 2000. Domain organization and flavin adenine dinucleotide-binding determinants in the aerotaxis signal transducer Aer of *Escherichia coli*. Proc. Natl. Acad. Sci. USA **97**:5830-5835.

13. **Bibikov, S. I. R. Biran, K. E. Rudd, K. E., and J. S. Parkinson.** 1997. A signal transducer for aerotaxis in *Escherichia coli*. J. Bacteriol. **179:**4075-4079.

14. **De Weert S., H. Vermeiren, I. H. Mulders, I. Kuiper, N. Hendrickx, G. V. Bloemberg, J. Vanderleyden, R. De Mot, B. J. Lugtenberg.** 2002. Flagella-driven chemotaxis towards exudate components is an important trait for tomato root colonization by *Pseudomonas fluorescens*. Mol. Plant-Microbe Interact. **15**:1173-1180.

15. **Falke, J. J., and G. L. Hazelbauer.** 2001. Transmembrane signaling in bacterial chemoreceptors. Trends Biochem. Sci. **26:**257-265.

16. **Fellay, R., J. Frey, and H. Krisch.** 1987. Interposon mutagenesis of soil and water bacteria: a family of DNA fragments designed for in vitro insertional mutagenesis of gram-negative bacteria. Gene **52:**147-154.

17. **Figurski, D. H., and D. R. Helinski.** 1979. Replication of an origin-containing derivative of plasmid RK2 dependent on a plasmid function provided in trans. Proc. Natl. Acad. Sci. USA **76:**1648-1652.

18. **Greer-Phillips, S. E., G. Alexandre, B. L. Taylor, and I. B. Zhulin.** 2003. Aer and Tsr guide *Escherichia coli* in spatial gradients of oxidizable substrates. Microbiology **149:**2661-2667.

19. **Grishanin, R. N., I. I. Chalmina, and I. B. Zhulin.** 1991. Behaviour of *Azospirillum brasilense* in a spatial gradient of oxygen and in a "redox" gradient of artificial electron acceptor. J. Gen. Microbiol. **137:**2781-2785.

20. **Hauwaerts, D., G. Alexandre, S. K. Das, J. Vanderleyden, and I. B. Zhulin.** 2002. A major chemotaxis gene cluster in *Azospirillum brasilense* and relationships between chemotaxis operons in alpha-proteobacteria. FEMS Microbiol. Lett. **208:**61-67.

21. **Ishikawa, J., and K. Hotta.** 1999. FramePlot: a new implementation of the frame analysis for predicting protein-coding regions in bacterial DNA with a high G + C content. FEMS Microbiol. Lett. **174:**251-253.

22. **Kumar, S. K. Tamura, and M. Nei.** 1994. MEGA: molecular evolutionary genetics analysis software for microcomputers. Comput. Appl. Biosci. **10:**189-191.

23. **Le Moual, H., and D. E. Koshland, Jr.** 1996. Molecular evolution of the C-terminal cytoplasmic domain of a superfamily of bacterial receptors involved in taxis. J. Mol. Biol. **261**:568-585.

24. **Letunic, I., R. R. Copley, S. Schmidt, F. D. Ciccarelli, T. Doerks, J. Schultz, C. P. Ponting, and P. Bork.** 2004. SMART 4.0: towards genomic data integration. Nucleic Acids Res. **32**:D142-D144.

25. **Lo Conte, L., C. Chothia, and J. Janin.** 1999. The atomic structure of protein-protein recognition sites. J. Mol. Biol. **285:**2177-2198.

26. **Okon, Y., and R. Itzigsohn.** 1995. The development of *Azospirillum* as a commercial inoculant for improving crop yields. Biotechnol. Adv. **13:**415-424.

27. **Okon, Y., and C. A. Labandera-Gonzalez.** 1994. Agronomic applications of *Azospirillum*: an evaluation of 20 years worldwide field inoculation. Soil Biol. Biochem. **26:**1591-1601.

28. **Okon, Y., and J. Vanderleyden.** 1997. Root-associated *Azospirillum* species can stimulate plants. ASM News **63:**366-370.

29. **Ramos, H. J. O., L. D. B. Roncato-Maccari, E. M. Souza, J. R. L. Soares-Ramos, M. Hungria, and F. O. Pedrosa.** 2002. Monitoring *Azospirillum*-wheat interaction using the *gfp* and *gusA* genes constitutively expressed from a new broad-host range vector. J. Biotechnol. **97:**243-252.

30. **Rebbapragada, A., M. S. Johnson, G. P. Harding, A. J. Zuccarelli, H. M. Fletcher, I. B. Zhulin, and B. L. Taylor.** 1997. The Aer protein and the serine chemoreceptor Tsr independently sense intracellular energy levels and transduce oxygen, redox, and energy signals for *Escherichia coli* behavior. Proc. Natl. Acad. Sci. USA **94:**10541-10546.

31. **Reinhold, B., T. Hurek, and I. Fendrik.** 1986. Strain-specific chemotaxis of *Azospirillum* spp. J. Bacteriol. **162:**190-195.

32. **Repik, A., A. Rebbapragada, M. S. Johnson, J. O. Haznedar, J. O., I. B. Zhulin, and B. L. Taylor.** 2000. PAS domain residues involved in signal transduction by the Aer redox sensor of *Escherichia coli*. Mol. Microbiol. **36:**806-816.

33. **Sambrook, J., E. F. Fritsch, and T. A. Maniatis.** 1989. Molecular cloning: a laboratory manual, 2nd ed. Cold Spring Harbor Laboratory Press, Cold Spring Harbor, N.Y.

34. **Simon, R., U. Priefer, and A. Pülher.** 1983. A broad host range mobilization system for *in vivo* genetic engineering transposon mutagenesis in gram-negative bacteria. Bio/Technology **1:**784-791.

35. **Steenhoudt, O., and J. Vanderleyden.** 2000. *Azospirillum*, a free-living nitrogen-fixing bacterium closely associated with grasses: genetic, biochemical and ecological aspects. FEMS Microbiol Rev. **24:**487-506.

36. **Stock, J. B., and M. G. Surette.** 1996. Chemotaxis. pp. 1103-1129. *In* C. N. Neidhart, R. Curtiss III, J. I. Ingraham, E. C. C. Lin, K. B. Low, B. Magasanik, W. S. Reznikoff, M. Riley, M. Schaechter, and H. E. Umbarger (ed.), *Escherichia coli* and *Salmonella*, vol. 1. ASM Press, Washington, D. C.

37. **Tarrand, J. J., N. R. Krieg, and J. Döbereiner.** 1978. A taxonomic study of the *Spirillum lipoferum* group, with description of a new genus, *Azospirillum* gen. nov. and two species, *Azospirillum lipoferum* (Beijerinck) comb. nov. and *Azospirillum brasilense* sp. nov. Can. J. Microbiol. **24:**967-980.

38. **Taylor, B. L., and I. B. Zhulin.** 1998. In search of higher energy: metabolism-dependent behaviour in bacteria. Mol. Microbiol. **28:**683-690.

39. **Taylor, B. L., I. B. Zhulin, and M. S. Johnson.** 1999. Aerotaxis and other energy-sensing behavior in bacteria. Annu. Rev. Microbiol. **53:**103-128.

40. **Thompson, J. D., T. J. Gibson, F. Plewniak, F. Jeanmougin, and D. G. Higgins.** 1997. The CLUSTAL_X windows interface: flexible strategies for multiple sequence alignment aided by quality analysis tools. Nucleic Acids Res. **25:**4876-4882.

41. **Vande Broek, A., M. Lambrecht, and J. Vanderleyden.** 1998. Bacterial chemotactic motility is important for the initiation of wheat root colonization by *Azospirillum brasilense*. Microbiology **144:**2599-2606.

42. **Vande Broek, A., and J. Vanderleyden.** 1995. The role of bacterial motility, chemotaxis, and attachment in bacteria-plant interactions. Mol. Plant-Microbe Interact. **8:**800-810.

43. **Vanstockem, M., K. Michiels, J. Vanderleyden, and A. P. Van Gool.** 1987. Transposon mutagenesis of *Azospirillum brasilense* and *Azospirillum lipoferum*, physical analysis of Tn*5* and Tn*5*-Mob insertion mutants. Appl. Environ. Microbiol. **53:**410-415.

44. **Verreth, C., B. Cammue, P. Swinnen, D. Crombez, A. Michielsen, K. Michiels, A. Van Gool, and J. Vanderleyden.** 1989. Cloning and expression in *Escherichia coli* of the *Azospirillum brasilense* Sp7 gene encoding ampicillin resistance. Appl. Environ. Microbiol. **55:**2056-2060.

45. **Wielbo, J., and A. Skorupska.** 2001. Construction of improved vectors and cassettes containing *gusA* and antibiotic resistance genes for studies of transcriptional activity and bacterial localization. J. Microbiol. Methods **45:**197-205.

46. **Wilson, K. J., A. Sessitsch, J. C. Corbo, K. E. Giller, A. D. Akkermans, and R. A. Jefferson.** 1995. ß-Glucuronidase (GUS) transposons for ecological and genetic studies of rhizobia and other gram-negative bacteria. Microbiology **141:**1691-1705.

47. **Wuichet, K., and I. B. Zhulin.** 2003. Molecular evolution of sensory domains in cyanobacterial chemoreceptors. Trends Microbiol. **11:**200-203.

48. **Yanish-Perron, C., J. Vieira, and J. Messing.** 1985. Improved M13 phage cloning vectors and host strains: nucleotide sequences of the M13mp18 and pUC19 vectors. Gene **33:**103-119.

49. **Yost, C. K., P. Rochepeau, and M. F. Hynes.** 1998. *Rhizobium leguminosarum* contains a group of genes that appear to code for methyl-accepting chemotaxis proteins. Microbiology **144:**1945-1956.

50. **Zamudio, M., and F. Bastarrachea.** 1994. Adhesiveness and root hair deformation capacity of *Azospirillum* strains for wheat seedlings. Soil Biol. Biochem. **26:**791-797.

51. **Zhulin, I. B.** 2001. The superfamily of chemotaxis transducers: from physiology to genomics and back. Adv. Microbiol. Physiol. **45:**157-198.

52. **Zhulin, I. B., V. A. Bespalov, M. S. Johnson, and B. L. Taylor.** 1996. Oxygen taxis and proton motive force in *Azospirillum brasilense*. J. Bacteriol. **178:**5199-5204.

53. **Zhulin, I. B., A. N. Nikolskaya, and M. Y. Galperin.** 2003. Common extracellular sensory domains in transmembrane receptors for diverse signal transduction pathways in bacteria and archaea. J. Bacteriol. **185:**285-294.

CHAPTER TWO

PART B: Identification of chemotaxis transducers in *Azospirillum brasilense*

INTRODUCTION

Chemotactic organisms use transducers to sense their environment and appropriately navigate to the most favorable niche. Chemotactic transducers (also called chemoreceptors or methyl-accepting chemotaxis proteins, mcp) have two distinct domains: one for sensing environmental cues and one for transducing appropriately the cues to a phosphorelay signal transduction system (18). Prototypical chemotaxis transducers have a topology in which a short N-terminal cytoplasmic segment and a large cytoplasmic C-terminal segment are joined together by a periplasmic domain flanked by two transmembrane regions (18). The N-terminal domain of chemotaxis transducers varies from species to species, reflecting the variety of environmental cues sensed by the organism (41). The N-terminal sensing domain and the C-terminal cytoplasmic domain are connected by a linker region (4). The C-terminal region is comprised of two methylation domains flanking a highly conserved domain, HCD, which is the site of interaction between the chemotaxis transducer and the CheW docking protein (9, 19, 33). The sequence of the HCD is highly conserved and found in transducer sequences of both Bacteria and Archaea (41). This conserved feature of the C-terminal region of chemotaxis transducers can be used to screen DNA libraries to find homolog chemotaxis transducers.

*Azospirillum brasilens*e is a free-living, nitrogen-fixing alpha-proteobacterium that live in association with the rhizosphere of various crops of agronomic importance,

promoting plant growth (25, 26). Motility and chemotaxis are hypothesized to be important for the colonization of plant roots (35, 36, 42). The chemotaxis transducer repertoire of bacteria depends on the environmental niche occupied by the organism and is responsible for sensing environmental cues. Various chemotaxis transducers can be limited to a small group of bacteria while others can be widespread. The characterization of the chemotaxis transducer repertoire of *A. brasilense* is necessary for the identification of environmental cues important for of colonization processes and development of this strain as a biofertilizer.

MATERIALS AND METHODS

Bacterial strains and plasmids

Wild type *A. brasilense* Sp7 (ATCC 29145) strain was used throughout this study. *A. brasilense* cells were grown at 28°C in the minimal medium (MMAB) (37). Cells were grown aerobically at 200 rpm on a rotary shaker. The growth medium was supplemented with the antibiotics kanamycin (30 μg ml^{-1}) and tetracycline (10 μg ml^{-1}). Kanamycin (50 μg ml^{-1}) and tetracycline (10 μg ml^{-1}) was added to media to grow *E. coli* when appropriate.

Identification of a new chemotaxis transducer

A.. brasilense Sp7 genomic DNA was digested with the *Avi*II restriction enzyme and southern hybridization was performed following standard protocols (27) using a 1 Kb probe generated from the C-terminal region of a known receptor, Tlp1. The probe was digoxigenin-11-ddUTP labeled using a PCR DIG Probe Synthesis Kit (Roche Applied

Science, Indianapolis, IN). Southern hybridization revealed approximately thirteen hybridizing bands. An *A. brasilense* Sp7 partial DNA library was constructed by digestion with *Avi*II followed by gel extraction (Qiagen gel extraction kit, Qiagen, Valencia, CA) of the 2-9 Kb region containing the largest number of bands possibly containing entire genes since chemotaxis transducers are less than 2 Kb in size. These fragments were then cloned into the pCR-blunt vector (Invitrogen, Carlsbad, CA) and transformed into *E,. coli* Top10 cells. Colonies were then screened using the 1 Kb probe following standard protocols (27). Plasmid DNA from putative positive clones were isolated, digested with *EcoR*I and subsequently screened again by Southern Hybridization with the 1 Kb probe in order to confirm the hybridization. Plasmids that consistently hybridized with the probe were sequenced using T7 promoter and M13 reverse primers (DNA Core Facility, G.S.U.). One such positive clone was identified (pBS5) and sequenced by primer walking (table 2.3). To obtain the flanking DNA sequence not contained in the clone, inverse PCR was performed by digesting Sp7 genomic DNA with *EcoR*I, diluting and self-ligating the DNA to form a circular template, and amplifying with Tlp2I-F3 and Tlp2I-R3 primers (table 2.3) designed to read outward from the end of the known Tlp2 sequence. The resulting PCR product was cloned into the pCR2.1-Topo vector (Invitrogen, Carlsbad, CA) and sequenced with T7 promoter and M13 reverse primers (DNA Core Facility, G.S.U.) and the DNA sequence obtained was aligned with the Tlp2 sequence.

Table 2.3 Primers used for the sequencing of *tlp2*

Primer Name	Sequence
T7 promoter	5’ AATACGACTCACTATAGG
AviIIF1	5’ CGATGGTGCCGACGATGC
AviIIF2	5’ GAAATCTCCTCGGTGGCG
AviIIF3	5’ CGTCGGCGGCGGAGTGGGTC
AviIIF4	5’ CGTTTCGGTGCGGAAGCGG
AviIIF5	5’ GTGTTCAGGTTGTCCAGCAG
AviIIF6	5’ GATTACGGCATCGGCTACG
AviIIF7	5’ CAATGGTCTTCATCGCCGC
AviIIF8	5’ CGAGCATCAGGGTGGTCC
AviIIF9	5’ CGGTGCGGAAGCGGATG
AviIIF10	5’ CGGTGCGGAAGCGGATG
M13 Rev	5’ GTCATAGCTGTTTCCTG
AviIIR1	5’CGCACCAACAGCACCATC
AviIIR2	5’ GCCGTGCTGGTCTTCCG
Tlp2IF3	5’ CATCGTCGGCACCATCG
Tlp2IR3	5’ GAAGCCCTTGCCAGCCTC

Computational DNA and protein sequence analysis

Computational gene finding was carried out using the FramePlot program, which is designed to predict protein-coding regions in bacterial DNA with a high G+C content(15). Similarity searches against the non-redundant database at the National Center for Biotechnology Information (Bethesda, Md.) were carried out with the BLASTP program (3). Domain architecture of the predicted Tlp2 protein was determined by searching against the SMART domain database (20). CLUSTAL W was used to align the N-terminal sequence of chemotaxis transducers homologous to that of the newly identified Tlp2 chemoreceptor in *A. brasilense* (7).

Tlp2 mutant construction

A *tlp2* insertion-deletion mutant was constructed using PCR. A 606 bp upstream region of *tlp2* was amplified using the primer pair Tlp2up F1 andTlp2up R1 (Table 2.4). This region contains the start codon of tlp2 and 151 bp downstream of this site. The resulting PCR product was cloned into pCR2.1-TOPO (Invitrogen) yielding pBS6. The fragment was then excised with *Kpn*I and *Not*I and cloned into pCM184 (24) digested with the same enzymes resulting in pBS7. *E. coli* SCS110 cells were then transformed with pBS7. A 533 bp downstream region of *tlp2* was amplified using the primer pair Tlp2down F1 and Tlp2down R1 (Table 2.4) and cloned into pCR2.1-TOPO resulting in pBS8. *E. coli* SCS110 cells were then transformed with pBS8. The fragment was then excised with *Apa*I and *Sac*I and cloned into pBS7 digested with the same enzymes , yielding pBS9. In pBS9, the upstream and downstream regions of *tlp2* flanked a

Table 2.4. Primers used for *tlp2* mutant construction

Primer Name	Sequence
Tlp2UF1	5’ CGGTGCCGCTGTAGTCC
Tlp2UR1	5’ CGATGGCTTCCGACTTGC
Tlp2DF1	5’ CGATAGCATCCGCAACAG
Tlp2DR1	5’ CGTTGGTGCTGATGTCGC

kanamycin resistance cassette present in pCM184 and yield a construct in which the *tlp2* gene is deleted for 784 bp and replaced by a kanamycin cassette. Next, the *Δtlp2*::kan construct generated using this approach was amplified from pBS9 using Tlp2up F1 and Tlp2down R1 and cloned into pCR2.1-TOPO. The the *Δtlp2*::kan construct was then excised with *Eco*RI and cloned into the suicide plasmid pSUP202 (29) digested with the same enzyme, resulting in pBS10. *E. coli* Top10 cells were transformed with pBS10. pBS10 was introduced into *A. brasilense* by triparental mating using pRK2013 (11) as a helper. Double homologous recombinants were selected by screening for loss of the plasmid on MMAB (37)with the appropriate antibiotics (Km, Tc). One such mutant, BS10 was characterized further.

RESULTS AND DISCUSSION

According to the SMART database (20), Tlp2 is predicted to have two transmembrane regions flanking an N-terminus periplasmic domain, and the C-terminal cytoplasmic region consisting of a HAMP domain (histidine kinase, adenylyl cyclase, methyl-accepting chemotaxis protein, and phosphatase) and a methyl-accepting chemotaxis-like domain (19) (Fig. 2.8). The HAMP domain has been shown to be essential transducing the signal from the sensing domain to the signaling domain The sensing specificity of chemotaxis transducer can be found within the N-terminal sensing domain (41). BLAST searches (April 11, 2006) using the N-terminal sensing region (between the 2 tranmsbrane domains) revealed homology of Tlp2 to several chemotaxis transducers and a histidine kinase with a methyl-accepting chemotaxis domain from *Bradyrhizobium* sp.

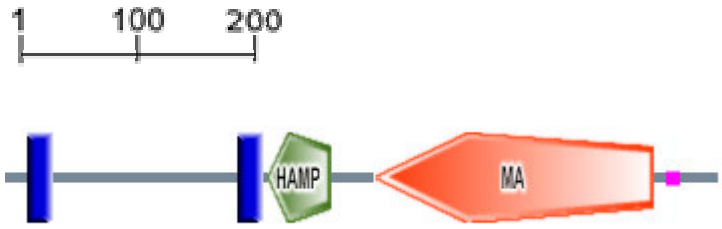

FIG. 2.8. Domain architecture of the predicted Tlp2 protein using the SMART database. The protein consists of an N-terminal transmembrane domain (blue bars represent predicted membrane-spanning regions), a HAMP domain (green pentagon), and a C-terminal methyl-accepting chemotaxis region. The scale bar represents amino acids.

BTAi1 all of unknown function. Homologs of the putative sensory domain of Tlp2 were found in a group of alpha-proteobacteria including *Agrobacterium tumefaciens*, *Bradyrhizobium japonicum*, *Bradyrhizobium* sp. BTAi1, *Magnetosprillum magnetotacticum*, *Rhizobium etli*, and *Sinorhizobium meliloti*. With the exception of *M. magnetotacticum*, all of these organisms are found in association with the rhizosphere of various plants, suggesting that Tlp2 may be a chemotaxis transducer specific for this niche. However, the presence of this sensing domain in *M. magnetotacticum*, which primarily inhabits fresh and salt water environmnets, raises questions regarding the specificity of this domain to this niche. *M. magnetotacticum* has the most chemotaxis transducers studied to date, and it has been hypothesized that this large number of transducers is related to energy taxis functions (1). Perhaps the function of this domain is sensing a particular energy parameter found in both environments. This is unlike the first chemotaxis transducer Tlp1 identified in *A. brasilense*, which has homology to a broad range of chemotaxis transducers and histidine kinases in closely and distantly related bacterial species (13). However, no known motif or domain was identified in this region. The sensory domain found in Tlp2 is thus a conserved domain of unknown function.

To characterize this domain further an alignment of the N-terminal regions of the homologous chemotaxis transducers and histidine kinase using CLUSTAL W showed several conserved and similar residues (Fig 2.9). The N-terminal alignment showed several aromatic (Phe, Tyr) and positively charged (Arg) residues that were conserved among all of the homologous proteins. There were also several similar aromatic (Phe, Tyr) and negatively charged (Asp, Gln, Glu) residues that are conserved among the homologous proteins. These data suggest that Tlp2 may sense environmental stimuli via a

Fig. 2.9. Multiple alignment of the N-terminal region of Tlp2 from *A. brasilense*. The start and end positions are shown to the right of each sequence. Identical residues are highlighted in black, and chemically similar residues are highlighted in gray. Each sequence in the alignment is identified by the abbreviated name of the organism its GenBank protein identification number. Abbreviations: Tlp, transducer like protein; HK, histidine kinase; Abra, *A. brasilense*; Atum, *A. tumefaciens*; Bjap, *B. japonicum*; Mmag, *M. magnetotacticum*, Bra, *Bradyrhizobium* sp. BTAi1.; Retl, *Rhizobium etli*; Smel, *Sinorhizobium meliloti*

ligand binding mechanism, since the presence of these charged residues suggests that this domain could bind ligands of the opposite charge. However, the presence of this domain in *M. magnetotacticum* suggests that this domain may sense energy. Located immediately downstream of Tlp2 is a putative adenine deaminase, which suggests that Tlp2 may be involved in sensing parameters related to this. Interestingly, the histidine kinase of *B. japonicum* sp. strain BTAi1 that has a sensing domain homologous to Tlp2 also has a methyl-accepting chemotaxis domain. This protein is located upstream of GTP cyclohydrolase, suggesting that this protein may sense parameters related to folic acid synthesis. A Tlp2 mutant has been constructed, and characterization of this mutant will reveal the substrate specificity of this chemotaxis transducer.

CHAPTER TWO

PART C: Localization of chemotaxis transducers in *Azospirillum brasilense*

INTRODUCTION

Motile bacteria navigate about their environment and detect chemical gradients with a high sensitivity and across a wide range of concentrations. The high sensitivity of the chemotaxis sensory machinery is due to the existence of a signal amplification system that allows for detection of differences of only a few molecules occupying ligand-binding transducers. Such sensitivity allows cells to integrate various environmental signals and respond appropriately. In the membrane of *E.coli*, chemotaxis transducers exist as trimers of dimers and are typically clustered at the cell poles (5). Chemotaxis transducer clustering,was first observed in *E. coli* and *Caulobacter crescentus* and then in several other bacterial and archaeal species, suggesting that it is a conserved feature of chemotaxis transducers (2, 12, 14, 17, 22, 23). A recent proposal suggests that clustering allows for interactions between transducers, and chemotaxis transducer clustering might be involved in signal amplification as well as signal transduction during chemotaxis (16, 28, 30, 31). Chemotaxis transducers exist in specific stoichiometric ratios within the cell. For example, in *E. coli* Tsr and Tar are highly abundant with thousands of copies per cell, while Tap, Trg, and Aer are of low abundance with only a few hundred copies per cell (21). Additionally, the other components of the chemotaxis signal transduction pathway (CheA, CheW etc.) in *E. coli* have been shown to localize to the pole of the cells (22, 32),

which is thought to be important for the formation of tight clusters of the chemotaxis proteins resulting in signal amplification and adaptation (6, 10).

Using an antibody raised against the HCD region of the *E. coli* chemotaxis transducer Tsr, immunofluorescence microscopy was used to determine if such cellular localization of chemoreceptor homologs is also present in *A. brasilense*. First we showed that this antibody recognized several bands in *A. brasilense* whole cell protein extracts. Next, in vivo methylation with [methyl-^{3}H] methionine revealed the presence of methylated proteins similar in molecular weight to those proteins identified by the anti-Tsr antibody in whole cell extracts. This suggested that this antibody could possibly be used to detect chemotaxis transducers in *A. brasilense*.

MATERIALS AND METHODS

Immunofluorescence for chemotaxis transducer localization

The appropriate conditions were established for visualizing the localization of chemoreceptors to the poles of the cells by adapting the protocol of Teleman, et al.(34). An overnight Sp7 culture was centrifuged at 14,000 rpm and re-suspended in 50 µl of its own medium. Cells were added to 1ml of 98% methanol, previously equilibrated at -20°C. The tube was inverted 6 times and incubated at -20°C for at least 10 minutes. Coverslips (Corning Cover Glass, No. 1.5, 22 x 30 mm) were coated with poly-L-lysine (Sigma, 0.01% solution) (15 µl) and allowed to dry. Cells (15 µl) were placed on the coverslip and allowed to dry. 350 µl of lysozyme (2 mg/ml) in GTE Buffer (50 mM glucose, 20 mM Tris-HCl pH 8.0, 10 mM EDTA) was added to each coverslip for 10 minutes. The lysozyme solution was then removed using a torn edge of a piece of

Whatman paper. Coverslips were incubated in blocking solution (2% dehydrated skim milk in PBS) overnight at 4°C. The coverslips were then incubated with primary antibody (anti-Tsr, 1:300 dilution in blocking solution) raised against the HCD region of the *E. coli* chemotaxis transducer Tsr for two hours. The coverslips were then rinsed ten times with PBS. The coverslips were then incubated with a secondary antibody (Alexa Fluor 488 goat anti-rabbit IgG in blocking solution) for two hours at room temperature. The coverslips were then placed on slides and viewed with a Nikon E800 microscope.

RESULTS AND DISCUSSION

A. brasilense was grown in both MMAB minimal medium and TY rich medium, and an anti-Tsr antibody, raised against the highly concerved domain (HCD) of the Tsr receptor in *E. coli*, was used for receptor localization . Under both growth conditions, localization was observed at either one or both cell poles (Fig. 2.10). The different media used did not result in a difference in localization or background, suggesting that this antibody cross-reacts with *A. brasilense* chemotaxis transducers that are expressed under a variety of environmental conditions. Different chemotaxis transducers could be expressed under the different conditions. For example, in *Pseudomonas aeruginosa*, the expression of some chemotaxis transducers is dependent on the nitrogen sources available (8). The expression of some chemotaxis transducers in *Rhodobacter sphaeroides* are regulated by light and oxygen (14). However, this assay is not sensitive enough to determine differences in expression for chemotaxis transducers localized to the cell poles since fluorescense cannot be quanitifed and the sub-cellular localization cannot be determined.due to lack of resolution. These data suggest that chemotaxis transducers in

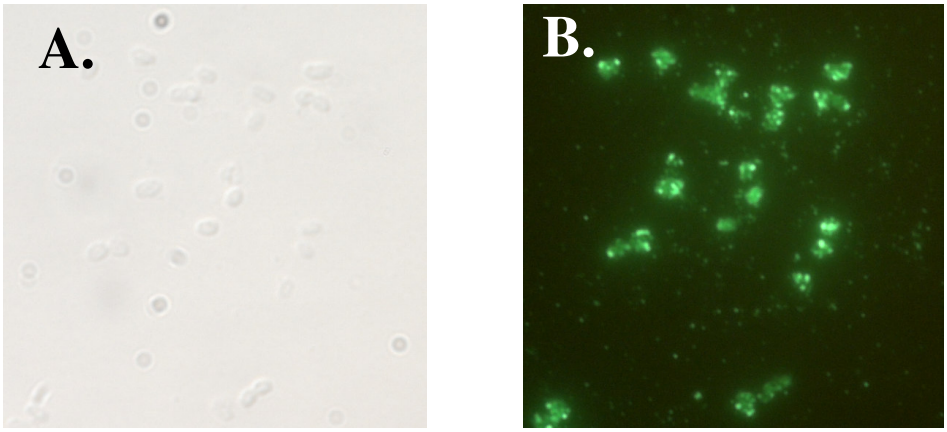

Fig. 2.10. Chemotaxis transducer localization in *A. brasilense*. (A.) *A. brasilense* cells grown in MMAB medium without excitation. (B.) *A. brasilense* cells grown in MMAB medium labeled with an anti-Tsr primary antibody (1:300 dilution) and a secondary antibody (Alexa Fluor 488 goat anti-rabbit IgG). Chemotaxis transducers are localized to either one or both cell poles as seen by the bright spots located at the ends of the cell. The picture in Fig. B. corresponds to the picture in Fig. A.

A. brasilense also form clusters, similar to those responses in other species. Future localization experiments with antibodies specific to chemotaxis transducers as well as components of the chemotaxis signal transduction system of *A. brasilense* will provide insight into the signaling mechanisms of this system. If the components of the chemotaxis system(s) are localized together this suggests that they interact with one another. *Rhodobacter sphaeroides* has components of two chemotaxis systems localized to different regions of the cell, presumably to prevent cross-talk between the two systems, and such a mechanism of a cross-talk prevention may also be present in *A. brasilense* (38-40). Since this antibody cross-reacts with the conserved C-terminal domain of the *E. coli* chemotaxis transducers Tsr and Tar, the ability of the antibody to cross-react with chemotaxis transducers of *A. brasilense* suggests that the organization of its signal transduction must be a similar to that of other chemotactic microorganisms.

REFERENCES

1. **Alexandre, G., S. E. Greer-Phillips, and I. B. Zhulin.** 2004. Ecological role of energy taxis in microorganisms. FEMS Microbiol. Rev. **28:**113-126.

2. **Alley, M. R., J. R. Maddock, and L. Shapiro.** 1992. Polar localization of a bacterial chemoreceptor. Genes Dev **6:**825-36.

3. **Altschul, S. F., T. L. Madden, A. A. Schaffer, J. Zhang, Z. Zhang, W. Miller, and D. J. Lipman.** 1997. Gapped BLAST and PSI-BLAST: a new generation of protein database search programs. Nucleic Acids Res **25:**3389-402.

4. **Ames, P., and J. S. Parkinson.** 1988. Transmembrane signaling by bacterial chemoreceptors: E. coli transducers with locked signal output. Cell **55:**817-26.

5. **Ames, P., C. A. Studdert, R. H. Reiser, and J. S. Parkinson.** 2002. Collaborative signaling by mixed chemoreceptor teams in Escherichia coli. Proc Natl Acad Sci U S A **99:**7060-5.

6. **Bray, D., M. D. Levin, and C. J. Morton-Firth.** 1998. Receptor clustering as a cellular mechanism to control sensitivity. Nature **393:**85-8.
7. **Chenna, R., H. Sugawara, T. Koike, R. Lopez, T. J. Gibson, D. G. Higgins, and J. D. Thompson.** 2003. Multiple sequence alignment with the Clustal series of programs. Nucleic Acids Res **31:**3497-500.

8. **Craven, R. C., and T. C. Montie.** 1983. Chemotaxis of Pseudomonas aeruginosa: involvement of methylation. J Bacteriol **154:**780-6.

9. **Danielson, M. A., R. B. Bass, and J. J. Falke.** 1997. Cysteine and disulfide scanning reveals a regulatory alpha-helix in the cytoplasmic domain of the aspartate receptor. J Biol Chem **272:**32878-88.

10. **Duke, T. A., and D. Bray.** 1999. Heightened sensitivity of a lattice of membrane receptors. Proc Natl Acad Sci U S A **96:**10104-8.

11. **Figurski, D. H., and D. R. Helinski.** 1979. Replication of an origin-containing derivative of plasmid RK2 dependent on a plasmid function provided in trans. Proc Natl Acad Sci U S A **76:**1648-52.

12. **Gestwicki, J. E., A. C. Lamanna, R. M. Harshey, L. L. McCarter, L. L. Kiessling, and J. Adler.** 2000. Evolutionary conservation of methyl-accepting chemotaxis protein location in Bacteria and Archaea. J Bacteriol **182:**6499-502.

13. **Greer-Phillips, S. E., B. B. Stephens, and G. Alexandre.** 2004. An energy taxis transducer promotes root colonization by Azospirillum brasilense. J Bacteriol **186:**6595-604.

14. **Harrison, D. M., J. Skidmore, J. P. Armitage, and J. R. Maddock.** 1999. Localization and environmental regulation of MCP-like proteins in Rhodobacter sphaeroides. Mol Microbiol **31:**885-92.

15. **Ishikawa, J., and K. Hotta.** 1999. FramePlot: a new implementation of the frame analysis for predicting protein-coding regions in bacterial DNA with a high G + C content. FEMS Microbiol Lett **174:**251-3.

16. **Keymer, J. E., R. G. Endres, M. Skoge, Y. Meir, and N. S. Wingreen.** 2006. Chemosensing in Escherichia coli: two regimes of two-state receptors. Proc Natl Acad Sci U S A **103:**1786-91.

17. **Kirby, J. R., T. B. Niewold, S. Maloy, and G. W. Ordal.** 2000. CheB is required for behavioural responses to negative stimuli during chemotaxis in Bacillus subtilis. Mol Microbiol **35:**44-57.

18. **Krikos, A., N. Mutoh, A. Boyd, and M. I. Simon.** 1983. Sensory transducers of E. coli are composed of discrete structural and functional domains. Cell **33:**615-22.

19. **Le Moual, H., and D. E. Koshland, Jr.** 1996. Molecular evolution of the C-terminal cytoplasmic domain of a superfamily of bacterial receptors involved in taxis. J Mol Biol **261:**568-85.

20. **Letunic, I., R. R. Copley, S. Schmidt, F. D. Ciccarelli, T. Doerks, J. Schultz, C. P. Ponting, and P. Bork.** 2004. SMART 4.0: towards genomic data integration. Nucleic Acids Res **32:**D142-4.

21. **Li, M., and G. L. Hazelbauer.** 2004. Cellular stoichiometry of the components of the chemotaxis signaling complex. J Bacteriol **186:**3687-94.

22. **Maddock, J. R., and L. Shapiro.** 1993. Polar location of the chemoreceptor complex in the Escherichia coli cell. Science **259:**1717-23.

23. **Maki, N., J. E. Gestwicki, E. M. Lake, L. L. Kiessling, and J. Adler.** 2000. Motility and chemotaxis of filamentous cells of Escherichia coli. J Bacteriol **182:**4337-42.

24. **Marx, C. J., and M. E. Lidstrom.** 2002. Broad-host-range cre-lox system for antibiotic marker recycling in gram-negative bacteria. Biotechniques **33:**1062-7.

25. **Okon, Y., and C. A. Labandera-Gonzalez.** 1994. Agronomic applications of Azospirillum: an evaluation of 20 years worldwide field inoculation. Soil Biol. Biochem. **26:**1591-1601.

26. **Okon, Y., and J. Vanderleyden.** 1997. Root-associated Azosprillum species can stimulate plants. ASM News **63:**366-370.

27. **Sambrook, J., E. F. Fritsch, and T. A. Maniatis.** 1989. Molecular cloning: a laboratory manual, 2nd ed. Cold Spring Harbor Laboratory Press, Cold Spring Harbor, N.Y.

28. **Shimizu, T. S., N. Le Novere, M. D. Levin, A. J. Beavil, B. J. Sutton, and D. Bray.** 2000. Molecular model of a lattice of signalling proteins involved in bacterial chemotaxis. Nat Cell Biol **2:**792-6.

29. **Simon, R., U. Priefer, and A. Pülher.** 1983. A broad host range mobilization system for in vivo genetic engineering transposon mutagenesis in gram-negative bacteria. Biotechnology **1:**784-791.

30. **Sourjik, V.** 2004. Receptor clustering and signal processing in E. coli chemotaxis. Trends Microbiol **12:**569-76.

31. **Sourjik, V., and H. C. Berg.** 2004. Functional interactions between receptors in bacterial chemotaxis. Nature **428:**437-41.

32. **Sourjik, V., and H. C. Berg.** 2000. Localization of components of the chemotaxis machinery of Escherichia coli using fluorescent protein fusions. Mol Microbiol **37:**740-51.

33. **Surette, M. G., and J. B. Stock.** 1996. Role of alpha-helical coiled-coil interactions in receptor dimerization, signaling, and adaptation during bacterial chemotaxis. J Biol Chem **271:**17966-73.

34. **Teleman, A. A., P. L. Graumann, D. C. Lin, A. D. Grossman, and R. Losick.** 1998. Chromosome arrangement within a bacterium. Curr Biol **8:**1102-9.

35. **Vande Broek, A., M. Lambrecht, and J. Vanderleyden.** 1998. Bacterial chemotactic motility is important for the initiation of wheat root colonization by Azospirillum brasilense. Microbiology **144 (Pt 9):**2599-606.

36. **Vande Broek, A., M. Lambrecht, and J. Vanderleyden.** 1995. The role of bacterial motility, chemotaxis, and attachment in bacteria-plant interactions. Mol. Plant-Microbe Interactions **8:**800-810.

37. **Vanstockem, M., K. Michiels, J. Vanderleyden, and A. P. Van Gool.** 1987. Transposon Mutagenesis of Azospirillum brasilense and Azospirillum lipoferum: Physical Analysis of Tn5 and Tn5-Mob Insertion Mutants. Appl Environ Microbiol **53:**410-415.

38. **Wadhams, G. H., A. C. Martin, and J. P. Armitage.** 2000. Identification and localization of a methyl-accepting chemotaxis protein in Rhodobacter sphaeroides. Mol Microbiol **36:**1222-33.

39. **Wadhams, G. H., A. C. Martin, S. L. Porter, J. R. Maddock, J. C. Mantotta, H. M. King, and J. P. Armitage.** 2002. TlpC, a novel chemotaxis protein in Rhodobacter sphaeroides, localizes to a discrete region in the cytoplasm. Mol Microbiol **46:**1211-21.

40. **Wadhams, G. H., A. V. Warren, A. C. Martin, and J. P. Armitage.** 2003. Targeting of two signal transduction pathways to different regions of the bacterial cell. Mol Microbiol **50:**763-70.

41. **Zhulin, I. B.** 2001. The superfamily of chemotaxis transducers: from physiology to genomics and back. Adv Microb Physiol **45:**157-98.

42. **Zhulin, I. B., V. A. Bespalov, M. S. Johnson, and B. L. Taylor.** 1996. Oxygen taxis and proton motive force in Azospirillum brasilense. J Bacteriol **178:**5199-204.

CHAPTER THREE

A published manuscript

The Role of CheB and CheR in the Complex Chemotactic and Aerotactic Pathway of *Azospirillum brasilense*

Bonnie B. Stephens[1], Star N. Loar[2], and Gladys Alexandre[3]

Stephens, B.B., S. N. Loar, and G. Alexandre. 2006. The Role of CheB and CheR in the Complex Chemotactic and Aerotactic Pathway of *Azospirillum brasilense.* J. Bacteriol. 188: 4759-4768.

1. Graduate student who performed chemotaxis assays (swarm plates, temporal, aerotaxis), methanol release assays, and wrote preliminary drafts of the manuscript

2. Undergraduate student who performed swarm plate assays

3. Professor and mentor who provided laboratory space and equipment and supervised the project

The Role of CheB and CheR in the Complex Chemotactic and Aerotactic Pathway of *Azospirillum brasilense*

Running title: CheB and CheR in *A. brasilense*

Bonnie B. Stephens[1], Star N. Loar[1], and Gladys Alexandre[1,2]*

Department of Biology, Georgia State University, Atlanta, Georgia 30303[1]

Department of Biochemistry, Cellular and Molecular Biology and Department of Microbiology, The University of Tennessee, Knoxville, TN 37996[2]

*Corresponding author. Mailing address: Department of Biochemistry, Cellular and Molecular Biology, M407 Walters Life Sciences Building, The University of Tennessee, Knoxville, TN 37996. Tel. (865) 974-0866. Fax (865) 974-6306, E-mail: galexan2@utk.edu.

ABSTRACT

It has been previously reported that the alpha-proteobacterium *Azospirillum brasilense* undergoes methylation-independent chemotaxis; however, a recent study revealed *cheB* and *cheR* genes in this organism. We have constructed *cheB, cheR* and *cheBR* mutants of *A. brasilense* and determined that CheB and CheR proteins under the study significantly influence chemotaxis and aerotaxis, but are not essential for these behaviors to occur. First, we found that although cells lacking CheB, CheR, or both were no longer capable of responding to the addition of most chemoattractants in a temporal gradient assay, they did show the chemotactic response (albeit reduced) in the spatial gradient assay. Second, in comparison to the wild type, *cheB* and *cheR* mutants under steady-state conditions exhibited an altered swimming bias, whereas the *cheBR* mutant and the *che* operon mutant did not. Third, *cheB* and *cheR* mutants were null for aerotaxis, whereas the *cheBR* mutant showed reduced aerotaxis. In contrast to the swimming bias for the model organism *Escherichia coli*, the swimming bias in *A. brasilense* cells was dependent on the carbon source present and cells released methanol upon addition of some attractants and upon removal of other attractants. In comparison to the wild type, the *cheB, cheR* and *cheBR* mutants showed various altered patterns of the methanol release upon exposure to attractants. This study reveals a significant difference between the chemotaxis adaptation system of *A. brasilense* and that of the model organism *E. coli* and suggests that multiple chemotaxis systems are present and contribute to chemotaxis and aerotaxis in *A. brasilense*.

INTRODUCTION

The ability of bacteria to detect and respond to a broad range of environmental conditions is important for their survival. The chemotaxis system allows coordination of flagellar movement with temporal sensing of the environment. Chemotaxis has been studied in great detail in the model organism *Escherichia coli* (27, 36). The chemotaxis system integrates environmental cues into a behavioral response using a dedicated signal transduction pathway. This pathway is composed of chemotaxis transducers, a histidine kinase protein CheA coupled to the chemotaxis transducers via a docking protein CheW, a response regulator CheY, and adaptation proteins CheB and CheR. Homologous chemotaxis systems have been identified in distantly related Bacteria and Archaea (33, 41).

Prototypical chemotaxis transducers have an N-terminal extracellular sensory domain that detects environmental cues and a cytoplasmic C-terminal signaling domain that interacts with CheA to convey the signal to the flagellar motor via the CheY protein (8, 36). In order to respond to chemical gradients, motile cells possess an adaptation mechanism that allows them to make temporal comparisons of the chemical conditions in the environment as they swim about. Adaptation in chemotaxis is due to the activity of the chemotaxis transducer-specific enzymes: the CheR methyltransferase and the CheB methylesterase (32). CheR constitutively adds methyl groups from S-adenosylmethionine to specific glutamate residues on the C-terminal domain of chemotaxis transducers. Upon activation by phosphotransfer from CheA, phosphorylated CheB removes the methyl groups as methanol, thereby resetting transducers into a “sensing mode”. The ability of CheB to remove methyl groups as methanol has been used to design a continuous flow

assay to detect CheB activity in *E. coli* (15). The covalent modification of chemotaxis transducers by methylation is accompanied by a return to a pre-stimulus swimming bias. In *E. coli*, CheB is activated in response to negative stimuli, such as the removal of an attractant, whereas positive stimuli, such as the addition of an attractant, suppress its activity and thus methanol release (15). These characteristics result in a single type of methanol release profile in *E. coli*. However, nonenteric bacteria diverge from this paradigm. As with *E. coli*, *Bacillus subtilis* also possess a single set of chemotaxis proteins including CheR and CheB. However, in *B. subtilis*, methanol is released in response to both the addition and the removal of an attractant (16, 34), resulting in a single type of methanol release profile which is different from that of *E. coli*. Not all chemotactic responses require methylation-dependent adaptation. For example, with *E. coli*, aerotaxis and chemotaxis to phosphoenolpyruvate transport system sugars are methylation-independent (6, 22).

The role of methylation in chemotaxis has been studied with other chemotactic organisms. The archaeon *Halobacterium salinarum* releases methanol in response to both positive and negative chemical and light stimuli (23, 24), showing the same type of methanol release profile as *B. subtilis* (16). The alpha-proteobacterium *Rhodospirillum centenum* releases methanol in response to a negative stimulus, a reduction in light intensity, similarly to the *E. coli* pattern (14). The most significant difference from the model organisms in methanol release was observed with another alpha-proteobacterium, *Rhodobacter sphaeroides,* where methanol release was detected only in response to positive stimuli (20). These variations suggest that there is significant diversity in the

adaptation mechanisms among bacteria and archaea and that some adaptation systems are considerably more complex than that described for *E. coli* (33, 36).

Azospirillum brasilense is a nitrogen-fixing alpha-proteobacterium that colonizes the rhizosphere of various agronomically important grasses and cereals, promoting plant growth (5, 30). The dominant motility responses of *A. brasilense* is a metabolism-dependent form of taxis known as energy taxis (1). It has been previously reported that *A. brasilense* undergoes methylation-independent taxis responses (42). A chemotaxis operon controlling motility and aerotaxis was recently identified in this species by complementation of generally non-chemotactic mutants (12). The operon contains genes encoding a CheB methylesterase and a CheR methyltransferase, suggesting a role for methylation-dependent motile behavior in *A. brasilense*. In this study, we investigated the role of these two proteins in *A. brasilense* chemotaxis and aerotaxis. Our data indicate that CheB and CheR contribute to a complex methylation-dependent and methylation-independent motility behavior and are important for chemotaxis and aerotaxis. These findings expand our current view of the diversity in bacterial chemotaxis.

MATERIALS AND METHODS

Bacterial strains and plasmids

A wild type *A. brasilense* Sp7 (ATCC 29145) strain was used throughout this study. Other bacterial strains and plasmids used are listed in Table 3.1. *A. brasilense* cells were grown at 28°C in minimal medium (MMAB) (35)**,** supplemented with a carbon source of choice. Cells were grown aerobically at 200 rpm on a rotary shaker. The growth medium was supplemented with the antibiotics kanamycin (30 μg ml^{-1}), tetracycline (10 μg ml^{-1}),

Table 3.1. Strains and plasmids used in this study.

Strain or plasmid	Properties	Reference or source
Strains		
A. brasilense Sp7	Wild type strain	ATCC 29145
GA3	*cheB* mutant, *cheB*::*gusAKm*, Km^r	This work
BS104	*cheBR* mutant, Km^r	This work
BS109	*cheR* mutant; Gm^r	This work
BS110	*che* mutant; *cheAΔ::gusAKm*; Km^r, Tet^r	This work
E. coli		
EC100	General cloning strain	Epicentre
DH5α	General cloning strain	Gibco BBL
EC100-pir16	General cloning strain with *pir-116*	Epicentre
JM110	General cloning strain; dam^-dcm^-	Stratagene
S17-1	*thi endA recA hsdR* with RP4-2Tc::Mu-Km::Tn*7* Integrated in chromosome	26
Plasmids		
pUCBR	*cheBR* from pFAJ451 cloned as a *Avi*II/*EcoR*I fragment into pUC18	This work
pBSKBR	pBluescript SK II(+) containing *cheBR* from pUCBR as a *EcoR*I/*BamH*I fragment	This work
pBS101	pBSKBR digested with *Ehe*I and *Sma*I; Δ*cheBR* with Km^r cassette from pHP45Ω	This work
pBS102	Δ*cheBR*::Km^r from pBS101 cloned into pCR-blunt	This work
pBS103	Δ*cheBR*::Kan^r cloned into pSUP202	This work
pBS107	*cheR* PCR fragment cloned into pCR 2.1 TOPO	This work
pBS108	*cheR* fragment from pBS107 cloned into pKNOCK-Gm	This work
pGA1	pUCBR containing *gusA*::Km^r cassette from pWM6; Δ*cheB*	This work
pGA2	Δ*cheBR*::Km^r from pGA1 cloned into pCR-blunt	This work
pGA3	Δ*cheBR*::Km^r from pGA2 cloned as an *EcoR*I fragment into pSUP202	This work
pGA111	pBluescript SK (+) containing *cheA* with 545 bp upstream cloned as a *Hind*III/*Xho*I PCR fragment	This work
pGA112	pGA111 with a 555 bp internal deletion of *cheA* by inverse PCR and digestion with *BglII*	This work
pGA113	pGA112 with a 1975 bp deletion containing a *gusA*::Km^r cassette from pWM6	This work

Table 3.1 (cont.). Strains and plasmids used in this study.

Strain or plasmid	Properties	Reference or source
pGA114	pCR-blunt containing *cheAΔ::gusA::Km* from pGA113	This work
pGA115	*cheAΔ::gusA::Km* from pGA114 cloned into pSUP202	This work
pFAJ451	pLAFR1 cosmid clone containing the *A. brasilense* chemotaxis operon	12
pUC18	cloning vector; Ap^r	39
pBluescript SK II(+)	cloning vector; Ap^r	Stratagene
pCR-blunt	cloning vector; Km^r	Invitrogen
pCR2.1 TOPO	cloning vector; Km^r	Invitrogen
pKNOCK-Gm	Mobilizable plasmid, suicide vector for *A. brasilense*; Gm^r	3
pRK2013	Helper plasmid, carries *tra* genes; Km^r	10
pSUP202	Mobilizable plasmid, suicide vector for *A. brasilense*; Cm^r Tc^r Ap^r	26
pWM6	Source of *gusA*-Km^r cassette; Ap^r Km^r	21
pHP45Ω-Km	Ap^r Km^r	9

and gentamycin (10 μg ml^{-1}). Kanamycin (50 μg ml^{-1}) and gentamycin (5 μg ml^{-1}) were added to media to grow *E. coli* when appropriate.

Mutant construction

All standard cloning steps were carried out as described previously (25). The cosmid pFAJ451 was digested with AviII and EcoRI to release a fragment containing the *cheB* and *cheR* genes which was then cloned into the SmaI and EcoRI sites of pUC18, resulting in pUCBR. pUCBR was transformed into *E. coli* JM110 competent cells. To create a *cheB* mutant, a SmaI-excised *gusA-km* cassette from pWM6 (21) was cloned into the SmaI and T4 Klenow fragment end-repaired BclI sites of pUCBR, yielding pGA1. pGA1 was digested completely with EcoRI and partially with BamHI, end-repaired (End-it repair kit, Epicentre, Madison, WI) and cloned into pCR-Blunt (Invitrogen, Carlsbad, CA), yielding pGA2. EcoRI digested pGA2 was cloned into the same site of pSUP202, resulting in pGA3. *E. coli* S17-1 competent cells were transformed with pGA3 and used as a donor in a biparental mating with *A. brasilense* (35). Recombinants were screened for double homologous recombination and in-frame insertion of the cassette by replica plating and testing for GusA activity (21). One such recombinant, GA3, was further characterized as a *cheB* mutant (Table 3.1).

To create a *cheBR* insertion-deletion mutant, an EcoRI/BamHI fragment was isolated from pUCBR and cloned into the same sites of pBluescript II SK (+), resulting in pBSKBR. A polar kanamycin cassette was excised from pHP45Ω by HindIII digestion, end-repaired, and blunt-cloned into the SmaI and end-repaired EheI sites of pBSKBR, yielding pBS101. An end-repaired EcoRI and NotI fragment from pBS101 containing the

Δ*cheBR*::Km^R construct was cloned into pCR-Blunt (Invitrogen), resulting in pBS102. PCR using pBS102 as a template and the primers CheBR-F (5'-CCGGAATTCGCAAGATGAGCGGCGGGGACA) and CheBR-R (5'-CGGAATTCGCGGAAGGAGGCCATCTGGCG) was used to amplify the Δ*cheBR*::Km^R construct, which was then digested with EcoRI (engineered restriction sites, underlined) and cloned into the EcoRI-digested pSUP202 (26), yielding pBS103. *E. coli* EC100 cells (Epicentre) were transformed with pBS103 and transferred to *A. brasilense* by triparental mating using pRK2013 as a helper (10), as described previously (12). Screening for double homologous recombination was performed as described above. Southern hybridization was used to verify the loss of the plasmid. One such *cheBR* mutant (BS104) was further characterized (Table 3.1).

To construct a *cheR* mutant, an internal fragment of *cheR* was amplified by PCR using the primers CheR-F1 (5'-CGACATCACGGAGGCG) and CheR-R1 (5'-CACTTGTCGCCCTGCTG) and cloned into pCR2.1TOPO (Invitrogen), resulting in pBS107. pBS107 was digested with EcoRI and cloned into the EcoRI site of pKNOCK-Gm (3), a plasmid that does not replicate in *A. brasilense*, resulting in pBS108. *E. coli* EC100D *pir*-116 cells were transformed with pBS108 and introduced into *A. brasilense* by triparental mating. Single homologous recombination resulted in a *cheR* gene interrupted by the insertion of the pKNOCK-Gm vector (*cheR* mutant, BS109) (Table 3.1). Because *cheR* is the last gene of the chemotaxis operon (12), no polar effects were expected.

A chemotaxis operon mutant was constructed by inserting a polar cassette in *cheA*, the first gene of the operon (12), thereby disrupting the entire operon. First, a

fragment comprising the entire *che*A gene and 545 bp of DNA sequence upstream of the chemotaxis operon was amplified from pFAJ451 using the primers cheAop-HindF (CCCAAGCTTCAGCGCGATGAACTGGTTGGACC) and cheAY-XhoR (GGGCTCGAGTCATGCGGCACCTTTCTGCTC) followed by digestion with HindIII and XhoI sites (engineered restriction sites, underlined) and cloned into the same sites of pBluescript II SK (+), yielding pGA111. An inverse PCR-based strategy (38) using primers CheA-Del-F (5' GAAGATCTGCGGTCGCGCGGGAATTC) and CheA-Del-R (5' GAAGATCTGACCGCGTCCGCCGCACG) (engineered BglII sites are underlined) and pGA111 as a template generated a linear product with BglII sites at both ends of an internal 555 bp fragment to be deleted, which was precisely deleted by digestion followed by self-ligation. The construct, pGA112, was verified by sequencing. BglII and NcoI digestion followed by end-repair of the restriction sites deleted an additional 1,975 bp internal fragment. A SmaI-digested *gusA-Km* cassette from pWM6 (21) was inserted into the deleted region, yielding pGA113. The *cheAΔ::gusA-Km* construct was released from pGA113 by digestion with XhoI, made blunt by end-repair and SmaI digestion and cloned into pCR-Blunt (Invitrogen, Carlsbad, CA), yielding pGA114. An EcoRI digestion of pGA114 released *cheAΔ::gusA-km* for cloning into EcoRI- digested pSUP202, yielding pGA115. pGA115 was introduced into *A. brasilense* by triparental mating using pRK2013 as a helper. Single homologous recombinants carrying a deletion-insertion in *cheA* and the inserted pSUP202 plasmid were selected. Southern hybridization and PCR were used to verify the insertion of the recombinant plasmid. One such *che* mutant (BS110) was further characterized (Table 3.1).

All final constructs were verified by sequencing (DNA Core Facility, The University of Tennessee) prior to transfer to *A. brasilense* for conjugation and mutant construction.

Behavioral assays

A. brasilense cells swim by rotating a single bidirectional polar flagellum (42). A change in swimming direction (reversal) is brought about by a short backward movement along the axis of the cell due to the switch in direction of flagellar rotation coupled to a reduction in swimming speed, which randomly reorients the cells in a new direction (42, 43). Cells were grown in MMAB supplemented with a carbon source of choice (10 mM) to early exponential phase, observed with a dark-field microscope, and videotaped. Reversal frequency was measured by determining the number of reversals of a single cell during a 5-s time frame, corresponding to the average time a single cell can be tracked. Increasing the tracking time did not change the results. The reversal frequencies of at least 90 cells (from three independent cultures) were measured in each experiment. The reversal frequency of cells washed in chemotaxis buffer (10 mM phosphate buffer [pH 7.0], 1 mM EDTA) prior to analysis was similar to that described above.

Soft agar plates (so called “swarm plates”) and temporal gradient assays for chemotaxis and aerotaxis were performed as previously described (1, 2, 42, 43). Temporal response to attractants was measured after growing cells in MMAB to an early exponential phase, washing the cells three times and resuspending them in chemotaxis buffer. To estimate the response time to the removal of an attractant, the cells were mixed with the attractant to be tested at a final concentration of 10 mM. The cells were then

stimulated by the addition of chemotaxis buffer to dilute the concentration of the attractant from 10 mM to 2.5 mM, eliciting a repellent response. The time taken for approximately 50% of the population to return to the prestimulus motility bias was measured. The temporal gradient assay for aerotaxis was performed in a microchamber ventilated with oxygen and nitrogen gases in a set up developed by Laszlo and Taylor (18) and adapted for *A. brasilense* (43). The spatial gradient assay for aerotaxis was performed as previously described (43) by placing motile cells in an optically flat capillary (inner dimensions 0.1 by 2 by 50 mm; Vitro Dynamics Inc, Rockaway, N. J.). The cells used were washed and resuspended in chemotaxis buffer supplemented with 10 mM malate.

Continuous flow assay

Continuous flow assays were performed as previously described for stimulation with chemicals in *E. coli* (15) and with oxygen in *Halobacterium salinarum* (19) with some modifications. Cells were grown to the late exponential phase in MMAB supplemented with 5 mM malate and 5 mM fructose. Cells were washed with chemotaxis buffer with chloramphenicol (100 μg ml^{-1}), incubated with 50 μCi L-[*methyl*-^{3}H] methionine (Amersham Biosciences) with chloramphenicol (100 μg ml^{-1}) for 2 h, and placed on a sterile in-line filter (Acrodisc 0.45 μm, Pall Gelman) connected to a peristaltic pump. The filter was washed at a flow rate of 3 ml/min for 35 minutes with chemotaxis buffer, 10 minutes with an attractant (10 mM) in chemotaxis buffer, and 5 minutes with chemotaxis buffer. Fractions were collected every 30 s. An aliquot (100 μl) from each fraction was placed in a microfuge tube in scintillation fluid (Beckman Ready solv-HP) and subjected

to vapor phase transfer for 48 hours. The samples were counted for 10 minutes in a scintillation counter (LS 6500; Beckman Instruments). For methanol release in aerotaxis, N_2 or O_2 (21%) was bubbled though chemotaxis buffer or attractant and washed over the filter assembly as described previously (19).

Statistical Analysis

Microsoft Excel was used for statistical analysis of results. A *t*-test assuming equal variances using a *P* value = 0.01 was used to determine whether there was a significant difference between the mutants and the wild type in behavioral assays.

RESULTS

Mutants lacking CheB and CheR are impaired in chemotaxis. We constructed mutants defective in the *cheB* and/or *cheR* gene and characterized their motile behavior. First, we tested chemotaxis of the wild type and the *cheB*, *cheR,* and *cheBR* mutants to strong chemoattractants (1) by using the soft agar plate assay. We define strong and weak attractants based on their ability to trigger a response in spatial and temporal gradient assays: strong attractants elicit longer response times in a temporal gradient assay and a lower threshold in a spatial gradient assay. Malate, succinate, fructose, and oxygen are strong attractants, while galactose is a weaker attractant for *A. brasilense* (1). We found that the *cheB*, *cheR,* and *cheBR* mutants were significantly impaired in their swimming ability in this assay. The chemotactic rings formed by the mutants were significantly smaller in diameter than those formed by the wild type strain for all substrates tested (Fig.

3.1). The growth rates of the mutants were measured and found to be statistically undistinguishable from that of the wild type (data not shown).

A temporal gradient assay provides a direct measurement of the frequency of flagellar rotation changes of individual cells challenged with a stimulus. Potent attractants cause free-swimming wild type *A. brasilense* cells to swim smoothly and then resume the pre-stimulus motility pattern. We measured the response times of free-swimming cells challenged with both positive and negative stimuli. Response times of the wild type strain *A. brasilense* upon addition of strongest attractants succinate, malate, and fructose were similar (Table 3.2). Surprisingly, cells lacking CheB and/or CheR were no longer capable of responding to the addition of these attractants. On the other hand, *cheB* and *cheBR* mutants not only responded, but also adapted upon addition of a weaker attractant galactose. Upon removal of malate, succinate, fructose, and galactose, wild type cells increased swimming reversal frequency, indicating a repellent response. The mutant cells either did not respond at all or showed no adaptation to the stimulus (Table 3.2). We analyzed the swimming bias of the wild-type cells in the presence of a constant concentration of an attractant (steady-state conditions). Under steady-state conditions, *E. coli* mutants lacking CheB and CheR have tumbly and smooth swimming biases, respectively, whereas the double mutant has a motility bias similar to that of the wild-type strain. The *A. brasilense cheBR* mutant had random steady-state swimming bias similar to that of the wild type. Interestingly, the wild type cells and the *cheBR* mutant had different swimming biases dependent on the substrate present: the reversal frequency was higher when cells were grown on fructose relative to malate. Similarly, the swimming bias of *cheB* and *cheR* mutants was also dependent on the substrate present;

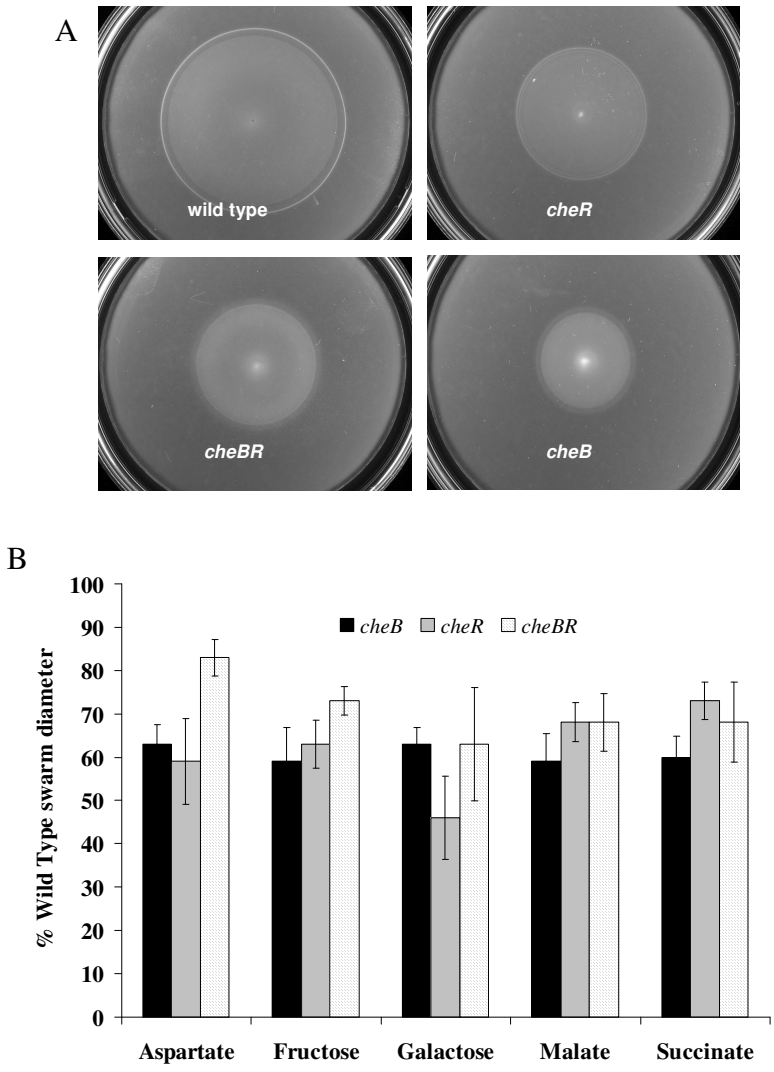

Fig. 3.1. *cheBR, cheB, and cheR* mutants are deficient in chemotaxis. Chemotaxis of the *A. brasilense* wild-type strain (Sp7) and that of the mutants were compared by soft agar plate assay. Chemotactic-ring diameters were measured after incubation at 28°C for 48 h. (A) Representative soft agar plates with 10 mM malate as the sole carbon source. (B) The average chemotactic-ring diameters are expressed as the percentage relative to that of wild-type strain (defined as 100%). Error bars represent standard deviations from the means calculated from at least three repetitions. Differences in the chemotactic-ring diameters of the wild type and the mutants were found to be statistically significant with all chemoeffectors tested.

Table 3.2. Chemotaxis of *A. brasilense* wild type strain, *cheBR*, *cheB*, and *cheR* mutants in a temporal gradient assay.

	Response time in a temporal assay (s) ± SD									
	malate[a]		succinate		fructose		galactose		oxygen	
	+[b]	-[c]	+	-	+	-	+	-	+	-
Wild type	56 ± 6	43 ± 3	52 ± 7	41 ± 4	63 ± 8	45 ± 3	34 ± 8	26 ± 4	33 ± 4	28 ± 2
cheBR	NR[d]	NR	NR	NR	NR	>300	38 ± 5	>300	NR	NR
cheB	NR	NR	NR	NR	NR	NR	82 ± 7	NR	NR	NR
cheR	NR	>300[e]	NR	NR	NR	NR	NR	NR	NR	NR

[a] Cells were grown with the chemical to be tested as an attractant or repellent and prepared as described in *Material and Methods*.

[b] +: addition of attractant; the chemicals were tested at a final concentration of 10 mM

[c] -: removal of attractant; the chemical concentration was reduced from 10 mM to 2.5 mM (final).

[d] NR: No response, i.e., no change in the swimming bias of cells upon addition or removal of the chemoeffector tested.

[e] Cells responded to the removal of the chemoeffector by changing the swimming bias but did not adapt within 300 seconds of observation.

however it was different from that of the wild-type cells on any given substrate. On malate, the *cheB* mutant had increased reversal frequency, which corresponds to tumbly bias in *E. coli*, and the *cheR* mutant had smooth swimming bias similar to that of its *E. coli* counterparts. However, on fructose, the phenotype displayed by these mutants was reversed (Fig. 3.2).

Mutants lacking CheB and CheR are impaired in aerotaxis. Aerotaxis is arguably the strongest behavioral response in *A. brasilense* (4, 43). We first used the spatial gradient assay for aerotaxis to analyze the role of CheB and CheR. In this assay, an oxygen gradient is established by oxygen diffusion through a suspension of motile cells that contain an electron donor (carbon source). Cells accumulate at the maximum energy levels generated by metabolizing the carbon source using an optimum concentration of oxygen as a terminal electron acceptor (43). We found that the *cheB* and *cheR* mutants were unable to form aerotaxis bands, although the cells were fully motile. Interestingly, the *cheBR* mutant did form an aerotaxis band (Fig. 3.3); however, it was formed with a significant delay (more than 5 min to form the band by the mutant versus less than 2 min by the wild type) and farther away from the meniscus than that formed by the wild type. Several independent studies previously showed that the time required for the formation of the aerotactic band by *A. brasilense* cells in this assay is very consistent (1 to 2 min) and reflects the ability of cells to efficiently sense the oxygen gradient and navigate toward its optimum concentration (1, 4, 43). The observation that the aerotaxis band formed by the CheBR mutant is significantly delayed and formed further away from the meniscus supports the proposition that the CheBR mutant is impaired in aerotaxis.

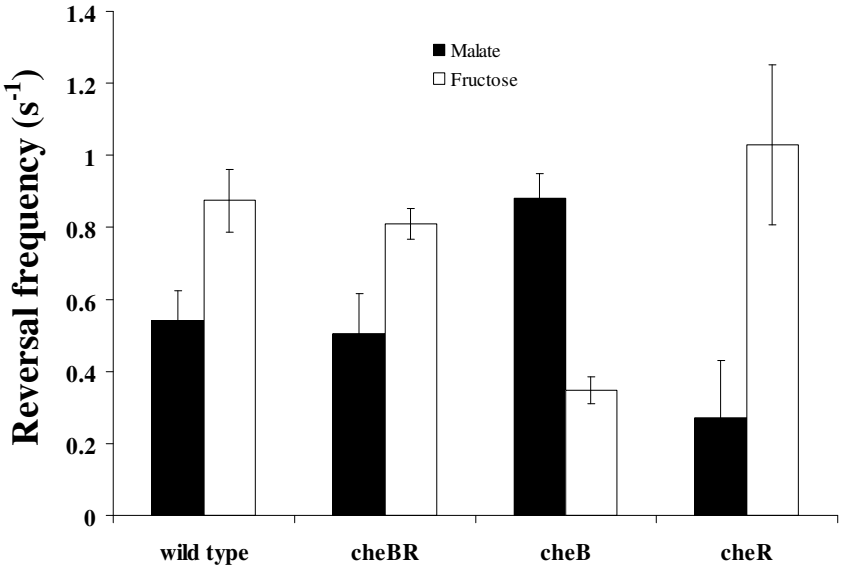

Fig. 3.2. Reversal frequencies of free-swimming cells of wild type *A. brasilense*, the *cheBR*, *cheB* and *cheR* mutants on different carbon sources (filled bars, malate; open bars, fructose). The reversal swimming frequency was determined as described in the Material and Methods section. Standard deviations to the means are indicated.

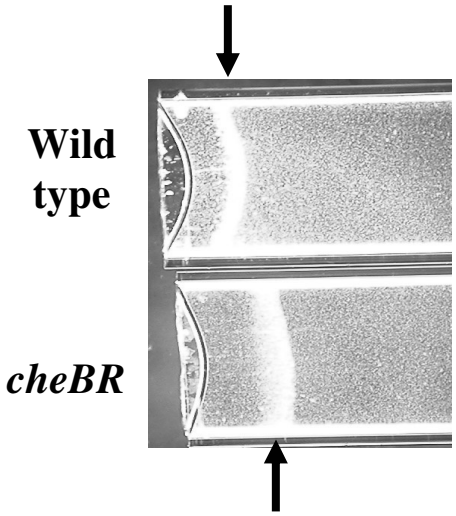

Fig. 3.3. The *cheBR* mutant is impaired in, but not null for, aerotaxis in a spatial gradient assay. The abilities of the *A. brasilense* wild-type strain (Sp7) and the *cheBR* mutant to form a sharp aerotaxis band in a gradient of oxygen in a capillary tube were compared. The wild-type strain (Sp7) forms a sharp aerotaxis band, while the *cheBR* mutant forms a diffuse band at a different position in the gradient. Malate (10 mM) was added as the sole carbon and energy source to the suspension of motile cells. The *cheB* and *cheR* mutants did not form any aerotaxis bands under similar conditions (not shown). Arrows point to the center of the aerotaxis bands.

Interestingly, none of the three mutants responded to either addition or removal of oxygen in a temporal gradient assay for aerotaxis, whereas the wild type had a positive and negative response, respectively (Table 3.2).

Methanol evolution upon chemostimulation. In order to determine the activities of CheB and CheR, we used the methanol release assay (15). We first determined the profile of methanol release from the wild-type cells upon stimulation with various chemoeffectors. The wild-type cells showed a release of methanol upon addition, but not upon removal of malate (Fig. 3.4A). Interestingly, the addition of malate resulted in continuous methanol release (rather than a peak) slowly decreasing over time. This is different from the profiles of methanol release in *E. coli* and *B. subtilis*, but similar to that in *R. sphaeroides*. The wild-type cells also released methanol upon removal of but not upon addition of a weaker attractant galactose (Fig. 3.4C). This type of a profile is typical of *E. coli*. There was no methanol release upon the addition or removal of fructose, succinate, or oxygen (Fig. 3.4B, D, E). Thus, different chemoeffectors induce different methanol release profiles in *A. brasilense*, and there is indication of methylation-independent taxis in response to succinate and oxygen.

Strains deleted of *cheB, cheR,* or both showed a wide spectrum of methanol release profiles (Fig. 3.5). None of the mutants showed methanol release upon either addition or removal of fructose (Fig. 3.5B) and oxygen (not shown). In contrast to wild-type cells, the *cheB* and the *cheR* mutants did not release methanol upon removal of galactose and they released significantly less methanol upon addition of malate (Fig.

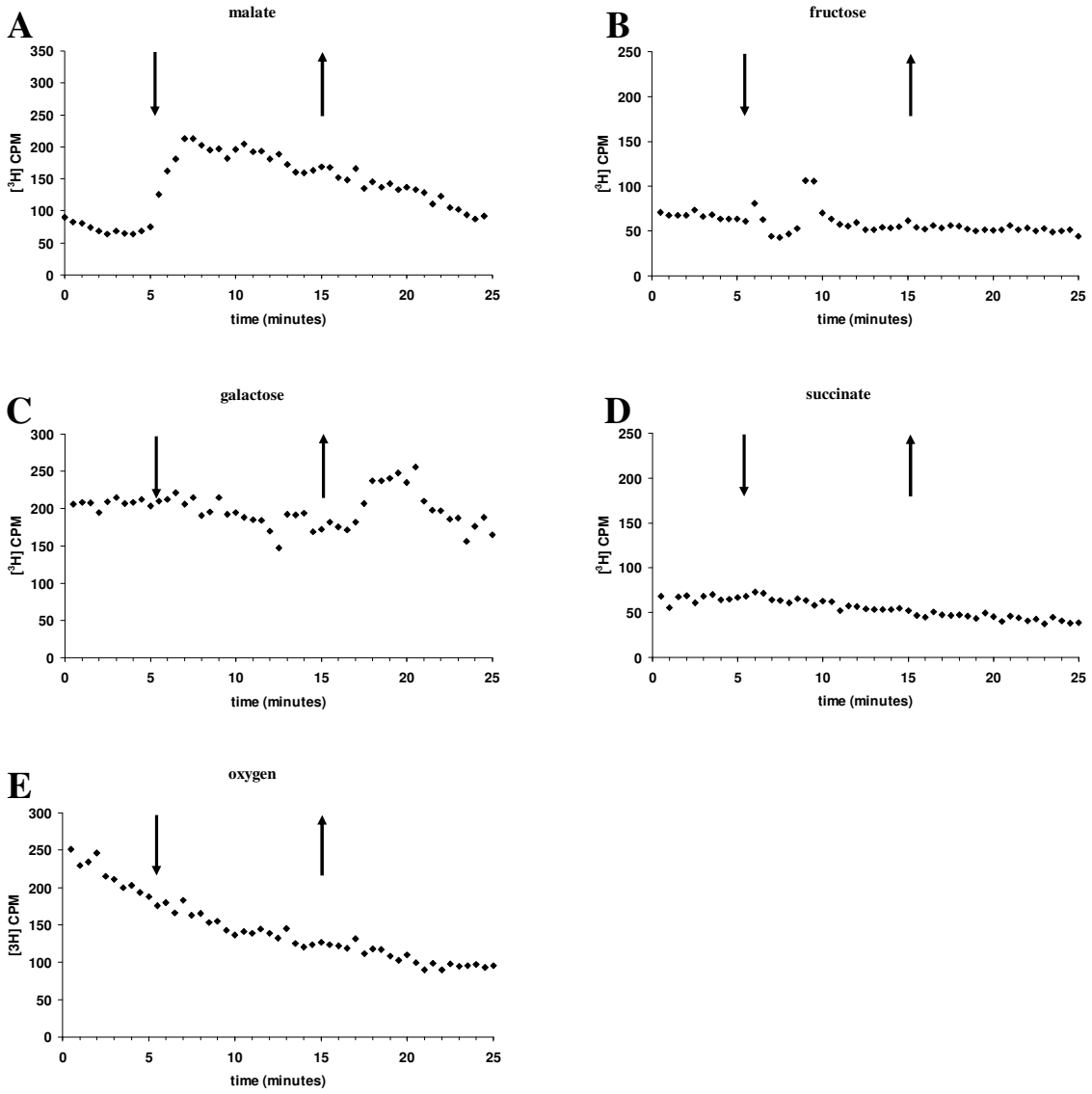

Fig. 3.4. Methanol release from *A. brasilense* wild-type strain upon the addition and removal of chemical attractants (10 mM) and oxygen (shown by arrows). The wild-type strain has different patterns of methanol release, represented as counts per minute (CPM), upon stimulation with malate (A), fructose (B), galactose (C), succinate (D) and oxygen (E). Representative results of at least two independent experiments are shown.

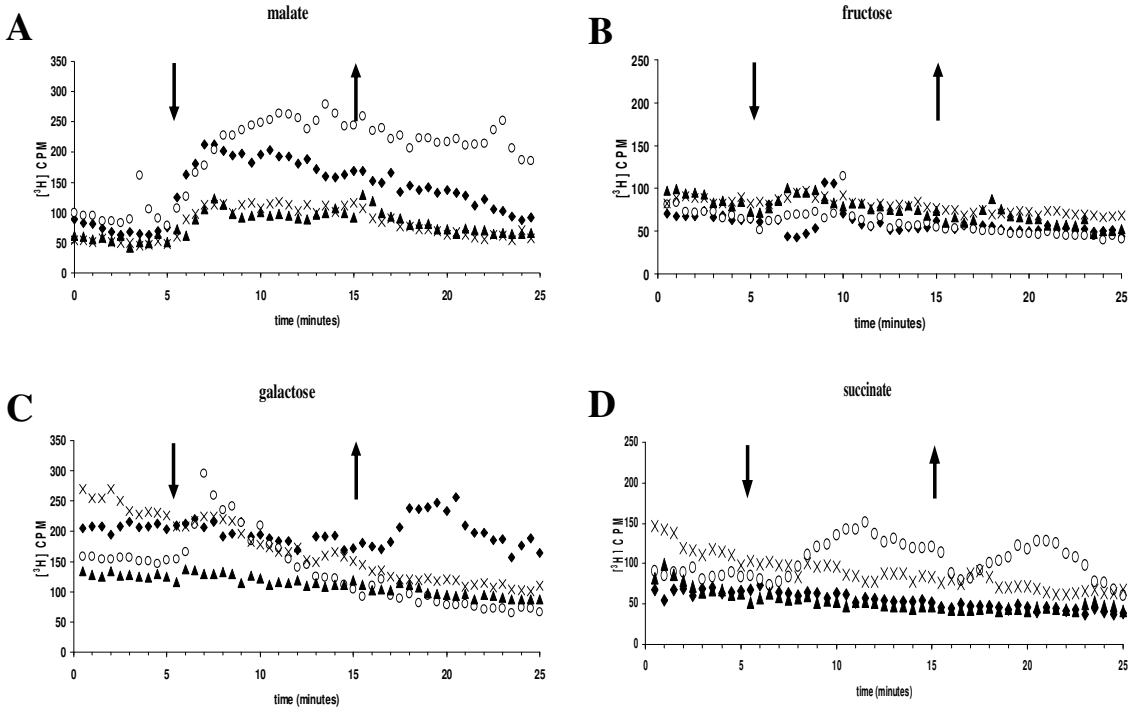

Fig. **3.5**. Methanol release from *A. brasilense* wild-type strain (Sp7) (◆), *cheBR* mutant (○), *cheB* mutant (▲), and *cheR* mutant (×) upon the addition and removal (shown by arrows) of chemoeffectors. Methanol evolution represented as counts per minute (CPM) observed in response to malate (A), fructose (B), galactose (C), succinate (D) is shown. Representative results from at least two independent experiments are shown.

3.5A and C). These results are consistent with a role for CheB and CheR in the induction of methanol release in response to these chemoeffectors.

Unexpectedly, the *cheBR* mutant did release methanol upon the addition of malate, succinate, and galactose as well as upon the removal of succinate (Fig. 3.5A, C, D). Furthermore, the methanol release profile in response to these chemostimuli was different from that of the *cheB* mutant and the wild-type strain. The *cheBR* mutant released methanol upon addition, but not removal of galactose, whereas the wild type did just the opposite (Fig. 3.5C). Also, in response to the addition of malate, this mutant released methanol in significantly higher amounts than the *cheB* mutant and the wild-type strain (Fig. 3.5A). While succinate did not induce methanol release in the wild-type strain, the *cheBR* mutant released methanol upon both addition and removal of succinate (Fig. 3.5D). These results strongly suggest that there are other methylation/demethylation system(s) in *A. brasilense* in addition to the one under investigation.

A *che* operon mutant has modest chemotaxis defects. The limited chemotaxis defects observed for the *cheB* and *cheR* mutants prompted us to further evaluate the function of the chemotaxis pathway in controlling motility. We have constructed a chemotaxis operon insertion mutant (*che* mutant) and characterized its motility (Fig. 3.6). We have found that relative to the wild type, the *che* mutant was impaired in chemotaxis in the soft agar plate assay, but it did form chemotactic rings (Fig. 3.6A, B). These results indicated that the *che* mutant was not null for chemotaxis. Under steady state conditions, the *che* mutant had a chemoeffector-dependent motility bias similar to that of the *cheBR* mutant and the wild-type strain (Fig. 3.6C). Altogether, these data suggest that this

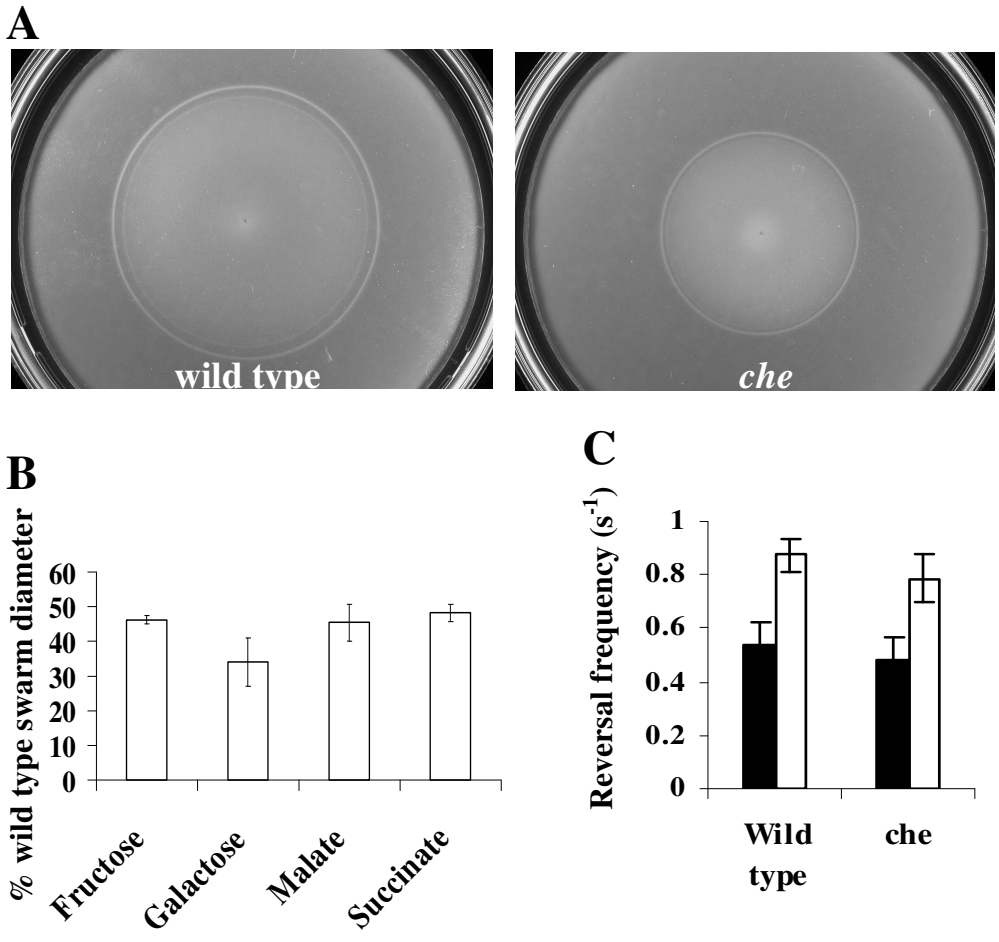

FIG. 3.6. The *che* operon mutant is impaired in, but not null for, chemotaxis. (A) Chemotaxis toward 10 mM malate, as determined by a soft agar plate assay. Both plates were inoculated with the same number of cells and incubated at 28°C for 48 h. (B) The average chemotactic-ring diameters are expressed as percentages relative to that of wild-type strain (defined as 100%). Error bars represent standard deviations from the means, calculated from at least three repetitions. Differences in the chemotactic-ring diameters of the wild type and the *che* operon mutant were found to be statistically significant with all chemoeffectors tested. (C) Reversal frequencies of free-swimming cells of the wild type and the *che* mutant on malate (filled bars) and fructose (open bars). The reversal swimming frequency was determined as described in the Material and Methods. Standard deviations to the means are indicated.

chemotaxis pathway contributes to controlling motility; however, it is probably not its primary function.

DISCUSSION

The identification of *cheB* and *cheR* genes (12) suggested the presence of a methylation-dependent chemotaxis pathway in *A. brasilense*. In this work, we used genetic and biochemical approaches to investigate the role of CheB and CheR in chemotaxis in this bacterium and found that there are both methylation-dependent and methylation-independent pathways for chemotaxis in *A. brasilense*. Our analysis also revealed unexpected phenotypes for the *cheB*, *cheR,* and *cheBR* mutants, further suggesting a more complex role for these proteins in *A. brasilense* than in other species.

CheB and CheR have an effect on but are not essential for chemotaxis and aerotaxis. We have demonstrated that *cheB* and *cheR* mutants contribute to chemotaxis and aerotaxis. Remarkably, all single and double mutants did not respond to stimulation with the strong attractants malate, succinate, fructose and oxygen in a temporal gradient assay. Addition of these attractants did not result in changes in the swimming behavior of the mutants, whereas the wild type cells responded to all stimuli by suppressing the reversal frequency. This is the most striking departure from the behavior of the model organisms *E. coli* and *B. subtilis*, where mutations in the corresponding genes abolish adaptation, but not excitation in the temporal gradient assay (31, 40). Similar behavior has been reported in *R. sphaeroides*, where the $cheB_1$ and $cheR_2$ mutants did not respond to temporal stimulation at all (20). We have found that *cheB* and *cheR* mutants in *A. brasilense* retained the ability (although significantly reduced) to form chemotactic rings

on semisoft agar. This is again different from results from analogous mutants in *E. coli* (40), but similar to those in *R. sphaeroides* (20). The apparent discrepancy between the results obtained in a temporal gradient assay (lack of the response) and in a spatial gradient assay (presence of the response) was also observed for aerotaxis: the *cheBR* mutant formed an aerotaxis band in the spatial gradient assay, but did not respond to the addition or removal of oxygen in a temporal gradient assay. It is noteworthy to mention that the chemotaxis and aerotaxis responses observed in the temporal and spatial gradient assays are not equivalent since the latter assay requires the metabolism of an attractant and cell growth (the chemotaxis assay only). Furthermore, with temporal gradient assays, cells are challenged with extremely steep step gradients of chemoeffectors (that are not physiological), while they respond to much more shallow gradients in the spatial gradient assays. Therefore, the sensitivity of the chemotaxis response tested is different for each of these assays, which could account for the discrepancies observed. Further deviations from the *E. coli* model were detected by analyzing the swimming motility bias of *cheB* and *cheR* mutants. Deletion of *cheB* and *cheR* in *E. coli* results in cells displaying tumbly and smooth-swimming phenotypes, respectively (29, 40) regardless of the substrate present. The *A. brasilense* cells showed a different type of behavior. The wild-type cells had different swimming biases on different substrates, and *cheB* and *cheR* mutants showed a spectrum of motility phenotypes that were dependent on the substrate present. On some substrates, the *cheB* mutant had a high reversal frequency while the *cheR* mutant had a smooth-swimming bias, whereas on other substrates it was just the opposite. These results indicate that CheB and CheR proteins play an important role in the overall chemosensory behavior of *A. brasilense* that does not conform to the *E. coli* model. Our

results also indicate that there are CheBR-independent responses in *A. brasilense*. For example, the *cheBR* mutant not only responded, but also adapted to the addition of galactose in a temporal gradient assay. Thus, mutations in *cheB* and *cheR* do not affect the ability of the cells to respond to temporal stimulation by all effectors. The swimming phenotypes of *cheB* and *cheR* mutants in *A. brasilense* are strikingly different from those of mutants in *E. coli* but similar to mutants lacking principle chemotaxis methylesterase and methyltransferase ($CheB_1$ and $CheR_2$) in *R. sphaeroides*, which is a distant alpha-proteobacterial relative of *A. brasilense*. The reason(s) for these significant differences from the *E. coli* model is currently unknown for either *R. sphaeroides* (20) or *A. brasilense*. In contrast to chemotaxis in *E. coli*, metabolism-dependent chemotaxis has been proposed as a major motility behavior in both *R. sphaeroides* (13) and *A. brasilense* (1, 2, 11) and may be one of the factors contributing to the observed differences.

Evidence for additional methylation/demethylation systems contributing to chemotaxis. We found that the profile of methanol release in *A. brasilense* is chemoeffector-specific: some attractants caused methanol release upon addition, whereas others caused release upon removal. This behavior represents another significant difference between *A. brasilense* and the model organisms and has not been previously reported for any microorganism. It is important to mention that the contribution of CheB and CheR to motility and methanol evolution upon chemostimulation in *A. brasilense* is chemoeffector dependent. One possible explanation is that additional methylation/demethylation system(s) in *A. brasilense* differentially modulates the responses observed. The strongest evidence for the presence of additional adaptation

enzymes comes from the results obtained with the *cheBR* mutant stimulated with succinate. While the wild-type cells did not release methanol upon either addition or removal of succinate, the mutant released a significant amount of methanol both upon addition and removal of attractant. Interestingly, the same profile of methanol release has been reported in the Δ*cheR*$_1$ mutant of *R. sphaeroides* lacking an additional methyltransferase, which did not seem to contribute to chemotaxis under conditions tested (20). Additional methylation/demethylation systems in *A. brasilense* might be responsible for most of the observed phenotypic differences between this bacterium and other organisms. Although the *A. brasilense* genome is not yet available, preliminary data from the on-going sequencing project (http://genomics.biology.gatech.edu/research/azo) indicate that *A. brasilense* might possess at least three additional chemotaxis operons containing CheB and CheR pairs. Future studies will determine whether these systems contribute to chemotaxis or to other cellular function in *A. brasilense*.

Complex contribution of CheB and CheR to aerotaxis. One of the most intriguing findings of the present study is that aerotaxis in *A. brasilense* appears to be methylation-independent. There was no methanol release from either the wild type or any of the mutants upon addition or removal of oxygen in a continuous flow assay, whereas there was methanol release in the same experimental set up when a gradient of malate was introduced instead of oxygen. Nevertheless, the *cheB* and *cheR* mutants had a null phenotype for aerotaxis in both temporal and spatial gradient assays. Aerotaxis was shown to be methylation-dependent in *B. subtilis* (37) and *H. salinarum* (19) and methylation-independent in *E. coli* (6, 22). Normal aerotaxis in *E. coli* requires a CheB

protein; however the absence of the enzyme only inverts (7), but does not abolish the response in a temporal gradient assay, as it does in *A. brasilense*. Our results indicate a similar methylation-independent and CheBR-dependent behavior in response to the strong attractants fructose and succinate. The exact mechanism of methylation-independent sensory adaptation is currently not known for any bacterial species including the model organism *E. coli* (6). However, it is conceivably a major adaptation mechanism in *A. brasilense.*

Model for the role of CheB and CheR. Although this study has established an important role for the CheB and CheR proteins in chemotaxis and aerotaxis in *A. brasilense*, it has revealed a significant departure from the role in model organisms. The contribution of these enzymes to the overall behavior in azospirilla appears to be different from that in the model organism for chemotaxis, *E. coli*, and in other organisms that possess a single set of chemotaxis genes, such as *B. subtilis*. On the other hand, there are many similarities with chemotaxis in *R. sphaeroides*, which emerges as a model to study the motility behavior in organisms with multiple chemotaxis pathways (36). Most of the observed deviations from known features of the chemotactic response are likely due to the presence of multiple chemotaxis pathways in *A. brasilense*. We have shown that not only *cheB* and *cheR* mutants, but also a mutant lacking the entire chemotaxis operon encoding the CheB and CheR proteins is impaired in, but not null for, chemotaxis. Therefore, other chemotaxis pathways contribute to the overall control of flagellar motility.

In order to reconcile the data, we propose a model in which the chemotaxis pathway under study does not primarily control motility and chemotaxis in *A. brasilense*. However, CheB and CheR from this pathway affect the methylation status of chemotaxis transducer(s) that is ultimately involved in controlling chemotaxis, perhaps via cross-regulation with another chemotaxis pathway(s) at the level of chemoreceptor methylation/demethylation (Fig. 3.7). Our findings that multiple methylation/demethylation systems contribute to methanol release in response to a single chemostimulation are consistent with such a model. For *E. coli*, it was proposed that the combined activity of CheB and CheR on chemotaxis transducers modulate signal amplification and sensitivity in chemotaxis (17, 28). We argue that multiple methylation/demethylation systems contribute to the overall methylation status of chemotaxis transducers, which in turn modulates the overall sensitivity of the chemotactic response and chemosensory adaptation. We also argue that in the absence of CheB and/or CheR, the overall methylation status of chemotaxis transducers is modified, altering the sensitivity of the chemotaxis response. This in turn may explain why mutants lacking CheB and/or CheR are unable to respond to essentially any stimuli in a temporal gradient assay while retaining chemotaxis in spatial gradients. Future studies aiming at the identification and characterization of other putative multiple chemotaxis homologs in *A. brasilense* will be critical for understanding the molecular details underlying such complex behavior and will likely lead to the modification of the working model proposed here.

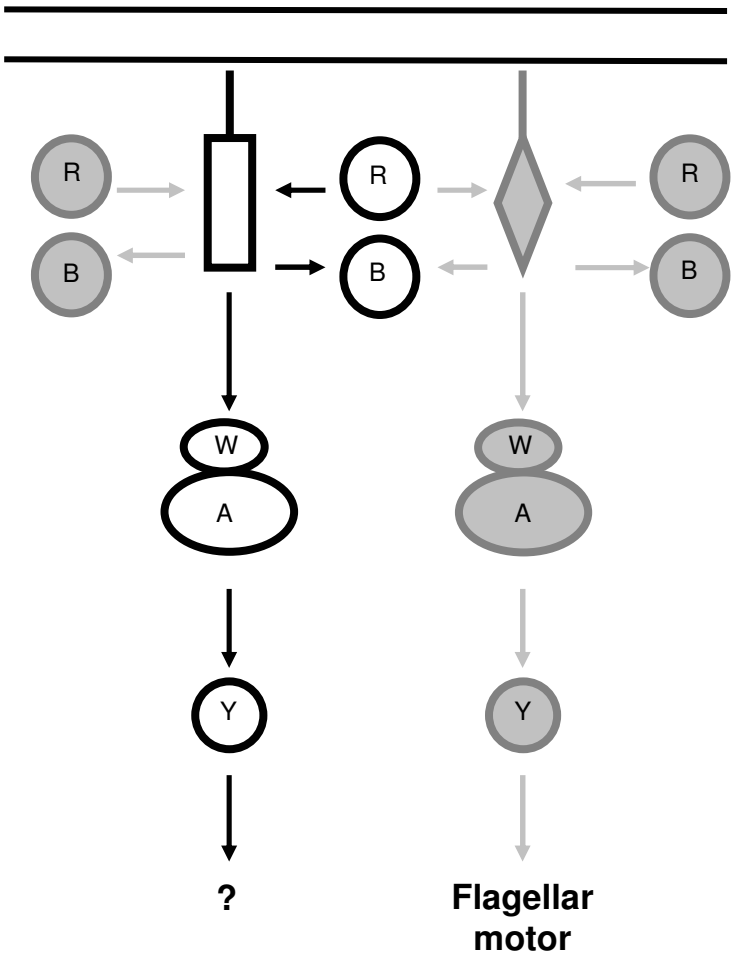

FIG. 3.7. Working model for the role of CheB and CheR proteins in *A. brasilense* chemotaxis. CheB (B) and CheR (R) proteins under study and the *che* pathway are shown in solid black lines. CheA (A), Che (W), and CheY (Y) putative chemotaxis homologs are shown in gray. Cytoplasmic C-terminal domains of putative chemotaxis transducers interacting with CheB and CheR are shown as a rectangle and a diamond. The model argues that the primary function of the chemotaxis pathway under study is probably not to control motility behavior. CheB and CheR may contribute to chemotaxis and aerotaxis because of their effect on the methylation status of the chemotaxis transducer(s) that is ultimately involved in controlling motility (see text for details).

ACKNOWLEDGEMENTS

We thank G. L. Hazelbauer for critical reading of the manuscript and many helpful suggestions and A. Lin and L. Hall for technical assistance.

This work was supported by a CAREER award from the National Science Foundation (MCB-0347218) to G.A. S. N. L. was supported by a NSF REU supplement to the CAREER award.

REFERENCES

1. **Alexandre, G, S. E. Greer, and I. B. Zhulin.** 2000. Energy taxis is the dominant behavior in *Azospirillum brasilense*. J. Bacteriol. **182**: 6042-6048.

2. **Alexandre, G., S. E. Greer-Phillips, and I. B. Zhulin.** 2004. Ecological role of energy taxis in microorganisms. FEMS Microbiol. Rev. **28**:113-126.

3. **Alexeyev, M. F.** 1999. The pKNOCK series of broad-host-range mobilizable suicide vectors for gene knockout and targeted DNA insertion into the chromosome of gram-negative bacteria. Biotechniques **26**:824-826.

4. **Barak, R., I. Nur, Y. Okon, and Y. Henis.** 1982. Aerotactic response of *Azospirillum brasilense*. J. Bacteriol**. 152**:643-649.

5. **Bashan, Y., G. Holguin, and L. E. de-Bashan.** 2004. *Azospirillum*-plant relationships: physiological, molecular, agricultural, and environmental advances (1997-2003). Can. J. Microbiol. **50**:521-577.

6. **Bibikov, S. I., A. C. Miller, K. K. Gosink, and J. S. Parkinson.** 2004. Methylation-independent aerotaxis mediated by the *Escherichia coli* Aer protein. *J Bacteriol* **186**: 3730-3737.

7. **Dang, C. V., M. Niwano, J. Ryu, and B. L. Taylor.** 1986. Inversion of aerotactic response in *Escherichia coli* deficient in CheB protein methylesterase. J. Bacteriol. **166**: 275-280.

8. **Falke, J. J., and G. L. Hazelbauer.** 2001. Transmembrane signaling in bacterial chemoreceptors. Trends Biochem. Sci. **26**:257-265.

9. **Fellay, R., J. Frey, and H. Krisch.** 1987. Interposon mutagenesis of soil and water bacteria: a family of DNA fragments designed for in vitro insertional mutagenesis of gram-negative bacteria. Gene **52:**147-154.

10. **Figurski, D. H., and D. R. Helinski.** 1979. Replication of an origin-containing derivative of plasmid RK2 dependent on a plasmid function provided in trans. Proc. Natl. Acad. Sci. USA 76:1648-1652.

11. **Greer-Phillips, S. E., B. B. Stephens, and G. Alexandre.** 2004. An energy taxis transducer promotes root colonization by *Azospirillum brasilense*. J. Bacteriol. **186**: 6595-6604.

12. **Hauwaerts, D., G. Alexandre, S. K. Das, J. Vanderleyden, and I. B. Zhulin.** 2002. A major chemotaxis gene cluster in *Azospirillum brasilense* and relationships between chemotaxis operons in alpha-proteobacteria. FEMS Microbiol. Lett. **208:** 61-67.

13. **Jeziore-Sassoon, Y., P.A. Hamblin, C. A. Bootle-Wilbraham, P. S. Poole, and J. P. Armitage.** 1998. Metabolism is required for chemotaxis to sugars in *Rhodobacter sphaeroides*. Microbiology **144**: 229–239.

14. **Jiang, Z. Y., and C. E. Bauer.** 2001 Component of the *Rhodospirillum centenum* photosensory apparatus with structural and functional similarity to methyl-accepting chemotaxis protein chemoreceptors. J. Bacteriol. **183**: 171-177.

15. **Kehry, M. R., T. G. Doak, and F. W. Dahlquist.** 1984. Stimulus-induced changes in methylesterase activity during chemotaxis in *Escherichia coli*. J. Biol. Chem. **259**: 11828-11835.

16. **Kirby, J. R., C. J. Kristich, S. L. Feinberg, and G. W. Ordal.** 1997. Methanol production during chemotaxis to amino acids in *Bacillus subtilis*. Mol. Microbiol. **24**: 869-78.

17. **Lamanna, A. C., J. E. Gestwicki, L. E. Strong, S. L. Borchardt, R. M. Owen, and L. L. Kiessling.** 2002. Conserved amplification of chemotactic responses through chemoreceptor interactions. J. Bacteriol. **184:** 4981-4987.

18. **Laszlo, D. J. , and B. L. Taylor.** 1981. Aerotaxis in *Salmonella typhimurium*: role of electron transport. J. Bacteriol. **145**:990-1001.

19. **Lindbeck, J. C., E. A. Goulbourne, Jr, M. S. Johnson, and B. L. Taylor.** 1995. Aerotaxis in *Halobacterium salinarum* is methylation-dependent. Microbiology **141**: 2945-2953.

20. **Martin, A. C., G. H. Wadhams, D. S. Shah, S. L. Porter, J. C. Mantotta, T. J. Craig, P. H. Verdult, H. Jones, and J. P. Armitage.** 2001. CheR- and CheB-dependent chemosensory adaptation system of *Rhodobacter sphaeroides*. J. Bacteriol. **183**: 7135-7144.

21. **Metcalf, W. W., and B. L. Wanner.** 1993. Construction of new β-glucuronidase cassettes for making transcriptional fusions and their use with new methods for allele replacements. Gene **129:**17-25.

22. **Niwano M, and B. L. Taylor**. 1982. Novel sensory adaptation mechanism in bacterial chemotaxis to oxygen and phosphotransferase substrates. Proc. Natl. Acad. Sci. USA **79**: 11-15.

23. **Nordmann, B., M. R. Lebert, M. Alam, S. Nitz, H. Kollmannsberger, D. Oesterhelt, and G. L. Hazelbauer.** 1994. Identification of volatile forms of methyl groups released by *Halobacterium salinarium*. J. Biol. Chem. **269**: 16449-16454.

24. **Perazzona B., and J. L. Spudich.** 1999. Identification of methylation sites and effects of phototaxis stimuli on transducer methylation in *Halobacterium salinarum*. J. Bacteriol. **181**: 5676-83.

25. **Sambrook, J., E. F. Fritsch, and T. A. Maniatis.** 1989. Molecular cloning: a laboratory manual, 2nd ed. Cold Spring Harbor Laboratory Press, Cold Spring Harbor, N.Y.

26. **Simon, R., U. Priefer, and A. Pülher.** 1983. A broad host range mobilization system for *in vivo* genetic engineering transposon mutagenesis in gram-negative bacteria. Biotechnology **1:** 784-791.

27. **Sourjik, V.** 2004. Receptor clustering and signal processing in *E. coli* chemotaxis. Trends Microbiol. **12**:569-576.

28. **Sourjik, V.**, **and H.C. Berg.** Receptor sensitivity in bacterial chemotaxis. Proc. Natl. Acad. Sci. USA **99**: 123-127.

29. **Springer, W. R., and D. E. Koshland, Jr.** 1997. Identification of a protein methyltransferase as the *cheR* gene product in the bacterial sensing system. Proc. Natl. Acad. Sci. USA **74**: 533-537.

30. **Steenhoudt, O. and J. Vanderleyden.** 2000. *Azospirillum*, a free-living nitrogen-fixing bacterium closely associated with grasses: genetic, biochemical and ecological aspects. FEMS Microbiol. Rev. **24**: 487-506.

31. **Stock, J. B., A. M. Maderis, and D. E. Koshland, Jr.** 1981. Bacterial chemotaxis in the absence of receptor carboxyl methylation. Cell **27**: 37–44.

32. **Stock, J. B., and M. G. Surette.** 1996. Chemotaxis. In *Escherichia coli* and *Salmonella typhimurium: Cellular and Molecular Biology*, 2nd edn. Neidhardt, F.C., Curtiss, R., III, Ingram, J.J., Lin, E.C.C., Low, K.B., Magasanik, B., *et al.* (eds). Washington, DC: American Society for Microbiology Press, pp. 1103–1129.

33. **Szurmant, H., and G. W. Ordal.** 2004. Diversity in chemotaxis mechanisms among the Bacteria and Archaea. Microbiol. Mol. Biol. Rev. **68**: 301-319.

34. **Thoelke, M. S., J. R. Kirby, and G. W. Ordal.** 1989. Novel methyl transfer during chemotaxis in *Bacillus subtilis.* Biochemistry **28**: 5585-5589.

35. **Vanstockem, M., K. Michiels, J. Vanderleyden, and A. P. Van Gool.** 1987. Transposon mutagenesis of *Azospirillum brasilense* and *Azospirillum lipoferum*, physical analysis of Tn*5* and Tn*5*-Mob insertion mutants. Appl. Environ. Microbiol. **53:** 410-415.

36. **Wadhams, G. H., and J. P. Armitage.** 2004. Making sense of it all: bacterial chemotaxis. Nat. Rev. Mol. Cell. Biol. 5:1024-37.

37. **Wong, L. S., M. S. Johnson, I. B. Zhulin, and B. L. Taylor.** 1995. Role of methylation in aerotaxis in *Bacillus subtilis.* J. Bacteriol. **177**:3985-3991.

38. **Wren, B.W., Henderson, J., and J. M. Ketley.** 1994. A PCR-based strategy for the rapid construction of defined bacterial deletion mutants. Biotechniques **16**:994-996.

39. **Yanish-Perron, C., J. Vieira, and J. Messing.** 1985. Improved M13 phage cloning vectors and host strains: nucleotide sequences of the M13mp18 and pUC19 vectors. Gene **33:**103-119.

40. **Yonekawa, H., H. Hayashi, J. S. Parkinson.** 1983. Requirement of the CheB function for sensory adaptation in *Escherichia coli*. J. Bacteriol. **156**:1228-1235.

41. **Zhulin, I. B.** 2001. The superfamily of chemotaxis transducers: from physiology to genomics and back. Adv. Microb. Physiol. **45:** 157-98.

42. **Zhulin, I. B., and J. P. Armitage.** 1993. Motility, chemokinesis, and methylation-independent chemotaxis in *Azospirillum brasilense*. J. Bacteriol. **175**: 952-958.

43. **Zhulin, I. B., V. A. Bespalov, M. S. Johnson, and B. L. Taylor**. 1996 Oxygen taxis and proton motive force in *Azospirillum brasilense*. J. Bacteriol. **178**:5199-204.

CHAPTER FOUR

A manuscript (in preparation)

Control of cell length in a bacterium

Bonnie B. Stephens[1] and Gladys Alexandre[2]

1. Graduate student who performed all experiments and wrote preliminary drafts of the manuscript

2. Professor and mentor who provided laboratory space and equipment and supervised the project

Control of cell length in a bacterium

Bonnie B. Stephens[1] and Gladys Alexandre[1,2]*

Department of Biology, Georgia State University, Atlanta, Georgia 30303[1]

Department of Biochemistry, Cellular and Molecular Biology and Department of Microbiology, The University of Tennessee, Knoxville, TN 37996[2]

*Corresponding author. Mailing address: Department of Biochemistry, Cellular and Molecular Biology, M407 Walters Life Sciences Building, The University of Tennessee, Knoxville, TN 37996. Tel. (865) 974-0866. Fax (865) 974-6306, E-mail: galexan2@utk.edu.

ABSTRACT

The ability to maintain a characteristic cell size is a fundamental property of cells from multicellular and unicellular organisms. Although relatively detailed molecular models for cell division and the coupling of cell growth with the cell cycle in both prokaryotes and eukaryotes have been developed, little is known concerning the mechanism by which cells maintain a characteristic cell size (2). Environmental conditions such as temperature and nutrients availability were shown to influence cell size in bacteria (14) while nutrients and ploidy affect cell size in eukaryotes (7, 13). Cell size varies throughout the cell cycle since newborn cells increase in size continually over the cell cycle until they reach a critical initiation mass (or critical size) and divide (4, 11). While cell size determination is dependent on the growth rate and cell size and growth are tightly regulated in most organisms, the size of some metazoans cells can change independently of cell divisions under specific developmental conditions (2, 5, 8, 12). However little is known about the signaling pathways that control cell growth and coordinate changes in cell size in response to environmental cues. Here, we show that a signal transduction pathway modulate cell length in response to changes in nutrient conditions, independently of the growth rate, in a bacterium.

INTRODUCTION

Motile bacteria can rapidly adapt to environmental changes by biasing their movement in order to navigate toward conditions optimum for growth using chemotaxis. The role of the chemotaxis machinery is to detect and respond to temporal changes in chemical gradients by modifying the swimming behavior. At the molecular level, a conserved

signal transduction pathway integrates sensory information and alters the swimming direction or velocity accordingly. Similar signal transduction pathways are found in all bacteria and archaea and may function to modulate motility as well as other cellular functions (18). Recent experimental evidence indicates that the primary function of a chemotaxis operon homolog in the alpha-proteobacterium *Azospirillum brasilense* does not control motility behavior (16). This signal transduction pathway is comprised of the conserved set of chemotaxis protein homologs CheA, CheY, CheW, CheB, and CheR that were shown to control the motility behavior of other bacterial species. We investigated the possibility that this signal transduction system could control cellular functions other than motility in *A. brasilense* by characterizing the physiology and growth of different mutants in this pathway.

RESULTS AND DISCUSSION

First, we tested the ability of various mutants in this signal transduction pathway to bind dyes known to interact with exopolysaccharides. We found that the mutants were all affected in their ability to bind congo red and calcofluor white, which stain beta-linked glucans found in exopolysaccharides produced by various bacterial species (Fig. 4.1A). Relative to the wild type strain colony, the mutant colonies bound the dye either more or less or with a different pattern (Fig. 4.1A). These data suggest that mutants in the chemotaxis operon are impaired in their ability to produce congo-red binding EPS.

The ability to bind congo red has been correlated with the aggregation of cells by cell-to-cell adhesion mediated by the production of abundant exopolysaccharides. Aggregated cells form large clumps that flocculate in liquid cultures (1). To investigate

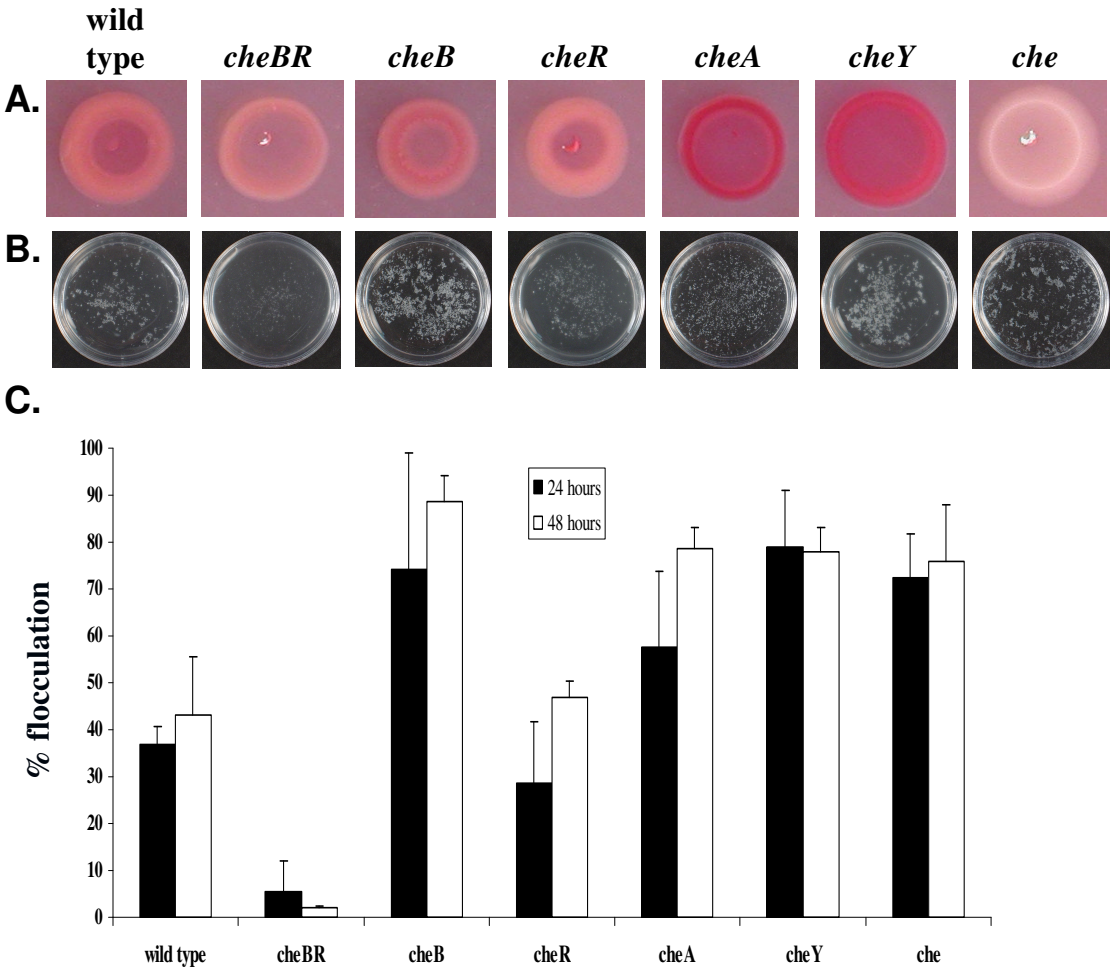

Fig. 4.1.EPS production in the wild type and mutants of the *A. brasilense* chemotaxis operon. Chemotaxis mutants have different abilities to bind congo red, indicating differences in EPS among the mutants strains (A). Chemotaxis mutants have different ability to flocculate relative to the wild type strain as shown qualitatively (B) and quantitatively. Flocculation defects are not due to differences in timing (B).

the role of the signal transduction pathway in flocculation, we compared the mutants with the wild type for their ability to flocculate. Relative to the wild type strain the *cheA, cheB, cheY,* and *che* mutants flocculated substantially more, while the *cheBR* mutant was greatly impaired and flocculated poorly even after extended incubation (Fig. 4.1B, C).

Interestingly, aggregated cells in flocs are smaller than the undifferentiated vegetative cells (10). We tested the possibility that the difference in the ability to flocculate correlated with morphological defects in the mutants. Transmission electron microscopy was used to further characterize the wild type and mutant strains. We found that relative the *cheA, cheB, cheR, cheY,* and *che* mutants were consistently shorter than the wild type strain (Fig.4.2). Cells of the *cheBR* mutant consistently appeared longer. In order to determine which characteristic of the cell size (length or width) was affected by the mutations, we determined the median cell length, width, and aspect ratio in cultures of actively growing cells (Table 4.1). We found that there was not a correlation between median cell length and width but that the aspect ratio changed. The length of the cells was changing under different conditions. These data suggest that the mutants are affected in their ability to elongate with no detectable effect on the width: the cheBR mutant strain is elongated relative to the wild type strain while the *cheB*, *cheR*, *cheA*, *cheY*, and *che* mutants are significantly shorter than the wild type strain (Table 4.1). Although the different cell lengths of the mutants were observed regardless of the growth conditions, we found that nutrients modulated the extent of cell elongation for a particular strain. Some nutrients promoted cell elongation in the wild type and most of the mutant strains regardless of their initial cell length. For example, the median cell length distribution of the wild type, *cheA*, and *cheBR* mutant strains increased when grown in presence of

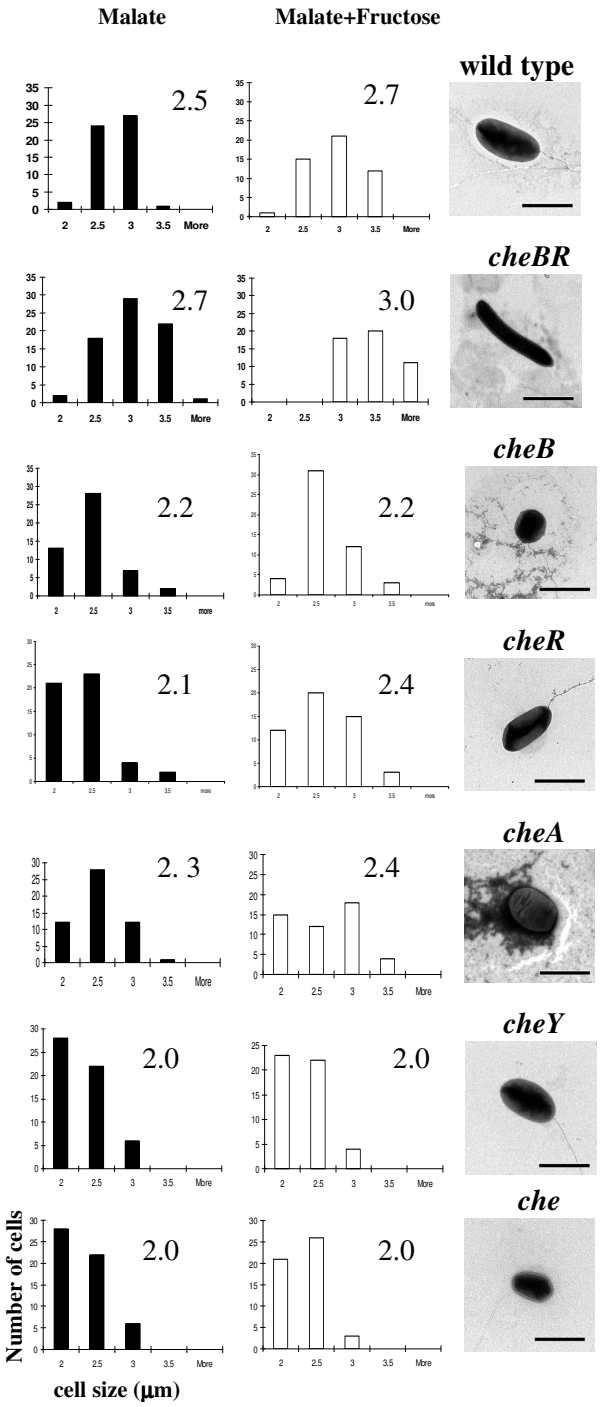

Fig. 4.2 Cell length distributions of the wild type and chemotaxis mutant strains under different nutrient conditions. The graphs represent the median distribution of cell lengths: black bars represent malate and white bars represent malate and fructose. Numbers on the graph indicate the median cell length. TEM pictures show representative cells under malate and fructose conditions. Black bars represent 2µm.

Table 4.1 Cell sizes of wild type and chemotaxis mutants

Strain	median cell length (μm)				median cell width (μm)		aspect ratio		correlation coefficient	
	fructose	alanine	malate	malate + fructose	malate	malate + fructose	malate	malate + fructose	malate	malate + fructose
wild type	2.1	2.0	2.5	2.7	1.3	1.6	1.9 ±0.2	1.7 ±0.2	0.42	0.20
cheBR	2.3	2.2	2.7	3.0	1.3	1.2	2.1 ±0.3	2.6 ±0.4	0.15	-0.18
cheB	2.2	2.1	2.2	2.2	1.3	1.4	1.8 ±0.2	1.7 ±0.3	0.40	0.25
cheR	2.1	1.9	2.1	2.4	1.4	1.3	1.5 ±0.2	1.6 ±0.3	0.32	0.26
cheA	2.1	2.1	2.3	2.4	1.3	1.3	1.8 ±0.3	1.9 ±0.5	0.30	0.42
cheY	2.0	2.0	2.0	2.0	1.3	1.2	1.6 ±0.2	1.7 ±0.3	0.50	0.26
che	2.0	1.8	2.0	2.0	1.4	1.3	1.5 ±0.2	1.6 ±0.2	0.39	0.34

malate and fructose relative to malate. However, median cell length distribution relative to that of the wild type was biased toward shorter cell lengths for the *cheA* mutant and longer cell lengths for the cheBR mutant (Table 4.1). We found that the effect of nutrients on cell elongation correlated with the growth rate (Fig. 4.3). For example, wild type cells were longer under conditions of fast growth. The correlation between growth rate, cell size and the effect of nutrient conditions on these parameters is similar to what has been previously established in many different cell types including bacteria and yeast.

The different cell lengths of the mutants raised the possibility that the mutations affected the growth rates. We determined the doubling time and the average length of septating cells of the wild type and mutants grown under different nutrient conditions (Fig. 4.3). The doubling times of the mutants were not significantly different from that of the wild type, but the average length of septating cells had the same bias as the corresponding mutant. Longer cells divided at a longer cell length relative to the wild type, and shorter cells divided at a shorter cell length with no discernable effect on growth rate. Similarly, there was not an apparent difference in septation length of the mutants between the carbon sources on which the cells were grown (Fig. 4.3). These data suggest that although the mutants maintain a cell length distribution biased toward either longer or shorter cell length relative to the wild type throughout the cell cycle, the doubling time was not affected. Furthermore, the biased cell length of the mutant was not adjusted to a wild type length prior to division since the length of septating cells was affected in the mutant. These data indicate that only cell length, but not cell division, per se, is altered in the mutants. The timing of chromosome replication and cytokinesis are independent from each other and independent of cell length at division in bacteria (5).

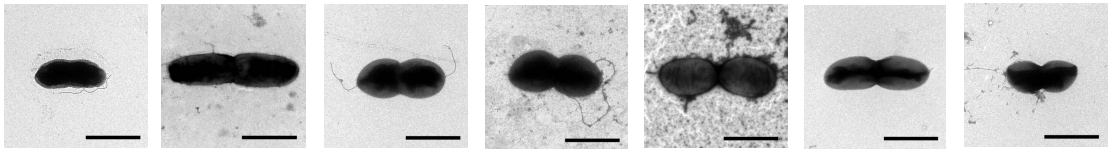

	wild type	***cheBR***	***cheB***	***cheR***	***cheA***	***cheY***	***che***
	doubling time (minutes)						
malate	136	138	135	141	137	138	133
malate + fructose	120	115	116	119	119	121	107
	Avg. length of septating cells (μm)						
malate	3.4 ±0.3	3.8 ±0.3	3.2 ±0.2	2.9 ±0.3	3.2 ±0.4	3.0 ±0.1	2.9 ±0.3
malate + fructose	3.5 ±0.5	3.9 ±0.4	3.1 ±0.3	2.9 ±0.2	3.1 ±0.3	2.8 ±0.2	2.9 ±0.2

Fig. 4.3 Doubling times and average septating lengths of the wild type and chemotaxis mutants under different nutrient conditions. TEM pictures show representative cells under malate and fructose conditions. Black bars represent 2μm.

Therefore, we hypothesize that the che-signal transduction pathway modulates cell length independent of cell divisions.

Interestingly, a *cheY* and a *che* mutant were no longer able to adjust their cell length in presence of different nutrients: these mutants were short regardless of the condition and were much shorter than all of the other cells, including the wild type. In homologous chemotaxis systems, CheY modulates the signaling output which results in a biased swimming motility toward or away from a particular environment. If CheY is the signaling output of this pathway, then we expect the *cheY* and *che* mutant to have similar phenotypes. Therefore, we propose that the main function of the *che* operon is to modulate cell length in response to changes in nutrients condition. Because the cheY and che operon mutants had doubling times similar to that of the wild type but are of a shorter size, we hypothesize that the signal(s) transduced by this pathway is independent of growth rate. In chemotaxis systems that control swimming motility, CheB and CheR comprise an adaptation system that allows motile cells to make temporal comparisons as they swim about and provide the motile cell with a molecular "memory". By analogy to chemotaxis systems that control motility bias we hypothesize that in the *cheBR* mutant cells receive the positive signal for increase in cell length, but fail to adapt and therefore keep elongating. We propose that the wild type cells can rapidly adjust their lengths between cell divisions.

We have shown that cells of different lengths differ in their ability to aggregate. Propensity for cell-to-cell aggregation and flocculation increase as the cells become shorter, implicating the signal transduction system in coordinating cell size modulation with cell-to-cell interactions. Modulation of cell lengths in response to environmental

cues and subsequent changes in cell-to-cell interaction properties is a general property of both prokaryotes and eukaryotes. For example, changes in cell size and cell surface properties are observed in bacteria growing as biofilms, some of which cause secondary antibiotic resistant infections (3). Cell size controls timing of development and final body size in *Drosophila* (12). Alteration in individual cell sizes with out change in cell division also influences the outcome of developmental processes in mammalian cells (2). Our results provide a mechanism by which a bacterium adjusts cell size and modulates cell-to-cell interaction in response to environmental cues using a dedicated signal transduction pathway. These findings complement recent experimental evidence that have demonstrated that the bacterial cell is highly organized and coordinate multiple cellular processes in both space and time, features that make it more similar to the complex eukaryotic cell than previously assumed. Although relatively detailed molecular models for cell division and the coupling of cell growth with the cell cycle in both prokaryotes and eukaryotes have been developed, much remains to be discovered on how cells maintain a characteristic cell size (2). Our results indicate that bacteria may be a valuable model to study the mechanism of cell size control.

MATERIALS AND METHODS

Bacterial strains and growth conditions

A wild type *A. brasilense* Sp7 (ATCC 29145) strain was used throughout this study. *A. brasilense* cells were grown at 28°C in the minimal medium (MMAB) (17), supplemented with a carbon source of choice. Cells were grown aerobically at 200 rpm on a rotary shaker. The *cheBR, cheB, cheR,* and *che* mutants were described previously

(16). To visualize dye binding by individual colonies, cells to be tested were first grown in liquid MMAB with malate as a coarbon source, washed in sterile phosphate buffer (PBS, pH 7.5), and placed as 5 µl drops on solid trytpone yeast extract (TY, per liter, tryptone, 5g and yeast extract, 3g) plates containing either Congo Red (40 µg ml^{-1}) or Calcofluor White (50 µg ml^{-1}). The plates were incubated at 28°C for 48 hours before being photographed. Cell aggregation and flocculation was performed as following. First, cultures in liquid TY medium were prapred and normalized to an O.D. $_{600\ nm}$ of 1.0. Next, 100 µl of the normalized cultures were inoculated into 5 ml of liquid MMAB containing 8 mM fructose and 0.5 mM NaNO3 as the sole carbon and nitrogen sources at 28 ^{o}C with shaking (230 rpm). Flocculation within the cultures was quantified after 24 and 48 hours incubation as previously described (10). At least three independent cultures were used for each strain. The doubling times of individual strains were determined as follows. First, 6 ml of liquid MMAB medium supplemented with a carbon source of choice was inoculated with cells from the edge of a 48-hour swarm plate. Cells of a swarm plate swim outward from the point of inoculation as the carbon source is metabolized; inoculating from this edge ensure that a culture will be inoculated with actively motile cells. Cultures were grown for five hours to early exponential phase. Every hour during exponential phase, an aliquot of the culture was removed, serially diluted in sterile PBS, and plated on MMAB plates. Plates were incubated for 48 hours at 28°C, and the resulting colonies were counted. Average plate counts were plotted as a function of time and linear regressions were calculated using Microsoft Excel (Microsoft, Inc.).

Mutant construction

To construct a *cheA* mutant, pGA115 (16) containing a *cheAΔ::gusA-Km* deletion-insertion was introduced into *A. brasilense* by triparental mating using pRK2013 as a helper. Double homologous recombinants carrying a deletion-insertion in *cheA* and loss of the plasmid were selected. Southern hybridization and PCR were used to verify the loss of the recombinant plasmid. One such *cheA* mutant BS111 was further characterized. The *cheY* mutant was constructed by deletion of an internal 320-bp fragment in-frame and inserting a nonpolar kanamycin cassette from pCM184 (9). First a 531–bp fragment directly upstream of *cheY* and containing the start codon was amplified from the pFAJ451 cosmid (6) using the primers pair: cheYUF (5'GCCACCACCAAGAAGTCCAAG) and cheYUR (5'CATGGTGAACGGGCCTCAGGC). This fragment was cloned in the pCR2.1TOPO vector (Invitrogen). Similarly, a 554-bp fragment directly downstream of *cheY* and encompassing the last 43-bp at the 3'-end of the gene was amplified from pFAJ451 using the primer pair: cheYDF (5'CGACATCATCCAGACCAAGTTC) and cheYDR (5'CTTGACCTTCGACACCAGCTC) and cloned into pGEM-T (Promega). The *cheY* fragments were verified by sequencing (Georgia State University) and subsequently isolated by digestion with *NcoI* and *NotI* (upstream fragment) and *ApaI* and *SacI* (downstream fragment) before being cloned into corresponding sites in the pCM184 vector. In the resulting construct, the kanamycin cassette from pCM184 is inserted in-frame between the two cloned fragments, yielding a Δ*cheY*::kan construct. The correct construct was verified by restriction analysis and sequencing. The entire Δ*cheY*::kan construct was amplified by using the primers cheYUF and cheYDR and blunt-cloned into the pSUP202 suicide vector (digested with

EcoRI followed by end-repair for blunt) (15) The suicide vector containing the Δ*cheY*::kan construct was used for allelic exchange as described above. One double homologous recombinant (BS116) was chosen.

Microscopy

Transmission electron microscopy was performed on a LEO 906e transmission electron microscope (80 kV). Cells were grown in MMAB supplemented with a carbon source of choice, washed in sterile PBS, spotted on formvar coated nickel grids, and negatively stained with 2% uranyl acetate for 1 minute. 50 Cells from at least three independent cultures were manually measured for length from cell pole to cell pole and for width along the widest part of the cell. Aspect ratios were calculated by dividing cell length by cell width.

Statistics

We found that the median cell length value best described the central tendency of the cell length distribution between the different populations of actively growing cells and between the different conditions. The mean cell length was not always similar to the median cell length value.

A two-sample T-test assuming equal variances was calculated using Microsoft Excel (Microsoft, Inc.) to compare the mean cell lengths of the mutant strains to the wild type under different growth conditions.

REFERENCES

1. Burdman, S. et al. Surface characteristics of Azospirillum brasilense in relation to cell aggregation and attachment to plant roots. *Crit. Rev. Microbiol*. **26**, 91-110 (2000

2. Conlon, I. & Raff, M. Size control in animal development. *Cell* **96**, 235-244 (1999).

3. Costerton, J.W. et al. Bacterial biofilms: a common cause of persistent infections. *Science* **284**, 1318-1322 (1999).

4. Donachie, W.D. Relationship between cell size and time of initiation of DNA replication. *Nature*. **219**, 1077-1079 (1968).

5. Donachie, W.D. et al. Cell length, cell growth and cell division. *Nature* **264**, 328-333 (1976).

6. Hauwaerts, D. et al. A major chemotaxis gene cluster in *Azospirillum brasilense* and relationships between chemotaxis operons in alpha-proteobacteria. *FEMS Microbiol Lett.* **208**, 61-67 (2002).

7. Johnston, G.C. et al. Regulation of cell size in the yeast *Saccharomyces cerevisiae*. *J Bacteriol*. 137, 1-5 (1979).

8. Jorgensen, P. & Tyers, M. How cells coordinate growth and division. *Curr. Biol*. **14**, R1014-R1027 (2004).

9. Marx, C.J. & Lidstrom, M.E. Broad-host-range cre-lox system for antibiotic marker recycling in gram-negative bacteria. *Biotechniques* **33**, 1062-1067 (2002).

10. Madi, L. & Henis, Y. Aggregation in *Azospirillum brasilense* Cd: Conditions and factors involved in cell-to-cell adhesion. *Plant and Soil* **115**, 89-98 (1989).

11. Mitchison, J.M. *The biology of the cell cycle*. Cambridge: Cambridge University Press. (1971).

12. Montagne, J. et al. *Drosophila* S6 kinase: a regulator of cell size. *Science* **285**, 2126-2129 (1999).

13. Mortimer, R.K. Radiobiological and genetic studies on a polyploid series (haploid to hexaploid) of *Saccharomyces cerevisiae*. *Radiat Res.* **9**, 312-326.

14. Schaechter, M. et al. Dependency on medium and temperature on cell size and chemical composition during balanced growth of *Salmonella typhimurium*. *J. Gen. Microbiol*. **19**, 592-606 (1958).

15. Simon, R. et al. A broad host range mobilization system for *in vivo* genetic engineering transposon mutagenesis in gram-negative bacteria. *Biotechnology* **1**, 784-791 (1983).

16. Stephens, B.B. et al. Role of CheB and CheR in the complex chemotactic and aerotactic pathway of *Azosprillum brasilense*. *J. Bacteriol*. **188**, 4759-4768 (2006).

17. Vanstockem, M. et al. Transposon Mutagenesis of *Azospirillum brasilense* and *Azospirillum lipoferum*: Physical Analysis of Tn5 and Tn5-Mob Insertion Mutants. Appl. Environ. Microbiol. 53, 410-415 (1987).

18. Wadhams, G.H. & Armitage, J.P. Making sense of it all: bacterial chemotaxis. *Nat. Rev. Mol. Cell Biol.* **5**, 1024-1037 (2004).

CHAPTER FIVE: CONCLUDING REMARKS

A. brasilense is a free-living diazotroph that lives in association with various grasses and cereals, promoting plant growth (9). Its dominant behavior is energy taxis, which allows the cell to occupy the most energetically favorable environmental niche (1). Energy taxis allows a cell to couple its metabolism and behavioral responses in accordance with the environmental conditions. While this type of behavioral response has been described for both *E. coli* and *B. subtilis*, is not the primary behavior of these organisms (7, 11). In *A. brasilense*, the strongest attractants are those that serve most efficiently as a growth substrate, such as organic acids and sugars, which are also the major organic compounds found in the rhizosphere (1). There is growing evidence that energy taxis is an important response in other rhizobial species, such as *Rhodobacter sphaeroides* and *Sinorhizobium meliloti* (2, 4, 12). Such a behavior would provide an advantage to motile cells by allowing the sensing and successful occupation of favorable environmental niches. Characterization of such a behavior is essential to the overall understanding of the ecology of *A. brasilense* as well as other important microbial species.

Characterization of a behavior such as energy taxis begins with identifying the first component of the signal transduction pathway, the “energy transducing sensors”. Only three types of energy sensors have been described in other microbial species. In *E. coli* Aer and Tsr are both energy sensors (10). Aer uses an FAD cofactor associated with a PAS domain to monitor changes in redox potential (3). Tsr is hypothesized to sense

proton motive force, although the mechanism of this sensing is unknown (10). *H. salinarum* and *B. subtilis* uses a heme-based sensor to mediate aerotactic responses (7). In *A. brasilense*, a novel chemotaxis transducer, Tlp1, was characterized and determined to be an energy taxis transducer that implicates energy taxis as important for the colonization of the rhizosphere of wheat. Analysis of the periplasmic sensing domain of Tlp1 revealed the lack of any known binding sites for oxygen- and redox-responsive cofactors. However, we found that the sensing domain of Tlp1 represents a new domain family, which is present in a wide variety of histidine kinases and chemotaxis transducers (5). Interestingly, non of the homologous proteins have been studied experimentally. The sensing domain of Tlp1 included the presence of several conserved aromatic amino acids, which are known to be important for protein-protein interactions, suggesting that Tlp1 may directly interact with proteins in addition to CheW and CheA when sensing energy. The presence of this new domain family implies that the energy sensing mechanism of this chemotaxis transducer is widespread and important to the biology of a variety of microorganisms.

The first obvious question that emerges from this study is how does Tlp1 sense energy? Understanding this mechanism will provide insight into energy sensing and bring a new level of knowledge to the mechanisms of signal propagation within signal transduction pathways. A homologous sensor protein in *Geobacter sulfurreducens* has been described to possibly contain a Cytochrome C in its sensing domain (8). The sensing of this protein may depend on the redox potential of its sensing domain. Downstream of Tlp1 is a predicted Cytochrome C protein homolog transcribed in the opposite direction. It is tempting to speculate that since Tlp1 is an energy sensor, this

component of the electron transport system could either directly or indirectly interact with Tlp1 to sense energy. Although difficult to perform with membrane-bound proteins, protein-protein interaction studies involving Tlp1 and Cytochrome C and/or other unknown proteins could possibly provide clues to the mechanism of sensing by Tlp1.

The identification of yet another type of energy sensor adds to the growing questions surrounding energy taxis. First, how do energy taxis transducers such as Tlp1 adapt? Adaptation involving ligand-binding chemotaxis transducers in organisms such as *E. coli* and *B. subtilis* is relatively well understood. In these model organisms, the ligand occupancy of the chemotaxis transducer results in a conformational change of the transducer, which ultimately activates the adaptation proteins resulting in cells that can appropriately respond to their new environment. How exactly do energy taxis transducers adapt to their environmental conditions? Is the mechanism of adaptation the same for energy sensors within the same species or is it dependent on the type of energy sensor present?

The next question is how do energy taxis transducers integrate their signals? It is easy to imagine a model in which several energy taxis transducers all contribute to the same signal transduction pathway controlling motility responses within the cell. This type of model is supported by the behavioral assays performed with the *tlp1* mutant, in which only a reduced, but not null, phenotype was observed in all cases. Additionally, in *E. coli* energy taxis is only abolished if both energy sensors *tsr* and *aer* are mutated. If this is the case, what is the advantage to having multiple energy sensors? One possiblility is that each energy sensor has the ability to sense different “levels” of energy and/or different parameters that reflect the intracellular energy status of the cell. An example of this type

of scenario would be the energy sensors of *E. coli* that are hypothesized to sense different energy parameters but signal to the same pathway. Another likely model would be in organisms containing multiple chemotaxis operons, multiple energy sensors signal to multiple pathways, each with a different output. If the target of the pathway is a step towards and energetically expensive process, it would be beneficial to have energy sensors as the first step to modulate such behaviors.

Experimental data suggests the presence of both energy sensing transducers (Tlp1) as well as hypothesized ligand binding transducers (Tlp2) in *A. brasilense*. In *E. coli*, it has been shown that chemotaxis transducers are localized to the poles of the cell in patches of mixed chemotaxis transducers, which aids in signal amplification. Localization of chemotaxis transducers has also been observed in *A. brasilense*. It would be interesting to know if chemotaxis transducers in *A. brasilense* are clustered together based on how they sense, either energy or ligand, and if mixed clusters are observed, how does signal amplification occur? In *R. sphaeroides*, chemotaxis transducers have been shown to localize to discrete regions within the cell, apparently due to the topology of the transducer. Membrane-anchored transducers cluster together while cytoplasmic transducers cluster together, along with the components of their respective chemotaxis-like systems to presumably prevent cross-talk between the systems. On the other hand, it has been shown in *Psuedomonas aeruginosa* that chemotaxis transducers from different pathways can cluster together although the components of each pathway are localized to the poles of the cell, but not localized together (6). This suggests that multiple chemotaxis transducers might signal to different chemotaxis pathways.

The identification of a chemotaxis operon in *A. brasilense* revealed the presence of a methylesterase CheB and methyltransferase CheR, suggesting methylation-dependent behavior responses, contrary to previous reports. Examination of the role of these proteins suggests a complicated contribution of these proteins to the the methanol release activity upon stimulation including methylation-independent, but CheBR-dependent responses, which is a significant departure from the model organism *E. coli*. In the model organisms *E. coli* and *B. subtilis*, the CheR methyltransferase is constitutively adding methyl groups to chemotaxis transducers, while the CheB methylesterase removes these groups as volatile methanol upon activation by CheA. This property of the adaptation system has allowed for the development of an assay that measures the activity of CheB in terms of methanol release.

The primary difference between these two model organisms is the sites of methylation/demethylation on the chemotaxis transducer, which accounts for the differences observed in methanol release. In *E. coli*, methanol release is observed upon a negative stimulus, while in *B. subtilis*, methanol release occurs upon both a positive and negative stimulus. The methanol release assay has been performed with several other species, resulting in patterns similar to either of the models. However, a strain with a deletion of $CheR_1$ of *Rhodobacter sphaeroides* displays a pattern of methanol release only upon a positive stimulus, which is unlike either of the models. In *A. brasilense*, the testing of various positive and negative stimuli resulted in a variety of methanol release profiles, which has not been observed in other organisms. Each chemical tested resulted in a different response, some reminiscent of *E. coli* or *B. subtilis*, some like *R. sphaeroides*, and others that are unique to *A. brasilense*. However, methanol release

experiments in other organisms have traditionally been performed with only one particular chemical as both the positive (addition of) and negative (removal of) stimulus. Further experimental evidence using a variety of chemicals in species such as *R. sphaeroides* where there is evidence of multiple adaptation mechanisms, could reveal patterns of methanol release similar to those of *A. brasilense* and provide insight into the possible "cross-talk" occurring between various systems within a single cell.

Mutations in the chemotaxis operon as well as a deletion of the entire operon itself revealed that this operon contributes to motility but it is not its primary function. There are numerous species that have multiple chemotaxis-like operons controlling functions other than motility. Since, it appeared that the chemotaxis-like operon in *A. brasilense* only contributes to, but does not dominantly control motility, we set out to characterize the function of this operon. Surprisingly, characterization of the chemotaxis operon in *A. brasilense* provides insight into the modulation of cell length in response to nutrient conditions. Mutations in the chemotaxis operon of *A. brasilense* result in strains that are either longer or shorter than the wild type but are not affected in the growth rates. These mutations also result in cells that have altered phenotypes influencing cell-to-cell interactions in response to environmental cues.

There are several questions that these results raise. First is in regards to the target of the response regulator CheY. In *E.coli* and other species where chemotaxis systems control flagellar motility, CheY binds to the flagellar motor, resulting in a change of direction of flagellar rotation. In *A. brasilense*, how is CheY modulating the ability of cells to change their length? Since this operon affects cell-to-cell interactions, perhaps the

target of this CheY (or CheY itself) is part of a quorum sensing system in *A. brasilense*, which could allow for successful colonization of the rhizosphere.

Another question arising from the cell size data is how is cell elongation controlled? An intriguing candidate for this is MreB, which is an actin homolog that polymerizes to form helical filament structures and has been shown to control cell shape in *E. coli* and *B. subtilis*. In *A. brasilense*, an *mreB* mutant displayed phenotypes similar to those displayed by mutants of the chemotaxis operon such as rounder cells, an altered ability to bind dyes such as Congo Red and Calcofluor white, and has been linked to cell differentiation. Construction of an *mreB* mutant in the wild type strain in addition to the chemotaxis mutants will provide insight as to if and how MreB regulates cellular processes such as elongation and EPS production.

I believe that as more information regarding chemotaxis and chemotaxis-like systems is uncovered, we will see that most processes within bacteria are either directly or indirectly linked to a chemotaxis-like system that temporally senses environmental conditions and can modulate behavioral responses. I think that this will be seen especially in bacteria that occupy environmental niches subject to drastic nutritional changes. The field of chemotaxis research is currently limited by roadblocks established by the model organisms, and as more species do not conform to the precedents already in place, more possibilities will become a reality and the complexities of such systems will be revealed.

A paradigm shift is beginning to take place as organisms such as *Azospirillum brasilense* shed light into the intricacies of signal transduction pathways more complex than the well-studied model chemotaxis systems of *Escherichia coli* and *Bacillus subtilis.* As more research in addition to genomic data from a broad range of bacteria becomes

available, it is apparent that the relatively simplistic systems of these model organisms will become exceptions to the rule instead of the standard to which everything is compared.

REFERENCES

1. **Alexandre, G., S. E. Greer, and I. B. Zhulin.** 2000. Energy taxis is the dominant behavior in Azospirillum brasilense. J Bacteriol **182:**6042-8.

2. **Armitage, J. P., and R. Schmitt.** 1997. Bacterial chemotaxis: Rhodobacter sphaeroides and Sinorhizobium meliloti--variations on a theme? Microbiology **143 (Pt 12):**3671-82.

3. **Bibikov, S. I., L. A. Barnes, Y. Gitin, and J. S. Parkinson.** 2000. Domain organization and flavin adenine dinucleotide-binding determinants in the aerotaxis signal transducer Aer of Escherichia coli. Proc Natl Acad Sci U S A **97:**5830-5.

4. **Gauden, D. E., and J. P. Armitage.** 1995. Electron transport-dependent taxis in Rhodobacter sphaeroides. J Bacteriol **177:**5853-9.

5. **Greer-Phillips, S. E., B. B. Stephens, and G. Alexandre.** 2004. An energy taxis transducer promotes root colonization by Azospirillum brasilense. J Bacteriol **186:**6595-604.

6. **Guvener, Z. T., D. F. Tifrea, and C. S. Harwood.** 2006. Two different Psuedomonas aeruginosa chemosensory signal transduction complexes localize to cell poles and form and remould in stationary phase. Mol Microbiol **61:**106-118.

7. **Hou, S., R. W. Larsen, D. Boudko, C. W. Riley, E. Karatan, M. Zimmer, G. W. Ordal, and M. Alam.** 2000. Myoglobin-like aerotaxis transducers in Archaea and Bacteria. Nature **403:**540-4.

8. **Londer, Y. Y., I. S. Dementieva, C. A. D'Ausilio, P. R. Pokkuluri, and M. Schiffer.** 2006. Characterization of a c-type heme-containing PAS sensor domain from Geobacter sulfurreducens representing a novel family of periplasmic sensors in Geobacteraceae and other bacteria. FEMS Microbiol Lett **258:**173-81.

9. **Okon, Y., and J. Vanderleyden.** 1997. Root-associated Azosprillum species can stimulate plants. ASM News **63:**366-370.

10. **Rebbapragada, A., M. S. Johnson, G. P. Harding, A. J. Zuccarelli, H. M. Fletcher, I. B. Zhulin, and B. L. Taylor.** 1997. The Aer protein and the serine

chemoreceptor Tsr independently sense intracellular energy levels and transduce oxygen, redox, and energy signals for Escherichia coli behavior. Proc Natl Acad Sci U S A **94:**10541-6.

11. **Taylor, B. L., I. B. Zhulin, and M. S. Johnson.** 1999. Aerotaxis and other energy-sensing behavior in bacteria. Annu Rev Microbiol **53:**103-28.

12. **Zhulin, I. B., A. F. Lois, and B. L. Taylor.** 1995. Behavior of Rhizobium meliloti in oxygen gradients. FEBS Lett **367:**180-2.

APPENDIX

A published manuscript

Lon protease of the α-proteobacterium *Agrobacterium tumefaciens* is required for normal growth, cellular morphology and full virulence

Shengchang Su[1], Bonnie B. Stephens[2], Gladys Alexandre[3] and Stephen K. Farrand[4]

Shengchang, S., B.B. Stephens, G. Alexandre, and S. K. Farrand. 2006. Lon protease of the α-proteobacterium *Agrobacterium tumefaciens* is required for normal growth, cellular morphology and full virulence. Microbiology. 152: 1197-1207.

1. Graudate student who performed UV sensitivity assays, motility and chemotaxis assays, β-galactosidas assays, RNA assays, immunoblotting assays, virulence assays, and contributed wrote the first draft of the manuscript

2. Graduate student who performed all electron microscopy and contributed to the writing of the first draft of the manuscript

3. Professor and mentor who provided laboratory space and equipment and supervised the project

4. Professor who provided laboratory space and equipment and supervised the project

Lon protease of the α-proteobacterium *Agrobacterium tumefaciens* is required for normal growth, cellular morphology and full virulence

Shengchang Su[1], Bonnie B. Stephens[2], Gladys Alexandre[2] and Stephen K. Farrand[1]

[1] Department of Microbiology, University of Illinois at Urbana-Champaign, B103 CLSL, 601 South Goodwin Avenue, Urbana, IL 61801, USA

[2] Department of Biology, Georgia State University, Atlanta, GA 30303, USA

Correspondence

Stephen K. Farrand

stephenf@uiuc.edu

ABSTRACT

The ATP-dependent Lon (La) protease is ubiquitous in nature and regulates a diverse set of physiological responses in bacteria. In this paper a *lon* mutant of the α-proteobacterium *Agrobacterium tumefaciens* C58 has been characterized. Unlike *lon* mutants of *Escherichia coli*, the *lon* mutant of *A. tumefaciens* grows very slowly, is not filamentous and exhibits normal resistance to UV irradiation. The mutant retains motility and chemotaxis, produces apparently normal amounts of exopolysacchride, but displays severe defects in cell morphology, with 80 % of the mutant cells appearing Y-shaped. Lon protease of *A. tumefaciens* shares high homology with its counterparts in *E. coli* and in *Sinorhizobium meliloti*, and functionally complements an *E. coli lon* mutant for defects in morphology and RcsA-mediated regulation of capsular polysaccharide production. Mutations at sites of Lon_{At} corresponding to the ATP-binding site and the active site serine of the *E. coli* Lon protease abolish complementation of phenotypes of the *A. tumefaciens* and *E. coli lon* mutants. The nucleotide sequence upstream of *A. tumefaciens lon* contains an element similar to the consensus σ^{32} heat-shock promoter of *E. coli*. Northern and Western blot analyses indicated that expression of *lon* is induced by elevated temperature, albeit to a much lower level than that of *groEL*. The *lon* mutant is highly attenuated for virulence, suggesting that Lon may be required for the proper expression, assembly or function of the VirB/D4-mediated T-DNA transfer system.

INTRODUCTION

The ATP-dependent Lon (La) protease is a conserved protein present in diverse organisms, including archaea, bacteria, yeast, plants and animals. Lon from *Escherichia*

coli (Lon_{Ec}) is an 87 kDa homo-oligomeric protein and contains highly conserved N-terminal ATPase and C-terminal protease domains (Goldberg *et al.*, 1994). Lon_{Ec} plays a primary role in the degradation of many abnormal proteins as well as unstable regulatory proteins. These latter targets include the λN protein, the SulA cell division regulator, the positive regulator of capsule synthesis, RcsA, and the F plasmid antidote protein CcdA (Gottesman, 1996). *lon* mutants of *E. coli* exhibit a pleiotropic phenotype that includes increased sensitivity to UV irradiation (Howard-Flanders *et al.*, 1964), cell division defects resulting in filamentation (Howard-Flanders *et al.*, 1964), mucoidy (Markovitz, 1964) and reduced degradation of various abnormal proteins (Gottesman & Zipser, 1978). The phenotypic properties of *lon* mutants are the result of a decreased ability to degrade specific regulatory proteins; SulA in the case of filamentation and RcsA in the case of overproduction of capsular polysaccharide.

Lon plays important roles in the regulation of developmental functions in a number of other bacteria, including normal cell morphogenesis and developmental progression in *Caulobacter crescentus* (Wright *et al.*, 1996), fruiting body formation in *Myxococcus xanthus* (Gill *et al.*, 1993) and lateral flagellar biosynthesis in *Vibrio parahaemolyticus* (Stewart *et al.*, 1997). Recent studies have shown that Lon from *Brucella abortus* functions as a general stress-response protease and is required for wild-type virulence during the initial stages of infection in BALB/c mice (Roberston *et al.*, 2000). In *Sinorhizobium meliloti*, Lon is involved in the regulation of exopolysaccharide synthesis and is required for effective nodulation of alfalfa (Summers *et al.*, 2000). The phytopathogenic α-proteobacterium *Agrobacterium tumefaciens*, a very close relative of *S. meliloti*, causes crown gall tumours on susceptible plants by transferring T-

strand DNA from its tumour-inducing (Ti) plasmid into a susceptible host plant cell. This bacterium has served as a model for studies concerning a number of important biological phenomena, including plasmid conjugation, pathogen–host signalling, Type IV secretion, *trans*-kingdom gene transfer and quorum sensing. Given the requirement for Lon protease in microbe–host interactions of other α-Proteobacteria, we constructed a *lon* null mutant of *A. tumefaciens* and characterized the effect of this mutation on a number of traits, including growth, cellular morphology and pathogenicity.

METHODS

Bacterial strains, media and growth conditions.

Strains of *A. tumefaciens* and *E. coli* and the plasmids used in this study are listed in Table A.1 . Strains of *E. coli* were grown at 37 °C in Luria broth (LB; Invitrogen) or in minimal A glucose medium (Miller, 1972), while strains of *A. tumefaciens* were grown at 28 °C in low salt LB, in MG/L medium (Cangelosi *et al.*, 1991), in AB minimal medium (Chilton *et al.*, 1974) supplemented with 0·2 % mannitol as sole carbon source (ABM) and on nutrient agar (NA; Difco). All liquid cultures were grown with agitation to ensure adequate aeration. Growth in liquid cultures was monitored turbidimetrically using a Klett–Summerson colorimeter fitted with a red filter or with a Spectronic 20 spectrophotometer at 600 nm. Antibiotics were used at the following concentrations in $\mu g\ ml^{-1}$: for *E. coli*, kanamycin, 50; tetracycline, 10; ampicillin, 100; and gentamicin, 10; for *A. tumefaciens*, kanamycin, 50; tetracycline, 2; carbenicillin, 100; and gentamicin, 50. Calcofluor (Sigma) was added to LB plates at a final concentration of 200 $\mu g\ ml^{-1}$. L-Arabinose was added at a final concentration of 0·1 % to induce expression of the *lon*

Table A.1. Bacterial strains and plasmids used in this study

Strain or plasmid	Genotype or description	Reference or source
A. tumefaciens		
NTL4	pTiC58-cured derivative of C58, Δ*tetRS*	Luo *et al.* (2001)
A136	pTiC58-cured derivative of C58, Rif^R Nal^R	Watson *et al.* (1975)
NTS1	NTL4 *lon* : : Gm^R, variable colony size	This study
NTS2	NTL4 *lon* : : Gm^R, stable colony size	This study
NTL4Δ*fla*	NTL4 in which *flaABC* is replaced with a *tet* cassette	This study
E. coli		
DH5α	F^- Φ80d*lacZ*Δ*M15 endA1 recA1 hsdR17* (r_K^- m_K^-) *supE44 thi-1 gyrA96* Δ(*lacZYA-argF*)U169	Invitrogen
S17-1	Pro^- Res^- Mod^+ *recA*; integrated RP4-Tet : : Mu-Kan : : Tn*7*, Mob^+	Simon *et al.* (1983)
HDB97	MC4100 (*ara714 cps* : : *lacZ*)	Bernstein & Hyndman (2001)
HDB98	HDB97 (*lon510*)	Bernstein & Hyndman (2001)
Plasmids		
pBAD22	ColE1 expression vector that contains P_{BAD}	Guzman *et al.* (1995)
pBADlon	lon_{At} cloned into pBAD22	This study
pBADlonK364Q	pBADlon expressing Lon_{At} with lysine at position 364 replaced by glutamine	This study
pBADlonS680A	pBADlon expressing Lon_{At} with serine at position 680 replaced by alanine	This study
pAW50	*E. coli*/*Agrobacterium* very low-copy-number shuttle vector	Wise *et al.* (2005)
pAWlon	lon_{At} cloned into pAW50	This study
pAWlonK364Q	pAWlon expressing Lon_{At} with lysine at position 364 replaced by glutamine	This study
pAWlonS680A	pAWlon expressing Lon_{At} with serine at position 680 replaced by alanine	This study
pUC19	Cloning vector	Our collection
pSlon	A 4988 bp PCR fragment containing the lon_{At} locus cloned into pUC19	This study

Table A.1 (cont.). Bacterial strains and plasmids used in this study

Strain or plasmid	Genotype or description	Reference or source
pMGm	Source of gentamicin resistance cassette	Murillo *et al.* (1994)
pSlonG	pSlon with a gentamicin resistance cassette inserted into the *lon* gene	This study
pSR47s	$oriT_{RP4}$/$oriV_{R6K}$, a mobilizable *pir*-dependent vector	Merriam *et al.* (1997)
pSRlonG	pSR47s carrying a *Bam*HI–*Xba*I fragment containing the *lon* gene from pSlonG	This study
pTiR10	Octopine-type Ti plasmid	Our collection
pTiC58	Nopaline-type Ti plasmid	Our collection

gene of *A. tumefaciens* from P_{BAD}.

Plasmids.

Plasmid pBADlon, a derivative of pBAD22 (Guzman *et al.*, 1995) expressing Lon from *A. tumefaciens* C58 (Lon_{At}) under the P_{BAD} arabinose-controlled promoter, was constructed as follows. The *lon* gene (lon_{At}) was amplified from *A. tumefaciens* NTL4 chromosomal DNA with *Pfu* DNA Polymerase (*Stratagene*) and cloned into the *Xba*I site of pBAD22. A clone containing lon_{At} correctly oriented downstream to the BAD promoter was identified and named pBADlon (Table A.1). A second PCR-amplified *lon* gene (lon_{At}) along with its own promoter region was cloned into the *Xba*I site of pAW50 (Wise *et al.*, 2005), creating plasmid pAWlon. This vector replicates at very low copy number in *A. tumefaciens* (Wise *et al.*, 2005). Site-directed mutations were introduced onto lon_{At} using the QuikChange Kit (Stratagene), according to the instructions of the manufacturer. Briefly, for construction of pBADlonK364Q, containing a mutation at lysine-364 in the ATP-binding motif, primers 5'-CTCCCGGCGTCGGCCAGACCTCGCTCGCCAAG-3' and 5'-CTTGGCGAGCGAGGTCTGGCCGACGCCGGGAGG-3' were used. pBADlonS680A, carrying a mutation at the active site serine-680, was constructed by using primers 5'-CCGAAGGACGGACCGGCCGCCGGTGTTGCCATG-3' and 5'-CATGGCAACACCGGCGGCCGGTCCGTCCTTCGG-3'. Similar strategies were used to introduce the two mutations into lon_{At} cloned in pAW50. Cloned inserts and the mutant alleles were confirmed by automated DNA sequencing performed at the Biotechnology Center of the University of Illinois at Urbana-Champaign.

Genetic manipulations.

Plasmids were introduced into *E. coli* by $CaCl_2$-mediated transformation and into *A. tumefaciens* strains by electroporation or by biparental mating using *E. coli* S17-1 (Simon *et al.*, 1983).

Disruption of the *A. tumefaciens* chromosomal *lon* gene.

Genomic DNA was prepared from an overnight culture of *A. tumefaciens* NTL4. A 4988 bp chromosomal fragment consisting of the entire coding sequences of *lon* and *clpX* along with the intergenic region between the two genes and an 879 bp sequence downstream from *lon* was amplified using *Pfu*Turbo DNA polymerase (Stratagene) (Fig. A.1a). The PCR product was cloned directly between the *Bam*HI and *Xba*I sites of pUC19 to create pSlon (Fig. A.1a). The gentamicin resistance cassette from pMGm (Murillo *et al.*, 1994) was excised by *Pst*I, made blunt by T4 DNA polymerase and inserted into the unique *Msc*I site within the *lon* gene in pSlon at a position corresponding to amino acid residue alanine-532, creating pSlonG (Fig. A.1a). The *Bam*HI–*Xba*I fragment containing *clpX* and the disrupted *lon* gene was excised from pSlonG and cloned between the *Bam*HI and *Spe*I sites of pSR47s (Merriam *et al.*, 1997). The resulting plasmid, pSRlonG, was transformed into S17-1 λ *pir* and the resultant strain was mated with NTL4 as described previously (Cook & Farrand, 1992). NTL4 carrying the chromosomal disruption in *lon* was selected by plating on medium containing the appropriate antibiotics and 5 % sucrose. Allelic exchange of the mutant *lon* gene for the wild-type allele was confirmed by Southern hybridization (data not shown). A similar strategy was used to construct NTL4Δ*fla*, a *fla*$^-$, non-motile strain of *A. tumefaciens* in

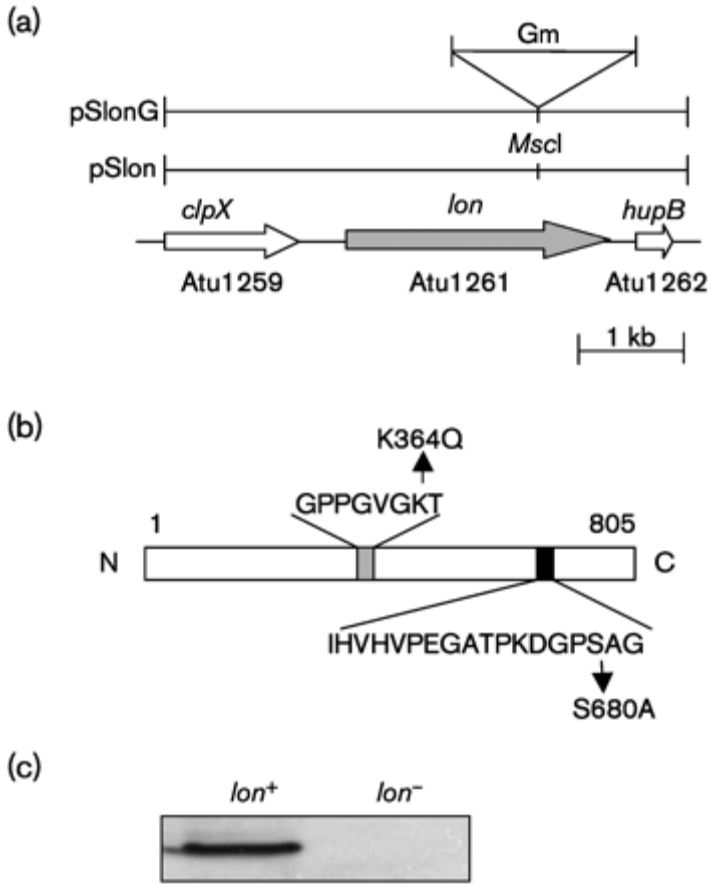

Fig. A.1. The *lon* gene of *A. tumefaciens* C58 and its protein product. (a) Genetic organization of the *lon* region from the chromosome of *A. tumefaciens* strain C58. The arrows indicate the direction of transcription. The fragment consisting of the entire coding sequences of *lon* and *clpX* along with the intergenic region between the two genes and an 879 bp sequence downstream from *lon* was cloned between the *Bam*HI and *Xba*I site of pUC19 to create pSlon. A gentamicin resistance cassette was inserted into the unique *Msc*I site to disrupt the coding sequence of the lon_{At} gene in pSlon, creating pSlonG. (b) Location of the two major consensus domains in Lon_{At}. The ATPase Walker A motif and the proteolytic active site serine are shown as well as the sites of the two amino acid substitution mutations, LonK364Q and LonS680A. (c) Proteins in total cell lysates of *A. tumefaciens* NTL4 (lon^+) and NTS2 (lon^-) were separated by 7·5 % SDS-PAGE and Lon was detected by immunoblotting with polyclonal rabbit antiserum directed against *B. abortus* Lon as described in Methods.

which the three tandem flagellum genes *flaA*, *flaB* and *flaC* were replaced with a tetracycline resistance cassette.

UV sensitivity.

Sensitivity to UV irradiation was assayed as described by Miranda & Kuzminov (2003). Briefly, a fresh overnight culture was diluted 100-fold into 2 ml ABM and grown with shaking at 28 °C to $2x10^8$ cells ml^{-1}. Tenfold serial dilutions were made in 0·9 % NaCl and 10 µl volumes of a set of the serial dilutions were spotted in rows of six onto a square Petri dish containing LB agar. The liquid in each spot was allowed to dry down, the plates were partially covered with a screen and exposed to a gradient of doses of UV light in the direction perpendicular to the dilution gradient, so that every dilution column (from 10^{-1} to 10^{-6}) received its own dose. A UV cross-linker (Amersham-Pharmacia), in which all the lamps except the central one were removed and 90 % of the remaining lamp was shielded, was used to deliver precise doses of UV (measured by the internal UV sensor). Immediately after exposure, the plate was covered with aluminium foil and incubated at 28 °C for 24 h. The titre of the culture at the zero dose was used to determine the survival at various UV doses.

Motility and chemotaxis assays.

Motility assays were conducted in ABM medium solidified with 0·3 % agar as described by Ding & Christie (2003). Cell cultures were normalized to an OD_{600} of 0·5 and a 2 µl volume of each strain was inoculated onto the surface of the motility plates. The plates were examined after 12, 24 and 48 h incubation at 28 °C. Chemotaxis assays were

performed on 0·3 % soft agar plates without carbon sources. A sterile Whatman paper disk saturated with 15 % (w/v) sucrose, glucose or mannitol was placed at the centre of the agar plate. Two microlitres of each cell culture normalized to an OD_{600} of 0·5 was inoculated onto the swarm plate 4 cm from the paper disk. The chemotaxis plates were maintained at 28 °C and examined throughout a 96 h incubation period.

Electron microscopy.

Agrobacterium strains were grown overnight with shaking at 28 °C in LB containing appropriate antibiotics to an OD_{600} of approximately 0·8. One millilitre of each culture was washed three times and resuspended in sterile PBS buffer. Cells from the washed cultures were absorbed to Formvar-coated nickel grids (EM sciences) for 1 min. Excess culture was blotted with Whatman filter paper and the grid was placed face down on a drop of 1 % uranyl acetate (EM Sciences) for 1 min. Excess stain was blotted with Whatman filter paper, the grid was air-dried and viewed with an LEO 906e transmission electron microscope operating at an accelerating voltage of 80 kV.

β-Galactosidase assay.

Production of β-galactosidase by *E. coli* strains grown in A medium was quantified using a modification of the Miller method (Miller, 1972). Activity was expressed as units of enzyme per 10^9 c.f.u. Samples were assayed in triplicate and the experiments were repeated three times. Results from a single representative experiment are shown.

RNA preparation.

Cultures of *A. tumefaciens* strains were grown to an OD_{600} of 0·5 in ABM medium at 20 °C or shifted to 37 °C and sampled after 5, 10, 15 and 30 min incubation at the elevated temperature. Total RNA was isolated using Trizol reagent (Invitrogen) as follows. Each 50 ml culture sample was rapidly chilled on ice and the cells were collected by centrifugation. The cell pellet was homogenized in 5 ml hot Trizol reagent (65 °C) and the mixture was shaken at 65 °C for 10 min. Chloroform (1 ml) was added, the tube was shaken vigorously by hand for 15 s and incubated at room temperature for 2–3 min. The phases were separated by centrifugation at 12 000 ***g*** for 15 min at 4 °C and the upper phase was removed to a new tube. One volume of isopropyl alcohol (2·5 ml) was added, mixed well and the mixture was incubated at room temperature for 10 min. The precipitated RNA was collected by centrifugation at 12 000 ***g*** for 10 min at 4 °C. The supernatant was removed and the pellet was washed once with 5 ml 75 % ethanol and air-dried to near completion. The RNA was dissolved in 300 µl RNase-free water and the preparation was treated with RNase-free DNase [RQ1 DNase (Promega)] to remove contaminating DNA. The preparation was extracted with phenol/chloroform to remove the DNase. The RNA was precipitated with isopropyl alcohol, collected by centrifugation, dried to near completion and dissolved in 100 µl RNase-free water. The RNA concentration was quantified using a Lambda 3B spectrophotometer (Perkin Elmer).

RNA blotting and hybridization.

RNA samples (20 µg) were separated on 1·5 % agarose gels containing 2·2 M formaldehyde and transferred to a positively charged nylon membrane (Roche) by capillary action in 20x SSC (3 M NaCl, 0·3 M tri-sodium citrate). An 887 bp *groEL* DNA probe and a 1·2 kb lon_{At} DNA probe were purified from agarose gels and labelled with digoxigenin [(DIG)-11-dUTP] using the DIG-High Prime labelling kit (Roche). DIG labelling, prehybridization, hybridization, posthybridization washes and detection with chemiluminescent substrate were performed according to the instructions of the manufacturer (Roche). DIG-labelled RNA molecular mass marker set II (Roche) was used as the RNA ladder.

Immunoblotting.

Cultures of *A. tumefaciens* were grown in ABM at 20 or 37 °C as described above. Proteins in total cell lysates were resolved by 7·5 % SDS-PAGE polyacrylamide gels loaded on a per cell equivalent basis and the separated proteins were transferred to nitrocellulose membrane after electrophoresis. Immunoblots were developed with polyclonal rabbit antiserum directed against *Brucella abortus* Lon obtained from Dr R. Martin Roop II (Department of Microbiology and Immunology, Louisiana State University Health Sciences Center, USA). Primary antibody was detected with horseradish peroxidase (HRP)-conjugated monkey anti-rabbit antiserum. Antibody–antigen interactions were visualized by chemiluminescence with an ECL kit (GE Healthcare). The intensity of protein bands was quantified by digital scanning and analysis of developed X-ray films with NIH Image 1.63 software.

Virulence assays.

Tumorigenesis was assessed on leaves of *Kalanchoë diagremontiana* using the culture dilution method as described by Nair *et al.* (2003) . Strains were grown in MG/L overnight at 28 °C with the appropriate antibiotics. Cells were collected by centrifugation, resuspended in 0·9 % (w/v) NaCl to an OD_{600} of 1·0 and further diluted as necessary in 0·9 % NaCl. Two-centimetre-long wounds made with an 18-gauge needle on the youngest expanded leaves of a 5-week-old *K. diagremontiana* plant with three pairs of leaves were inoculated with 3 µl of these dilutions. Tumour formation was monitored over a period of 25 days. Assays were done in triplicate and the experiments were repeated three times.

RESULTS

A. tumefaciens lon locus

Based on the whole-genome sequence of *A. tumefaciens* C58 (Wood *et al.*, 2001, the lon_{At} gene (Atu1261), located on the circular chromosome, is 2418 bp in length and encodes a protein of 805 aa with a calculated molecular weight of 88 750. Lon_{At} shares 86 % amino acid identity and 92 % similarity with the Lon protease from *S. meliloti* (Lon_{Sm}) (Summers *et al.*, 2000), 81 % identity and 90 % similarity with Lon from *B. abortus* (Lon_{Ba}) (Roberston *et al.*, 2000), and 61 % identity and 75 % similarity with Lon_{Ec} from *E. coli* (Chin *et al.*, 1988). The deduced amino acid sequence of Lon_{At} contains a typical ATP-binding motif, $GPPGVGK_{364}T$ and KAKKANPLFLLD (Chin *et al.*, 1988) at amino acid coordinates 358–365 and 414–425, respectively, and a consensus serine protease active site motif $IHVHVPEGATPKDGPS_{680}AG$ (Amerik *et al.*, 1991) at amino acid

coordinates 665–682 (Fig. A.1b). These features are conserved in all known Lon proteases. The *A. tumefaciens lon* gene is preceded by an ORF encoding a homologue of ClpX, another ATP-dependent protease (Fig. A.1a), which is separated from lon_{At} by a 414 bp intergenic region predicted to encode the promoter of the *A. tumefaciens lon* gene. Located 275 bp downstream from the *lon* gene, a *hupB* homologue could encode a histone-like protein whose counterpart in *E. coli* is involved in regulating transcription by constraining DNA supercoils and DNA accessibility to regulatory proteins (Drlica & Rouvière-Yaniv, 1987).

The *lon* mutation impairs cell growth

To explore the role of Lon protease in *A. tumefaciens*, we constructed a null mutant by inserting a gentamicin resistance cassette into the *lon* gene by double-crossover homologous recombination as described in Methods (Fig. A.1a). On the selection plates, we noted two obviously different-sized colonies, both of which grew slower than the wild-type parent. One such clone, named NTS1, formed very small colonies and grew very slowly. The second, named NTS2, formed relatively larger colonies and grew faster than NTS1. When streaked out for single colony isolation, NTS1 gave two colony sizes, the small one like its parent and larger sized colonies resembling NTS2. When similarly streaked out, NTS2 gave colonies of homogeneous size which grew faster than those of NTS1, but slower than the wild-type parent. Southern blot analysis indicated that the *lon* gene of both NTS1 and NTS2 was disrupted as predicted (data not shown). Strain NTL4 grew with a doubling time of about 2·5 h in ABM minimal medium (Fig. A.2). However, strains NTS1 and NTS2 grew with a doubling time of around 8 and 4 h, respectively, in

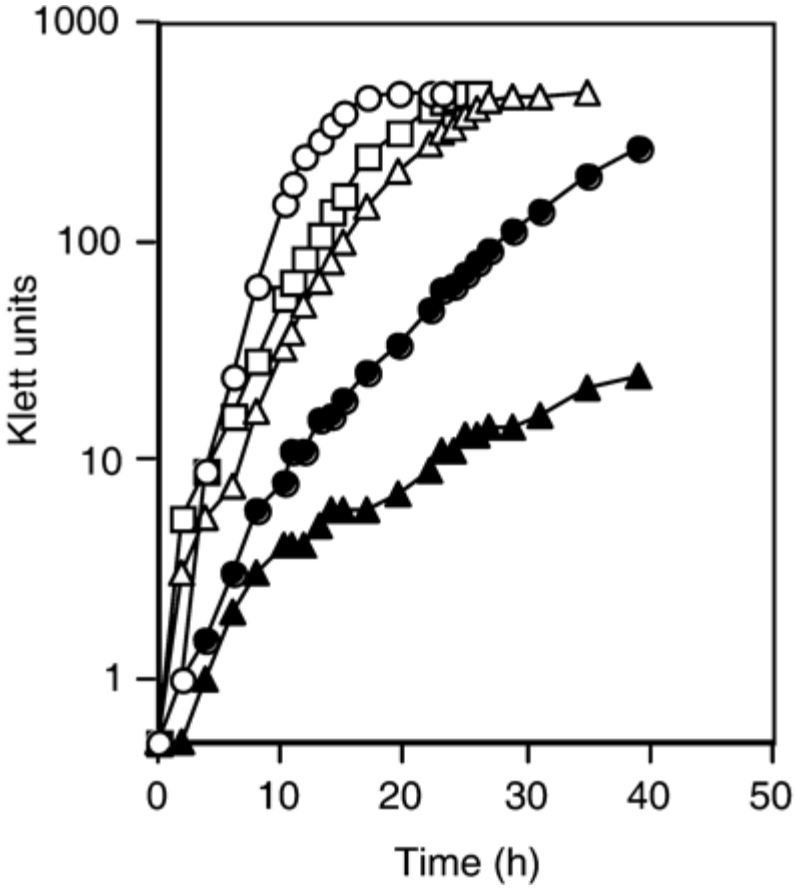

Fig. A.2. Growth of *A. tumefaciens* wild-type and *lon* mutant strains in ABM minimal medium. Turbidity values of cultures, expressed as Klett units, were determined at the given times. Data points are from a single culture for each strain and are representative of one of three experiments. ○, Wild-type strain NTL4; ▲, *lon* mutant NTS1; △, NTS1(pAWlon); ●, *lon* mutant NTS2; □, NTS2(pAWlon).

this medium (Fig. A.2). To verify that the slow growth phenotype of the *lon* mutants is due to the *lon* mutation, the two strains were complemented with lon_{At} cloned with its own promoter in the low-copy-number plasmid pAW50 (Table A.1). Derivatives of NTS1 and NTS2 harbouring pAWlon exhibited growth rates similar to that of the wild-type parent (Fig. A.2). Viability assays showed that the mutant gave the same number of c.f.u. as its parent strain at the equivalent levels of turbidity (data not shown). Because of its consistent growth properties, we chose NTS2 for further studies. As assessed by Western analysis, NTS2 failed to produce any protein that interacts with the Lon antiserum (Fig. A.1c). The wild-type strain NTL4 yielded a single reactive protein with a mobility corresponding to 89 kDa.

Exopolysacchride production

Succinoglycan is the major acidic exopolysacchride produced by *A. tumefaciens* and can be easily detected by the binding of the optical brightening agent Calcofluor. When streaked out on LB medium containing Calcofluor, colonies of NTS2 fluoresced under UV light with an intensity indistinguishable from those of NTL4 (data not shown).

UV sensitivity and cellular morphology

lon mutants of *E. coli* exhibit enhanced UV sensitivity and filamentation. Strain NTS2 was no more sensitive to UV irradiation at doses ranging from 20 to 60 J m^2 than its parent, NTL4 (data not shown). Unlike *lon* mutants of *E. coli*, NTS2 did not produce filaments even following UV irradiation (Fig. A.3a, panels 1 and 2, and data not shown). However, as seen by phase-contrast microscopy, the *lon* mutant, grown under normal

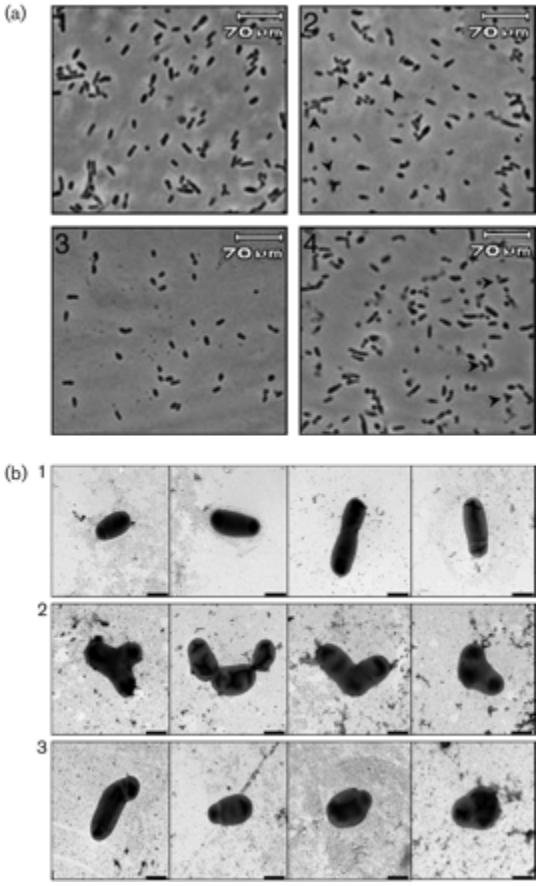

Fig. A.3. A *lon* mutation affects cell morphology in *A. tumefaciens*. (a) Phase-contrast microscopy; (b) electron microscopy. Cells of wild-type strain NTL4 (a, 1; b, row 1) show a typical short rod shape while most cells of the *lon* mutant NTS2 (a, 2; b, row 2) are branched, appearing as Y shapes. Complementation of the *lon* mutant cells by expression of a wild-type *lon* gene from pAWlon restored the wild-type cell morphology (a, 3; b, row 3). No complementation was observed in the *lon* mutant complemented with the clone expressing $Lon_{At}S680A$ (a, 4). The arrows in (a) 2 and 4 indicate aberrant cell shapes. The bars in (b) indicate 1 µm.

conditions, displayed obvious differences in cell morphology (Fig. A.3a, panel 2). Electron microscopic examination showed that cells of the wild-type strain NTL4 exhibited a typical short rod shape (Fig. A.3b, row 1). However, approximately 80–85 % of the mutant cells were branched, appearing as distinct Y shapes (Fig. A.3b, row 2). NTS2 harbouring pAWlon took on a near wild-type shape, although the complemented cells exhibited a somewhat swollen appearance (Fig. A.3a, panel 3, and Fig. A.3b, row 3). Plasmids expressing the two Lon_{At} mutants, LonK364Q and LonS680A, did not restore normal cell morphology (Fig. A.3a, panel 4, and data not shown).

Motility and chemotaxis

Given its aberrant cell morphology, we assessed the influence of the *lon* mutation on motility and chemotaxis using soft agar medium. As shown in Fig. A.4 (a), the *fla*$^-$ strain NTL4Δ*fla*, which is deleted for the three flagellum genes *flaA*, *flaB* and *flaC*, is completely non-motile. In contrast, wild-type strain NTL4 is strongly motile. The *lon* mutant NTS2 is also motile, although the zone of spreading is smaller than that of its parent (Fig. A.4a). The complemented mutant NTS2(pAWlon) is as motile as the wild-type NTL4. When viewed by phase-contrast microscopy, the percentage of NTS2 cells that were motile appeared to be similar to that of its wild-type parent (data not shown). The wild-type strain NTL4, the mutant NTS2 and the complemented mutant NTS2(pAWlon) all exhibited chemotaxis toward glucose (Fig. A.4b), as well as toward sucrose and mannitol (data not shown).

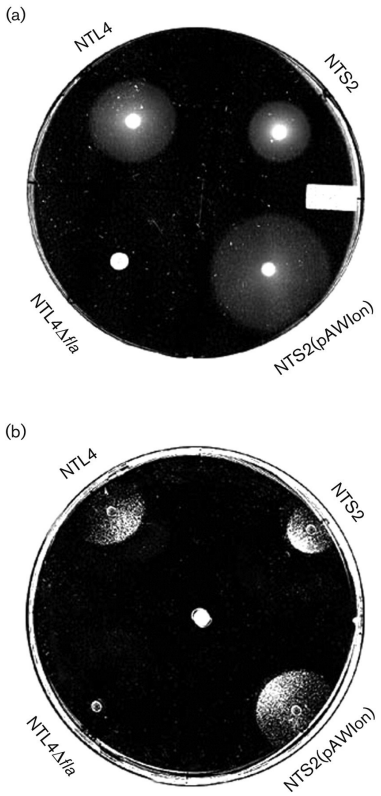

Fig. A.4. The *lon* mutant of *A. tumefaciens* is motile and exhibits chemotaxis. (a) Motility was assayed on 0·3 % agar plates as described in Methods. (b) Taxis by the strains toward glucose applied to a Whatman filter disk at the centre of plate was assessed as described in Methods.

Genetic complementation of an *E. coli lon* mutant

We determined whether Lon_{At} is equivalent to its *E. coli* homologue using two tests. In the first, we examined whether Lon_{At} could correct the SulA-associated filamentous phenotype exhibited by *E. coli lon* mutants. *E. coli* HDB98 (*lon510*) formed long filaments (Fig. A.5a, panel 2), while the strain expressing Lon_{At} exhibited normal cell morphology (Fig. A.5a, panel 3). However, neither of the two Lon_{At} mutants complemented the cell division defect (Fig. A.5a, panel 4, and data not shown). We also assessed the ability of Lon_{At} to complement the defect in regulation of *cpsB* by RcsA. The Lon^+ *E. coli* strain HDB97, which contains a *cpsB* : : *lacZ* fusion, expressed very little β-galactosidase activity, whereas its near isogenic *lon* mutant, HDB98 in which RcsA is not turned over, expressed the reporter at a high level (Fig. A.5b). Expression of Lon_{At} from pBADlon in HDB98 resulted in a strong depression of expression of the *cpsB* : : *lacZ* reporter while the same strain expressing either of the two Lon_{At} mutants exhibited high levels of β-galactosidase activity characteristic of the host *lon* mutant (Fig. A.5b).

Transcription of the *A. tumefaciens lon* gene is induced by growth at elevated temperature

In *E. coli*, *lon* is part of the heat-shock regulon. We assessed the effect of a temperature shift from 20 to 37 °C on the expression of lon_{At} in *A. tumefaciens* using two assays. In the first, we examined the level of mRNA transcripts of *lon* accumulated in the cells upon shifting to elevated temperature. In Northern blot analysis, levels of *groEL* mRNA, which appeared as two bands at 2·1 and 1·7 kb, increased to a maximum after 15 min incubation at the elevated temperature (Fig. A.6a). In a similar analysis using the *lon* probe, the *lon*-

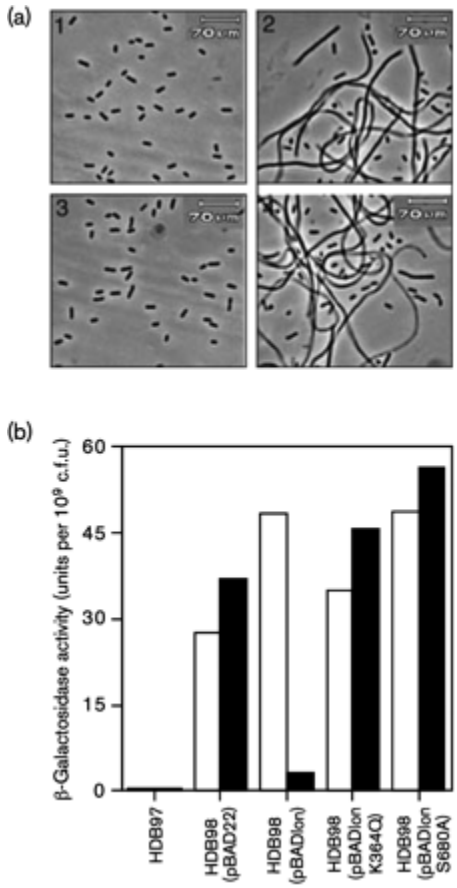

Fig. A.5. Lon_{At} complements the filamentous and mucoid phenotypes of a *lon* mutant of *E. coli*. (a) Phase-contrast microscopy of strains: 1, HDB97 (*lon*$^{+}$); 2, HDB98 (*lon*); 3, HDB98(pBADlon); 4, HDB98(pBADlonS680A). (b) Cultures of *E. coli* HDB97 (*cpsB* : : *lacZ*) and its *lon* mutant HDB98 with or without a lon_{At}-expressing plasmid as noted, were grown in minimal A medium with (black bars) or without (white bars) 0·1 % arabinose. Cultures were sampled and assayed for β-galactosidase activity.

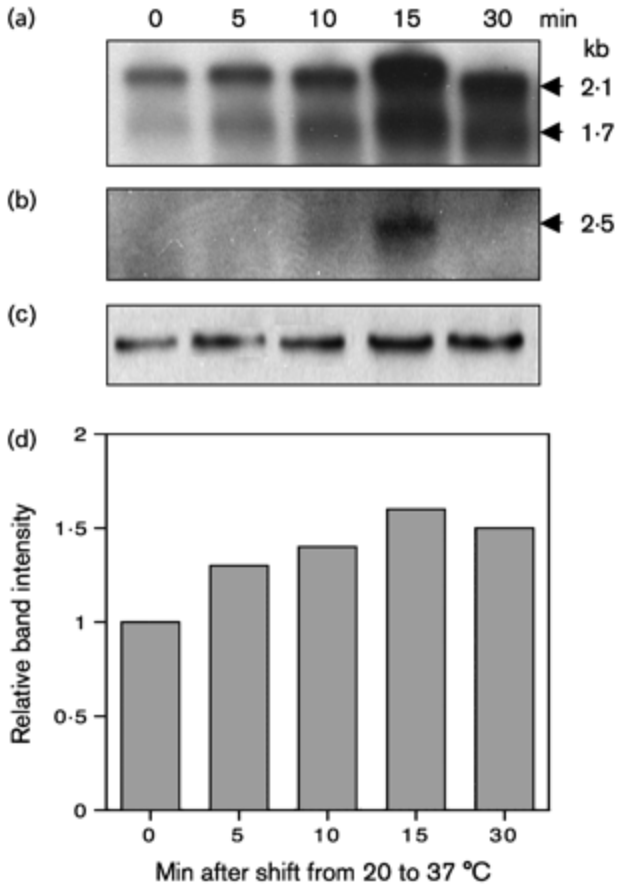

Fig. **A.6**. Expression of lon_{At} responds to elevated temperature. (a, b) Northern analysis of the *groEL* and *lon* genes. Total RNA of *A. tumefaciens* was isolated before and at different times (5, 10, 15 and 30 min) after raising the incubation temperature from 20 to 37 °C. An 887 bp *groEL* DNA fragment and a 1·2 kb *lon* DNA fragment were labelled with digoxigenin (DIG)-11-dUTP and used as probes for hybridization. (a) Hybridization with the *groEL* probe; (b) hybridization with the *lon* probe. (c) Immunoblot analysis of the levels of Lon protein in cells before and at different times (5, 10, 15 and 30 min) after raising the incubation temperature from 20 to 37 °C. Proteins in total cell lysates were separated by 7·5 % SDS-PAGE and Lon was detected by immunoblotting with polyclonal rabbit antiserum directed against *B. abortus* Lon as described in Methods. (d) The intensity of protein bands in (c) was quantified by digital scanning and analysis of developed X-ray films with NIH image 1.63 software. Experiments were repeated two times and data are representative of one of two experiments.

specific mRNA was not detectable in cells grown at 20 °C, but produced a strong signal at 2·5 kb in cells grown for 15 min at the elevated temperature (Fig. A.6b). The *lon* mRNA was not detectable in cells grown for 5 and 10 min at 37 °C and disappeared from cells grown for 30 min at the elevated temperature (Fig. A.6b). In the second, we evaluated the level of Lon protein after temperature shift using an immunoblot assay. The amount of Lon protein increased slightly but reproducibly after heat shock, reaching its maximum at 15 min followed by a small decrease in level after 30 min (Fig. A.6c and d).

The *lon* mutant is highly attenuated for virulence

Given that *lon* mutants of *B. abortus* and *S. meliloti* exhibit defects in interaction with their eukaryotic hosts (Roberston *et al.*, 2000; Summers *et al.*, 2000), we determined if the *lon* mutation influences the virulence of *A. tumefaciens*. Strains NTL4, NTS2 and their derivatives harbouring pTiC58 or pTiR10 were inoculated onto *K. diagremontiana* leaves at decreasing cell concentrations as described in Methods. Strains NTL4 and NTS2 which lack Ti plasmids were avirulent (Fig. A.7). Strains NTL4(pTiC58) and NTL4(pTiR10) induced tumours at all infection doses, although NTL4(pTiC58) yielded less tumour mass than did NTL4(pTiR10) at the lowest inoculation dose (OD_{600}=0·01). However, NTS2(pTiC58) and NTS2(pTiR10) failed to induce tumours at the lowest inoculation dose (OD_{600}=0·01) and induced much less tumour mass at the higher inoculation doses (OD_{600}=0·1 and 1·0, respectively) as compared to the wild-type parent (Fig. A.7). Introducing pAWlon into strains NTS2(pTiC58) and NTS2(pTiR10) restored wild-type levels of virulence to the *lon* mutant harbouring either Ti plasmid (Fig. A.7). Mutations in the ATPase or the proteolytic domains of Lon expressed from

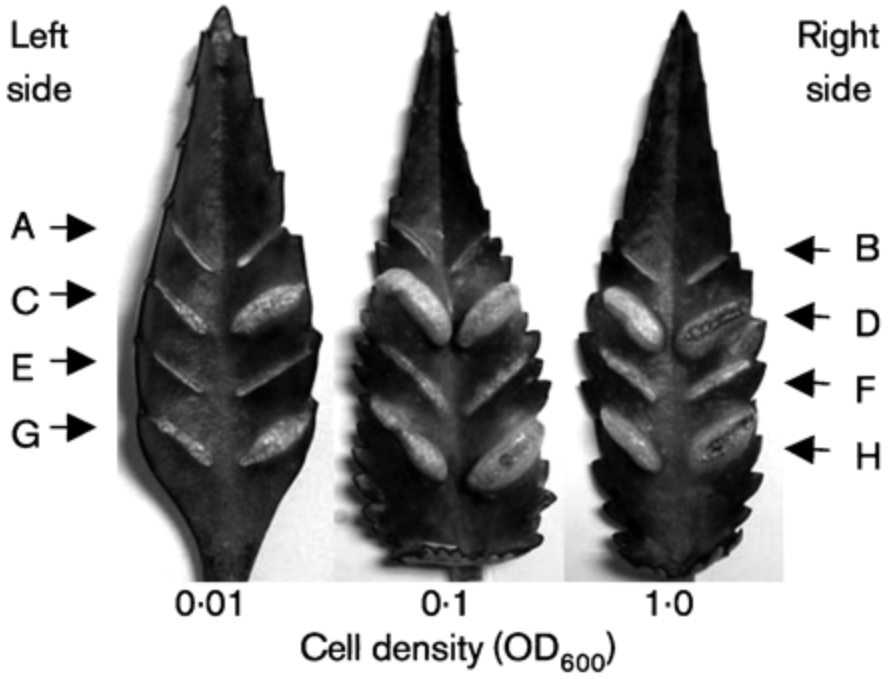

Fig. A.7. The *lon* mutant of *A. tumefaciens* is attenuated for virulence. Strains were grown and inoculated onto *K. diagremontiana* leaves as described in Methods. Wounds in leaves were inoculated with strains diluted to population sizes indicated by the OD_{600} values at the bottom: A, NTL4; B, NTS2; C, NTL4(pTiC58); D, NTL4(pTiR10); E, NTS2(pTiC58); F, NTS2(pTiR10); G, NTS2(pTiC58, pAWlon); H, NTS2(pTiR10, pAWlon). Labels to the left indicate strains inoculated on the left side of each leaf while labels to the right indicate strains inoculated on the right side of each leaf.

pAWlonK364Q or pAWlonS680A abolished complementation of the attenuated phenotype (Fig. A.8b).

We considered the possibility that the decrease in virulence of NTS2 is due to its slow growth. Our isolate of *A. tumefaciens* A136, a Rif^R Nal^R derivative of strain C58 (Watson *et al.*, 1975), grows slower than its parent strain NTL4 and, with a generation time of 3·5 h in minimal medium, grows at a rate similar to that of NTS2 (Fig. A.8a). The presence of pTiR10 had no effect on their respective growth rates (data not shown). While NTS2 harbouring pTiR10 was highly attenuated, A136 harbouring the same Ti plasmid was strongly tumorigenic (Fig. A.8b).

DISCUSSION

Given its strong conservation across phylogenetic lines, it is not surprising that Lon protease from *A. tumefaciens* is closely related to that of *E. coli* and in particular to that of *S. meliloti*, a very close relative in the family *Rhizobiaceae*. It also is not surprising that Lon_{At} requires both the Walker box motif and the active site serine; both domains are required for the activity of the *E. coli* enzyme. Consistent with these genetic, phylogenetic and enzymic relationships, the organization of the entire *lon* locus is conserved; the region flanking *lon* encodes *clpX* and *hupB* (Fig. A.1) on the circular chromosome of *A. tumefaciens* C58 as well as on the chromosomes of many prokaryotes (Chin *et al.*, 1988; Roberston *et al.*, 2000; Stewart *et al.*, 1997; Summers *et al.*, 2000). However, despite these similarities, Lon from *A. tumefaciens* targets at least a subset of proteins quite different from those turned over by this protease in *E. coli*.

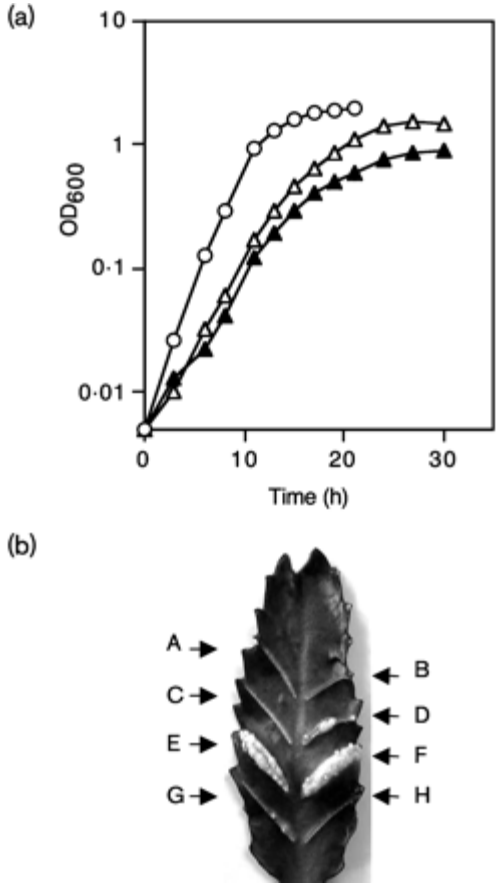

Fig. A.8. The attenuated virulence of the *lon* mutant NTS2 is not due to its slow growth. (a) Growth of Lon$^+$ *A. tumefaciens* strains NTL4 and A136 and the *lon* mutant NTS2 in ABM minimal medium. The optical density at 600 nm of the cultures was determined at the indicated times. Data are representative of one of three experiments. ○, NTL4; △, A136; ▲, *lon* mutant NTS2. (b) Virulence assays on *K. diagremontiana* leaves. Wounds in leaves were inoculated with strains: A, NTL4; B, NTS2; C, A136; D, NTS2(pTiR10); E, A136(pTiR10); F, NTS2(pTiR10, pAWlon); G, NTS2(pTiR10, pAWlonK364Q); H, NTS2(pTiR10, pAWlonS680A). All strains were inoculated at a population size corresponding to an OD_{600} of 1·0.

The influence of Lon on cell shape provides an example of such target diversity. Lon mutants of *A. tumefaciens* and *E. coli* both exhibit altered cell morphologies. However, while *lon* mutants of *E. coli* produce long filaments, cells of the *A. tumefaciens lon* mutant exhibit swellings and branching morphologies (Figs A.3 and A.5). Clearly, at the cellular level Lon is important to the regulation of cell division in both *E. coli* and *A. tumefaciens*. However, the protease contributes to this process by recognizing quite different targets in these two bacteria. In *E. coli*, *lon* mutants fail to degrade SulA, a cell division inhibitor, resulting in filamentation (Mizusawa & Gottesman, 1983; Schoemaker *et al.*, 1984). On the other hand, among the α-Proteobacteria, in the most well-studied relative of *A. tumefaciens*, *C. crescentus*, Lon contributes to the regulation of cell division by controlling the intracellular levels of CcrM, a DNA methylase. The levels and thereby the activity of this enzyme signal the initiation of DNA replication (Wright *et al.*, 1996). CcrM is a target of Lon and the unregulated accumulation of this essential methylase in *lon* mutants results in abnormal timing of initiation of DNA replication (Wright *et al.*, 1996). The defect in the timing of initiation most probably results in the altered cellular morphology through a pathway that couples chromosome replication to cell division. While *A. tumefaciens* lacks SulA, it contains an orthologue of the *C. crescentus ccrM* gene (Kahng & Shapiro, 2001). This gene also is essential in *A. tumefaciens* and overexpression of *ccrM* results in altered cellular morphologies very similar to that of the *lon* mutant (Kahng & Shapiro, 2001). Moreover, overexpression of CcrM in *S. meliloti* results in cells with morphologies indistinguishable from that of the *Agrobacterium lon* mutant (Wright *et al.*, 1995). We hypothesize that in *A. tumefaciens* CcrM is degraded by Lon and that aberrant accumulation of CcrM in the *lon* mutant causes inappropriate DNA

methylation which interferes with the timing of DNA replication and subsequent cell division. CcrM, but not SulA, is present and strongly conserved in all of the -Proteobacteria for which sequence data are available (Wright et al., 1995). We conclude that while Lon plays a central role in controlling cell division in both groups of prokaryotes, the targets of this protease, and therefore the mechanism of regulation, differs between the α- and γ-Proteobacteria. Moreover, while the role of Lon in modulating cell morphology is most pronounced during the SOS response within the γ-Proteobacteria, the protease is more completely integrated into normal cell division processes in the α-subgroup.

Lon_{At} complements *E. coli lon* mutants for filamentation and regulation of expression of *cps*, the operon encoding production of colonic acid capsule (Fig. A.5). Thus, while the protease controls cell division in the two groups of bacteria by targeting different regulatory elements, Lon from *Agrobacterium* retains its ability to recognize SulA and also RcsA, the positive activator of the *cps* regulon from *E. coli*. Lon also is required for proper regulation of extracellular polysaccharide synthesis in the close relative, *S. meliloti* (Summers *et al.*, 2000). However, Lon apparently does not control extracellular polysaccharide in *A. tumefaciens*; as judged by Calcofluor binding, the level of extracellular polysaccharide production by the *lon* mutant is not detectably altered from that of its wild-type parent.

On initial isolation, the *lon* mutants formed two colony morphotypes, one slow-growing and unstable, the other growing somewhat faster but stable (Fig. A.2 and data not shown). Given the instability of the NTS1-type and the stability of the NTS2-type colonies, we consider it likely that the stable morphotype contains a second, spontaneous

mutation that suppresses some strongly deleterious effect of the *lon* mutation on growth. The nature of this suppressor mutation is not known, but it is unlikely to contribute to the other *lon* phenotypes exhibited by NTS2. All such phenotypes are complementable by wild-type *lon* expressed from its own promoter from a low-copy-number vector.

Two lines of evidence indicate that Lon is a member of the heat-shock regulon in *A. tumefaciens*. First, the transcription of lon_{At} was transiently stimulated by elevated temperature (Fig. A.6b). Second, the increase in mRNA level was accompanied by a small but reproducibly detectable increase in the intracellular levels of the Lon protein (Fig. A.6c and d). Analysis of the nucleotide sequence upstream of lon_{At} revealed an element similar to the consensus σ^{32} heat-shock promoter of the -proteobacterium, *E. coli* (Fig. A.9a). Significantly, a σ^{32} homologue, RpoH, plays a major and global role in regulating the heat-shock response in *A. tumefaciens* (Mantis & Winans, 1992; Segal & Ron, 1995; Rosen *et al.*, 2002; Nakahigashi *et al.*, 1999). No sequences upstream of the –35 region of the *lon* promoter were found conserved in the corresponding upstream region of other heat-shock promoters in *Agrobacterium* or *E. coli*. However, a 16 bp inverted repeat (IR) is located between the putative –10 and –35 regions, and a second 14 bp IR is located downstream of the putative transcriptional start site (Fig. A.9b). While these IR elements are not conserved in other α-Proteobacteria, they may play a role in the transcriptional or posttranscriptional regulation of *lon* in *A. tumefaciens*. Expression of *lon* is also induced by elevated temperature in *B. abortus* (Roberston *et al.*, 2000) and *S. meliloti* (Mitsui *et al.*, 2004), suggesting that, as in the γ-Proteobacteria, inclusion of *lon* in the heat-shock regulon may be a common feature in the α-Proteobacteria. Interestingly, given that NTS2 does not display increased sensitivity to UV irradiation it is unlikely that

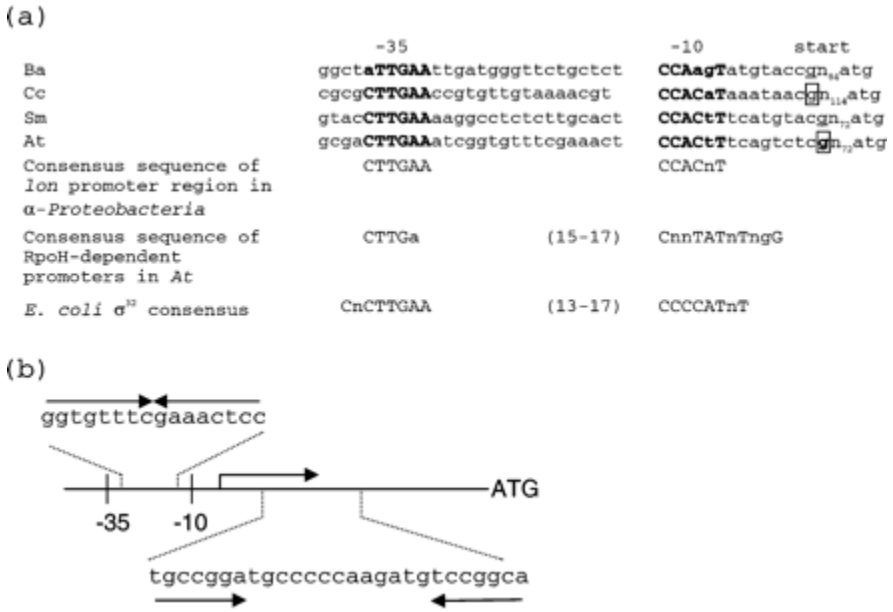

Fig. A.9. Promoter region of *A. tumefaciens lon* contains a σ^{32}-like sigma factor recognition site and two inverted repeats. (a) Alignment ofpromoter sequences of *lon* in α-Proteobacteria. Bacteria are abbreviated as follows: *Ba*, *B. abortus*; *Cc*, *C. crescentus*; *Sm*, *S. meliloti*; *At*, *A. tumefaciens*. The identified and putative start sites of heat-inducible transcripts are underlined and boxed, respectively. $N_x$atg indicates the number of nucleotide bases between the transcriptional start site and the translation start codon of *lon*. Bases found in at least three of four promoters are indicated in upper case and bold type. Consensus promoter sequences deduced from upstream untranslated regions of *lon* in α-Proteobacteria and those of the RpoH-dependent promoters in *A. tumefaciens* (Nakahigashi *et al.*, 1999) and *E. coli* σ^{32} (Yura *et al.*, 1993) are shown for comparison. (b) A 16 bp inverted repeat (IR) located between the putative –10 and –35 regions and a second, 14 bp IR located downstream of the putative transcriptional start site are shown.

Lon is part of the SOS response in *A. tumefaciens*.

Lon in its wild-type form is required for full pathogenicity by *A. tumefaciens* (Fig. A.7). Hence, ours joins a growing list of reports regarding the influence of this protease on the interaction of bacteria with their eukaryotic hosts. For example, among the α-*proteobacteria*, Lon of *B. abortus* is required during the initial stages of infection in BALB/c mice (Roberston *et al.*, 2000) while in *S. meliloti* Lon is required for formation of effective, nitrogen-fixing nodules in alfalfa (Summers *et al.*, 2000). In the γ-Proteobacteria Lon is important for systemic infection of mice by *Salmonella enterica* serovar Typhimurium (Takaya *et al.*, 2003). Pathogenesis of *A. tumefaciens* is a complex process involving signalling, gene regulation, assembly and function of a Type IV secretion system (T4SS), and physical interactions between the bacterium and its host plant. At present we do not know how the *lon* mutation affects these processes. Lon might target some protein involved in controlling expression of the *vir* regulon, the functions of which are involved in T-strand processing, transfer and integration into the plant genome. Alternatively, the mutation might interfere mechanistically with T-strand processing or with the assembly or function of the VirB T4SS. Interestingly, a mutant of strain C58 defective in the TAT transport system shows defects in cell morphology and virulence that phenocopy those of the *lon* mutant (Ding & Christie, 2003). It will be interesting to determine whether the loss of virulence associated with defects in Lon protease and the TAT secretory system reflect common or different targets.

ACKNOWLEDGEMENTS

We thank Dr R. Martin Roop II, Department of Microbiology and Immunology, Louisiana State University Health Sciences Center for providing us with the polyclonal rabbit antiserum directed against *B. abortus* Lon, and Dr. Andrei Kuzminov, Department of Microbiology, University of Illinois at Urbana-Champaign, for kind assistance with the UV sensitivity assay. We also thank Dr Zhao-Qing Luo, Department of Biological Sciences, Purdue University, for the generous gift of plasmid pSR47s, and the other members of the laboratory for helpful discussions. This work was supported by grant No. R01 GM52465 from the NIH to S. K. F.

REFERENCES

Amerik, A. Y., Antonov, V. K., Gorbalenya, A. E., Kotova, S. A., Rotanova, T. V. & Shimbarevich, E. V. (1991). Site-directed mutagenesis of La protease: a catalytically active serine residue. *FEBS Lett* **287**, 211–214.

Bernstein, H. D. & Hyndman, J. B. (2001). Physiological basis for conservation of the signal recognition particle targeting pathway in *Escherichia coli*. *J Bacteriol* **183**, 2187–2197.

Cangelosi, G. A., Best, E. A., Marinetti, G. & Nester, E. W. (1991). Genetic analysis of *Agrobacterium*. *Methods Enzymol* **204**, 384–397.

Chilton, M.-D., Currier, T. C., Farrand, S. K., Bendich, A. J., Gordon, M. P. & Nester, E. W. (1974). *Agrobacterium tumefaciens* DNA and PS8 bacteriophage DNA not detected in crown gall tumors. *Proc Natl Acad Sci U S A* **71**, 3672–3676.

Chin, D. T., Goff, S. A., Webster, T., Smith, T. & Goldberg, A. L. (1988). Sequence of the *lon* gene in *Escherichia coli*. A heat-shock gene which encodes the ATP-dependent protease La. *J Biol Chem* **263**, 11718–11728.

Cook, D. M. & Farrand, S. K. (1992). The *oriT* region of the *Agrobacterium tumefaciens* Ti plasmid pTiC58 shares DNA sequence identity with the transfer origins of RSF1010 and RK2/RP4 and with T-region borders. *J Bacteriol* **174**, 6238–6246.

Ding, Z. & Christie, P. J. (2003). *Agrobacterium tumefaciens* twin-arginine-dependent translocation is important for virulence, flagellation, and chemotaxis but not type IV secretion. *J Bacteriol* **185**, 760–771.

Drlica, K. & Rouvière-Yaniv, J. (1987). Histone-like proteins of bacteria. *Microbiol Rev* **51**, 301–319.

Gill, R. E., Karlok, M. & Benton, D. (1993). *Myxococcus xanthus* encodes an ATP-dependent protease which is required for developmental gene transcription and intercellular signaling. *J Bacteriol* **175**, 4538–4544.

Goldberg, A. L., Moerschell, R. P., Chung, C. H. & Maurizi, M. R. (1994). ATP-dependent protease La (Lon) from *Escherichia coli*. *Methods Enzymol* **244**, 350–375.
Gottesman, S. (1996). Proteases and their targets in *Escherichia coli*. *Annu Rev Genet* **30**, 465–506.

Gottesman, S. & Zipser, D. (1978). Deg phenotype of *Escherichia coli lon* mutants. *J Bacteriol* **133**, 844–851.

Guzman, L. M., Belin, D., Carson, M. J. & Beckwith, J. (1995). Tight regulation, modulation, and high-level expression by vectors containing the arabinose P_{BAD} promoter. *J Bacteriol* **177**, 4121–4130.

Howard-Flanders, P., Simson, E. & Theriot, L. (1964). A locus that controls filament formation and sensitivity to radiation in *Escherichia coli* K-12. *Genetics* **49**, 237–246.
Kahng, L. S. & Shapiro, L. (2001). The CcrM methyltransferase of *Agrobacterium tumefaciens* is essential, and its activity is cell cycle regulated. *J Bacterial* **183**, 3065–3075.

Luo, Z.-Q., Clemente, T. E. & Farrand, S. K. (2001). Construction of a derivative of *Agrobacterium tumefaciens* C58 that does not mutate to tetracycline resistance. *Mol Plant Microbe Interact* **14**, 98–103.

Mantis, N. J. & Winans, S. C. (1992). Characterization of the *Agrobacterium tumefaciens* heat shock response: evidence for a σ^{32}-like sigma factor. *J Bacteriol* **174**, 991–997.

Markovitz, A. (1964). Regulatory mechanisms for synthesis of capsular polysaccharide in mucoid mutants of *Escherichia coli* K-12. *Proc Natl Acad Sci U S A* **51**, 239–246.

Merriam, J. J., Mathur, R., Maxfield-Boumil, R. & Isberg, R. R. (1997). Analysis of the *Legionella pneumophila fliI* gene: intracellular growth of a defined mutant defective for flagellum biosynthesis. *Infect Immun* **65**, 2497–2501.

Miller, J. (1972). *Experiments in Molecular Genetics*, pp. 352–355. Cold Spring Harbor, NY: Cold Spring Harbor Laboratory.

Miranda, A. & Kuzminov, A. (2003). Chromosomal lesion suppression and removal in *Escherichia coli* via linear DNA degradation. *Genetics* **163**, 1255–1271.

Mitsui, H., Sato, T., Sato, Y., Ito, N. & Minamisawa, K. (2004). *Sinorhizobium meliloti* RpoH1 is required for effective nitrogen-fixing symbiosis with alfalfa. *Mol Gen Genomics* **271**, 416–425.

Mizusawa, S. & Gottesman, S. (1983). Protein degradation in *Escherichia coli*: the *lon* gene controls the stability of the SulA protein. *Proc Natl Acad Sci U S A* **80**, 358–362.

Murillo, J., Shen, H., Grehold, D., Sharma, A., Cooksey, D. A. & Keen, N. T. (1994). Characterization of pPT23B, the plasmid involved in syringolide production by *Pseudomonas syringae* pv. *tomato* PT23. *Plasmid* **31**, 275–287.

Nair, G. R., Liu, Z. & Binns, A. N. (2003). Reexamining the role of the accessory plasmid pAtC58 in the virulence of *Agrobacterium tumefaciens* strain C58. *Plant Physiol* **133**, 989–999.

Nakahigashi, K., Ron, E. Z., Yanagi, H. & Yura, T. (1999). Differential and independent roles of a σ^{32} homolog (RpoH) and an HrcA repressor in the heat shock response of *Agrobacterium tumefaciens*. *J Bacteriol* **181**, 7509–7515.

Roberston, G. T., Kovach, M. E., Allen, C. A., Ficht, T. A. & Roop, R. M., II (2000). The *Brucella abortus* Lon functions as a generalized stress response protease and is required for wild-type virulence in BALB/c mice. *Mol Microbiol* **35**, 577–588.

Rosen, R., Buttner, K., Becher, D., Nakahigashi, K., Yura, T., Hecker, M. & Ron, E. Z. (2002). Heat shock proteome of *Agrobacterium tumefaciens*: evidence for new control systems. *J Bacteriol* **184**, 1772–1778.

Schoemaker, J. M., Gayda, R. C. & Markovitz, A. (1984). Regulation of cell division in *Escherichia coli*: SOS induction and cellular location of the SulA protein, a key to Lon-associated filamentation and cell death. *J Bacteriol* **158**, 551–561.

Segal, G. & Ron, E. Z. (1995). The *dnaKJ* operon of *Agrobacterium tumefaciens*: transcriptional analysis and evidence for a new heat shock promoter. *J Bacteriol* **177**, 5952–5958.

Simon, R., Priefer, U. & Pühler, A. (1983). A broad host range mobilization system for *in vivo* genetic engineering: transposon mutagenesis in gram negative bacteria. *BioTechnology* **1**, 784–791.

Stewart, B. J., Enos-Berlage, J. L. & McCarter, L. L. (1997). The *lonS* gene regulates swarmer cell differentiation of *Vibrio parahaemolyticus*. *J Bacteriol* **179**, 107–114.

Summers, M. L., Botero, L. M., Busse, S. C. & Mcdermott, T. R. (2000). The *Sinorhizobium meliloti* Lon protease is involved in regulating exopolysaccharide synthesis and is required for nodulation of alfalfa. *J Bacteriol* **182**, 2551–2558.

Takaya, A., Suzuki, M., Matsui, H., Tomoyasu, T., Sashinami, H., Nakane, A. & Yamamoto, T. (2003). Lon, a stress-induced ATP-dependent protease, is critically important for systemic *Salmonella enterica* serovar Typhimurium infection of mice. *J Bacteriol* **71**, 690–696.

Watson, B., Currier, T. C., Gordan, M. P., Chilton, M.-D. & Nester, E. W. (1975). Plasmid required for virulence of *Agrobacterium tumefaciens*. *J Bacteriol* **123**, 255–264.

Wise, A. A., Voinov, L. & Binns, A. N. (2005). Intersubunit complementation of sugar signal transduction in VirA heterodimer and posttranslational regulation of VirA activity in *Agrobacterium tumefaciens*. *J Bacteriol* **187**, 213–223.

Wood, D. W., Setubal, J. C., Kaul, R., Monks, D. E., Kitajima, J. P. & 46 other authors (2001). The genome of the natural genetic engineer *Agrobacterium tumefaciens* C58. *Science* **294**, 2317–2323.

Wright, R., Stephens, C. & Shapiro, L. (1995). The CcrM DNA methyltransferase is widespread in the alpha subdivision of proteobacteria, and its essential functions are conserved in *Rhizobium meliloti* and *Caulobacter crescentus*. *J Bacteriol* **179**, 5869–5877.

Wright, R., Stephens, C., Zweiger, G., Shapiro, L. & Alley, M. R. (1996). *Caulobacter* Lon protease has a critical role in cell-cycle control of DNA methylation. *Genes Dev* **10**, 1532–1542.

Yura, T., Nagai, H. & Mori, H. (1993). Regulation of the *Escherichia coli* heat-shock response. *Annu Rev Microbiol* **47**, 321–350.